*Searches for Axions at the University of Western Australia*

Prof. Michael Tobar

THE UNIVERSITY OF WESTERN AUSTRALIA

QDm Quantum Technologies and Dark Matter Research Lab





DARK MATTER

EQUS Australian Research Council Centre of Excellence for Engineered Quantum Systems

# Searches for Axions at UWA

# QUANTUM TECHNOLOGIES AND DARK MATTER RESEARCH LAB

EQUS
Australian Research Council Centre of Excellence for Engineered Quantum Systems

THE UNIVERSITY OF WESTERN AUSTRALIA

QDm
Quantum Technologies and Dark Matter Research Lab

ARC CENTRE OF EXCELLENCE FOR DARK MATTER




## Our Team

**ACADEMIC**
Michael Tobar
Eugene Ivanov
Maxim Goryachev

**POSTDOCS**
Ben McAllister
Cindy Zhao
Jeremy Bourhill

**TECHNICIAN**
Steven Osborne

**ADJUNCT**
Alexey Veryaskin (Trinity Labs)

**HDR/PHD STUDENTS**
Graeme Flower
Catriona Thomson
William Campbell
Aaron Quiskamp
Elrina Hartman

**UNDERGRAD STUDENTS**
Jay Mummery (Masters)
Bryn Roughan (MPE)
Robert Limina (MPE)
Robert Crew (BPhil)
Daniel Tobar (BPhil)
Michael Hatzon (BPhil)

# QDM Laboratory

Welcome to the Quantum Technology and Dark Matter Laboratory at UWA!
Come inside and check out our world class facilities, home to nodes of the ARC Centre of Excellence for Engineered Quantum Systems, and the ARC Centre of Excellence for Dark Matter Particle Physics.

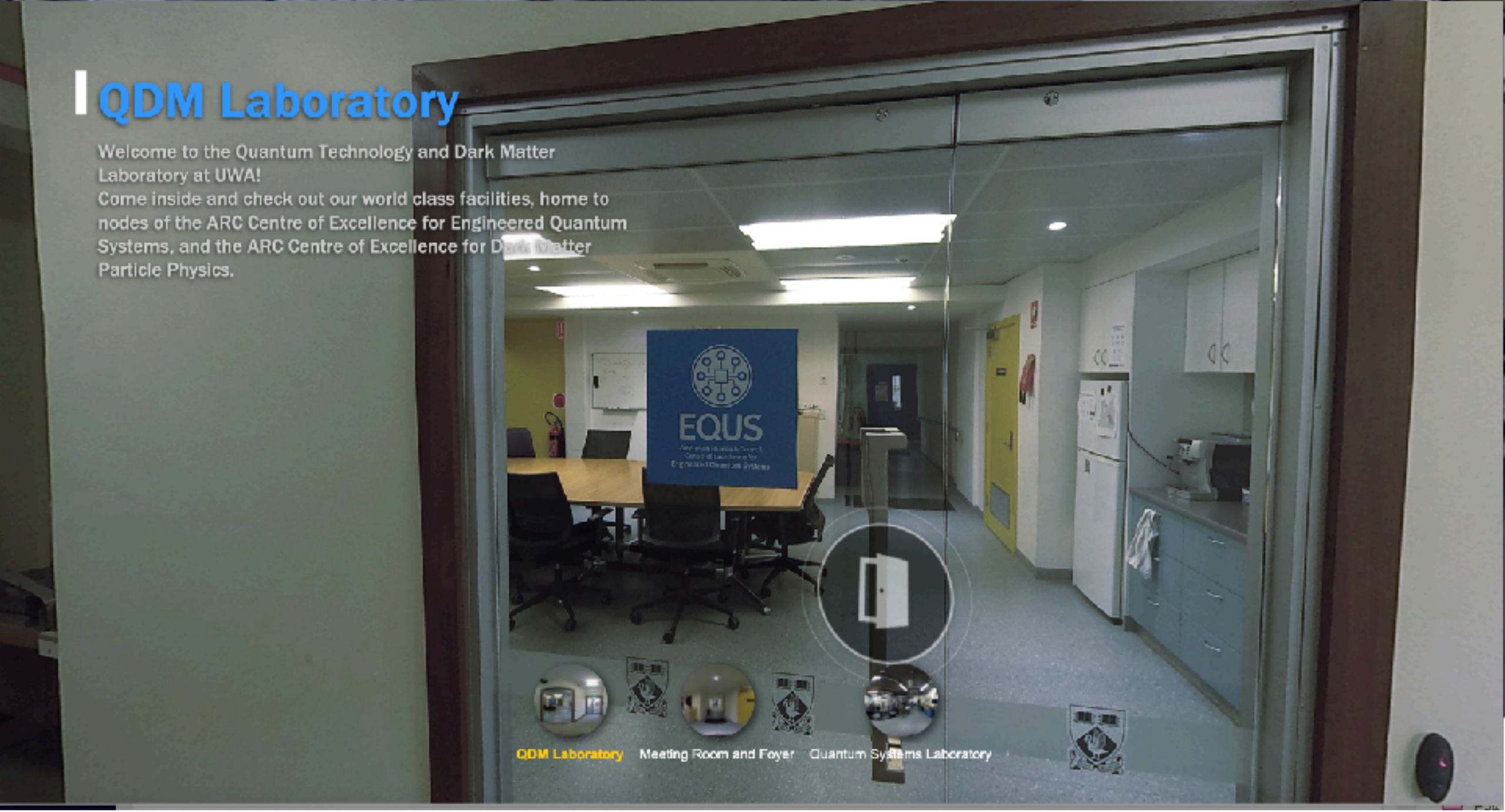

# WAVE LIKE DARK MATTER PROGRAM @ UWA

(1) Axion Dark Matter eXperiment (**ADMX**) Project run by Fermilab, run out of Seattle at Washington University. UWA Officially a group member since 2019. PI Gray Rybka

(2) **Oscillating Resonant Group AxioN experiment (ORGAN).** The first Axion experiment at UWA, currently testing Axion Cogenesis.

(3) AC Halloscope with Low Noise Oscillators (UPconversion Loop Oscillator Axion Detector (**UPLOAD**) UWA

(4)Low mass detectors for axions with LCR Circuits, **ADMX-SLIC** (Superconducting Lc-circuit Investigating Cold axions) UF (Sikivie and Tanner) and Broadband Electrical Action Sensing Technique (**BEAST**) UWA

(5)Searches for axions through coupling with electron spins, on hold until axion detected; **Magnon-Cavity** UWA

(6) **Light Scalar Dark Matter** (Dilaton) Clock Comparisons, Acoustic Detectors UWA

## (2) ORGAN

PHYSICAL REVIEW APPLIED 14, 044031 (2020)

# Dielectric-Boosted Sensitivity to Cylindrical Azimuthally Varying Transverse-Magnetic Resonant Modes in an Axion Haloscope

Aaron P. Quiskamp,[1,*] Ben T. McAllister,[1] Grey Rybka,[2] and Michael E. Tobar[1,†]

[1]ARC Centre of Excellence for Engineered Quantum Systems and ARC Centre of Excellence for Dark Matter Particle Physics, Department of Physics, University of Western Australia, 35 Stirling Highway, Crawley WA 6009, Australia

[2]Center for Experimental Nuclear Physics and Astrophysics, University of Washington, 1410 NE Campus Parkway, Seattle, Washington 98195, USA

(Received 15 June 2020; revised 6 August 2020; accepted 28 September 2020; published 27 October 2020)



Axions are a popular dark-matter candidate that are often searched for in experiments known as "haloscopes," which exploit a putative axion-photon coupling. These experiments typically rely on transverse-magnetic (TM) modes in resonant cavities to capture and detect photons generated via axion conversion. We present a study of a resonant-cavity design for application in haloscope searches, of particular use in the push to higher-mass axion searches (above approximately 60 $\mu$eV). In particular, we take advantage of azimuthally varying $TM_{mnl}$ modes that, while typically insensitive to axions due to field uniformity, can be made axion sensitive (and frequency tunable) through the strategic placement of dielectric wedges, becoming a type of resonator known as a dielectric-boosted axion-sensitivity (DBAS) resonator. Results from finite element modeling are presented and compared with a simple proof of concept experiment. The results show a significant increase in axion sensitivity for these DBAS resonators over their empty-cavity counterparts and high potential for application in high-mass axion searches when benchmarked against simpler more traditional designs that rely on fundamental TM modes.

DOI: 10.1103/PhysRevApplied.14.044031

## (3) UPLOAD

PHYSICAL REVIEW LETTERS 126, 081803 (2021)

# Upconversion Loop Oscillator Axion Detection Experiment: A Precision Frequency Interferometric Axion Dark Matter Search with a Cylindrical Microwave Cavity

Catriona A. Thomson,[*] Ben T. McAllister, Maxim Goryachev, Eugene N. Ivanov, and Michael E. Tobar[†]

ARC Centre of Excellence for Engineered Quantum Systems and ARC Centre of Excellence for Dark Matter Particle Physics, Department of Physics, University of Western Australia, 35 Stirling Highway, Crawley, Western Australia 6009, Australia

(Received 5 January 2020; revised 11 November 2020; accepted 15 January 2021; published 24 February 2021)



First experimental results from a room-temperature tabletop phase-sensitive axion haloscope experiment are presented. The technique exploits the axion-photon coupling between two photonic resonator oscillators excited in a single cavity, allowing haloscope detection to be performed in microwave frequencies, acting as a source of frequency modulation on the microwave carriers. This new pathway to axion detection has certain advantages over the traditional haloscope method, particularly in targeting axions below 1 $\mu$eV (240 MHz) in energy. At the heart of the dual-mode oscillator, a tunable cylindrical microwave cavity supports a pair of orthogonally polarized modes ($TM_{020}$ and $TE_{011}$), which, in general, enables simultaneous sensitivity to axions with masses corresponding to the sum and difference of the microwave frequencies. However, in the reported experiment, the configuration was such that the sum frequency sensitivity was suppressed, while the difference frequency sensitivity was enhanced. The results place axion exclusion limits between 7.44–9.38 neV, excluding a minimal coupling strength above $5 \times 10^{-11}$ 1/GeV, after a measurement period of two and a half hours. We show that a state-of-the-art frequency-stabilized cryogenic implementation of this technique, ambitious but realizable, may achieve the best limits in a vast range of axion space.

DOI: 10.1103/PhysRevLett.126.081803

## (4) LCR Circuits

Physics of the Dark Universe 30 (2020) 100624

Contents lists available at ScienceDirect

Physics of the Dark Universe

journal homepage: www.elsevier.com/locate/dark



# Broadband electrical action sensing techniques with conducting wires for low-mass dark matter axion detection

Michael E. Tobar *, Ben T. McAllister, Maxim Goryachev

ARC Centre of Excellence For Engineered Quantum Systems, Department of Physics, University of Western Australia, 35 Stirling Highway, Crawley WA 6009, Australia

## (6) SCALAR DARK MATTER

PHYSICAL REVIEW LETTERS 126, 071301 (2021)

# Searching for Scalar Dark Matter via Coupling to Fundamental Constants with Photonic, Atomic, and Mechanical Oscillators

William M. Campbell, Ben T. McAllister, Maxim Goryachev, Eugene N. Ivanov, and Michael E. Tobar[*]

ARC Centre of Excellence for Engineered Quantum Systems and ARC Centre of Excellence for Dark Matter Particle Physics, Department of Physics, University of Western Australia, 35 Stirling Highway, Crawley, Western Australia 6009, Australia

(Received 15 October 2020; revised 25 November 2020; accepted 15 January 2021; published 18 February 2021)



We present a way to search for light scalar dark matter (DM), seeking to exploit putative coupling between dark matter scalar fields and fundamental constants, by searching for frequency modulations in direct comparisons between frequency stable oscillators. Specifically we compare a cryogenic sapphire oscillator (CSO), hydrogen maser (HM) atomic oscillator, and a bulk acoustic wave quartz oscillator (OCXO). This work includes the first calculation of the dependence of acoustic oscillators on variations of the fundamental constants, and demonstration that they can be a sensitive tool for scalar DM experiments. Results are presented based on 16 days of data in comparisons between the HM and OCXO, and 2 days of comparison between the OCXO and CSO. No evidence of oscillating fundamental constants consistent with a coupling to scalar dark matter is found, and instead limits on the strength of these couplings as a function of the dark matter mass are determined. We constrain the dimensionless coupling constant $d_e$ and combination $|d_m - d_p|$ across the mass band $4.4 \times 10^{-14} \lesssim m_\phi \lesssim 5.8 \times 10^{-10}$ eV $c^{-2}$, with most sensitive limits $d_e \gtrsim 1.59 \times 10^{-1}$, $|d_m - d_p| \gtrsim 6.97 \times 10^{-1}$. Notably these limits do not rely on maximum reach analysis (MRA), instead employing the more general coefficient separation technique. This experiment paves the way for future, highly sensitive experiments based on state-of-the-art acoustic oscillators, and we show that these limits can be competitive with the best current MRA-based exclusion limits.

DOI: 10.1103/PhysRevLett.126.071301

# Axion Haloscope Dark Matter Experiments at UWA




3 Dilution Fridges  14T, 7T and 3T Magnets

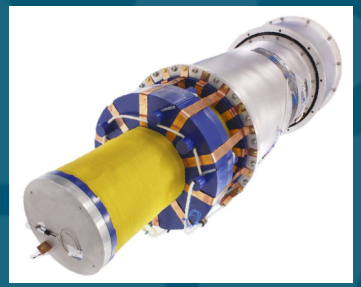

Network Analysers and components from RF to 100GHz

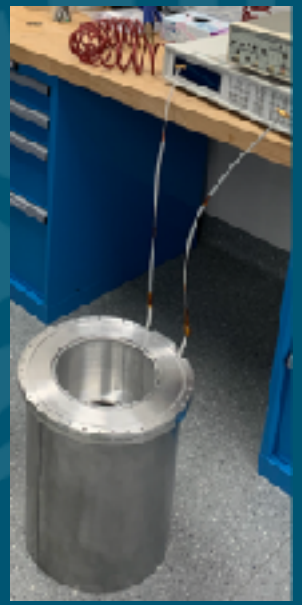

This Presentation

1) ORGAN: Current Status & Future Plans
2) UPLOAD experiment, Searching below 1micro eV
3) Low Mass Axion Searches: Reactive Poynting Theorem in Axion Modified ED














# ORGAN: Current Status & Future Plans

Aaron Quiskamp, Ben McAllister, Graeme Flower, Catriona Thomson, Will Campbell, Cindy Zhao, Maxim Goryachev, Eugene Ivanov, Michael Tobar (UWA)

Paul Altin (ANU)





















# **ORGAN**: **O**scillating **R**esonant **G**roup **A**xio**N** Experiment

- High frequency (>15 GHz) axion haloscope at UWA, path finding run in 2017
- High frequency parameter space is largely un-probed and ripe for exploration
- SMASH model predicts axion mass ($m_a$) between 50 and 200 $\mu eV$

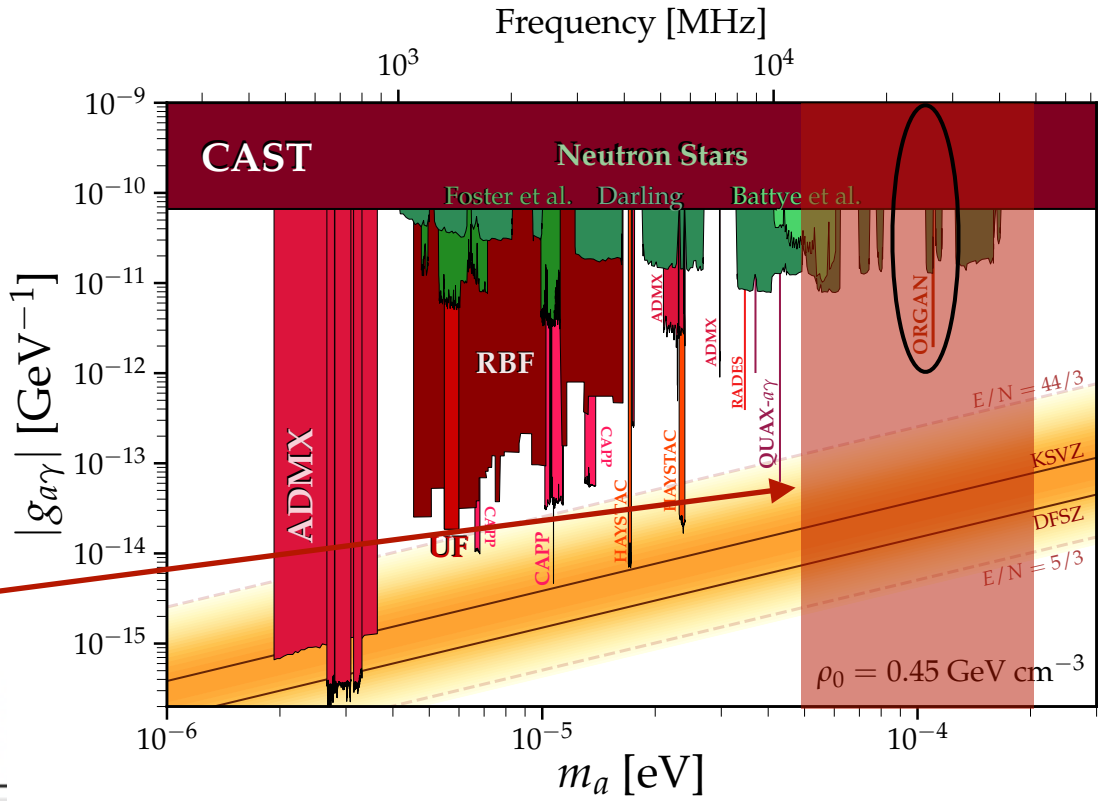




# ORGAN: Axion Detection

- Critical research areas to improve scan rate and axion model sensitivity:
  - Tuneable sensitive resonators
  - Low noise amplification
  - Data acquisition and analysis

    - Haloscope scan rate:

$$\frac{df}{dt} \propto \frac{1}{SNR_{goal}^2} \frac{g_{a\gamma\gamma}^4 B^4 C^2 V^2 \rho_a^2 Q_L Q_a}{m_a^2 (k_B T_n)^2}$$

    - Three aspects to this:
      - Magnet/dilution fridge: Look to purchasing larger magnet with larger bore
      - Resonator design: Dielectric, with novel tuning
      - Amplifier noise temperature: Single photon counter

ARC CENTRE OF EXCELLENCE FOR DARK MATTER PARTICLE PHYSICS

# ORGAN Dilution Refrigerator and Magnet

- Dedicated dilution refrigerator (Nov 2019), BF-XLD1000
- Equipped with 12.5 T magnet

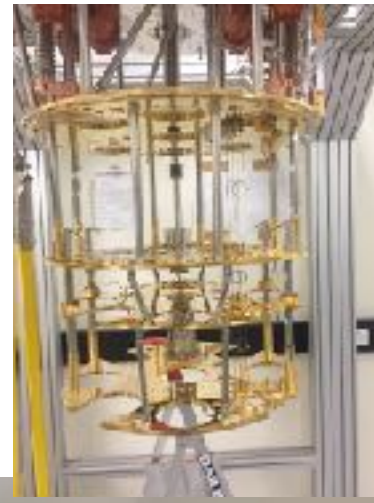






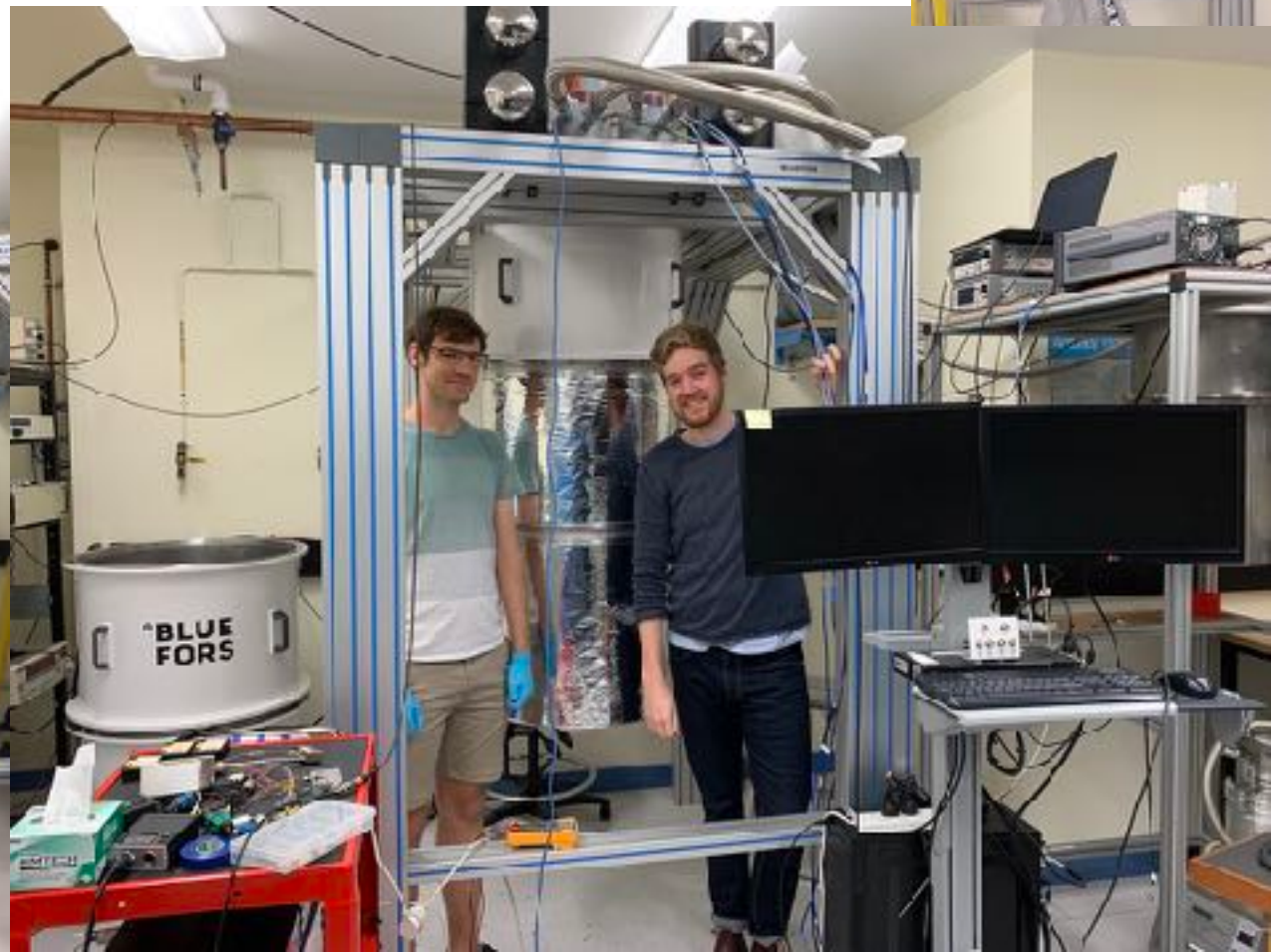

# Cavity Characterisation

- By **moving the rod radially** the mode is perturbed, shifting the frequency
- Some difficulty tuning when cold
- Solution: ramp the magnet to 11T



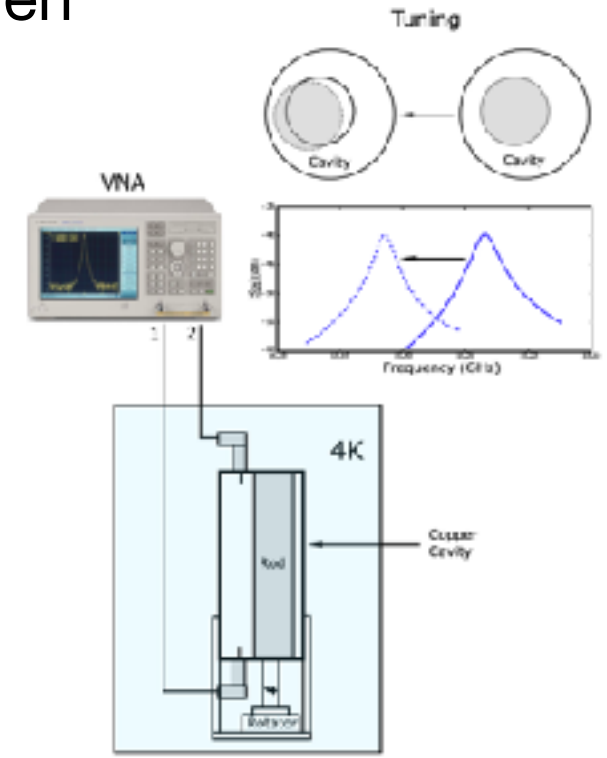


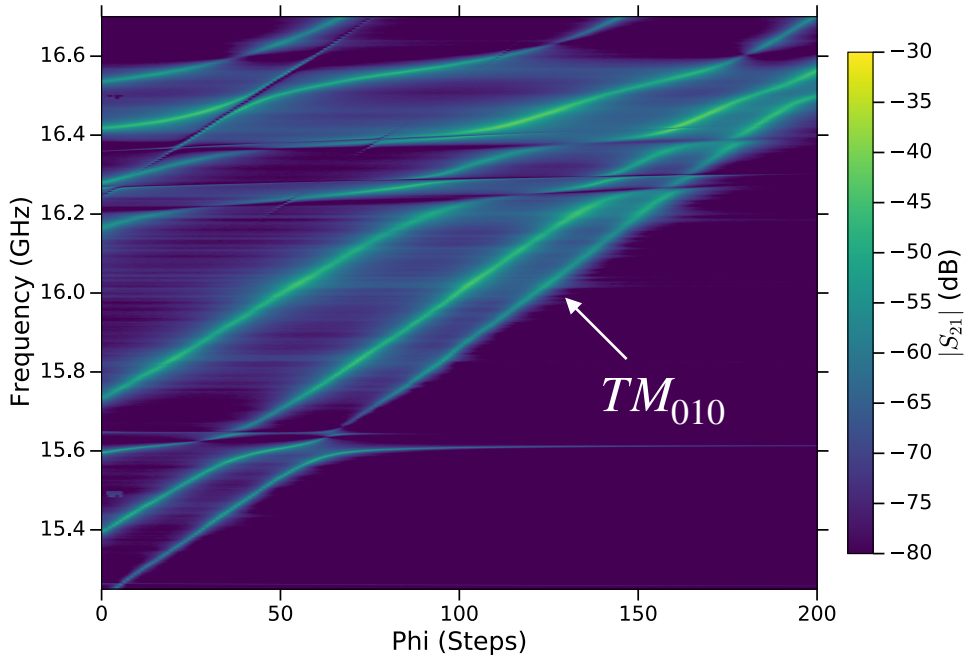


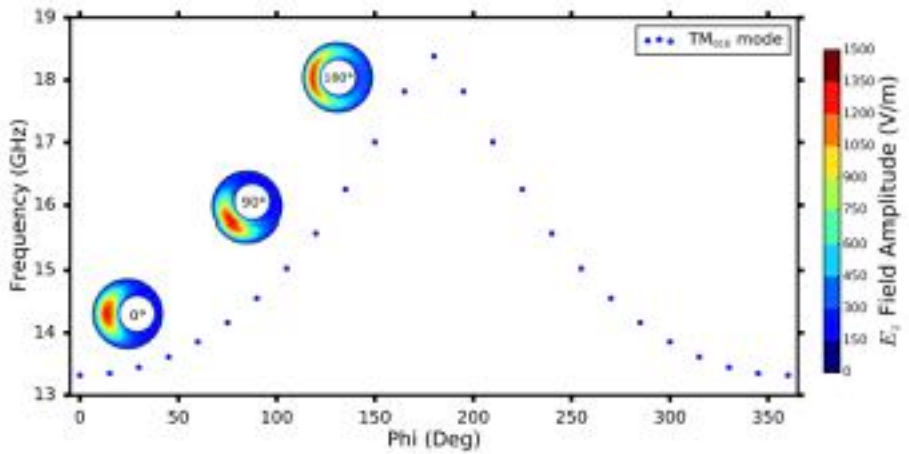

# Improving The Cavity: A Potential Solution?

- Dielectric Boosted Axion Sensitivity (DBAS)
- Take a higher order TM mode and make it axion sensitive by placing dielectric in out of phase regions.
- Result → decreased $E^z$ field in those regions → increase in C

PHYSICAL REVIEW APPLIED 9, 014028 (2018)

**Tunable Supermode Dielectric Resonators for Axion Dark-Matter Haloscopes**

Ben T. McAllister,[1,*] Graeme Flower,[1] Lucas E. Tobar,[1,2] and Michael E. Tobar[1,†]
[1]ARC Centre of Excellence for Engineered Quantum Systems, School of Physics, The University of Western Australia, Crawley 6009, Australia
[2]Department of Electrical and Computer Systems Engineering, Monash University, Clayton 3800, Australia

PHYSICAL REVIEW APPLIED 14, 044051 (2020)

**Dielectric-Boosted Sensitivity to Cylindrical Azimuthally Varying Transverse-Magnetic Resonant Modes in an Axion Haloscope**

Aaron P. Quiskamp,[1,*] Ben T. McAllister,[1] Giny Rybka,[2] and Michael E. Tobar[1,†]
[1]ARC Centre of Excellence for Engineered Quantum Systems and ARC Centre of Excellence for Dark Matter Particle Physics, Department of Physics, University of Western Australia, 35 Stirling Highway, Crawley WA 6009, Australia
[2]Centre for Experimental Nuclear Physics and Astrophysics, University of Washington, 1410 NE Campus Parkway, Seattle, Washington 98195, USA

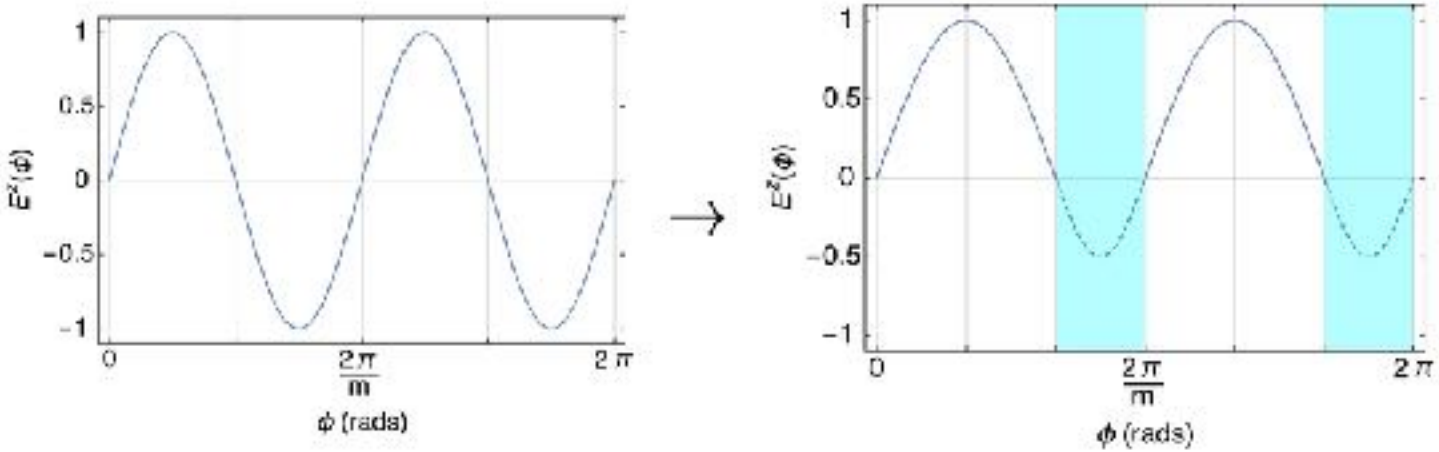


$TM_{410}$

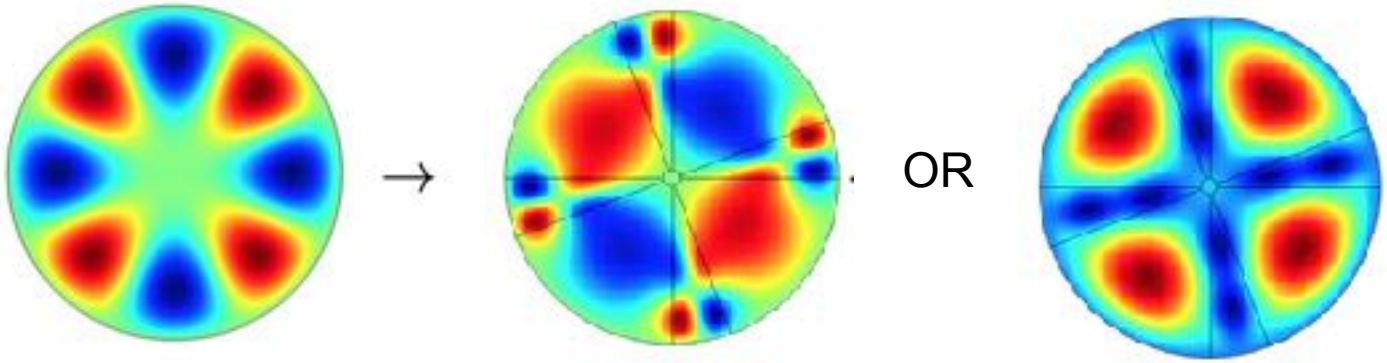

OR

# FEM Modelling with 4 Sapphire Wedges

Built-in tuning → 2-wedges remain stationary, while the other 2 are allowe to move relative to the stationary ones.

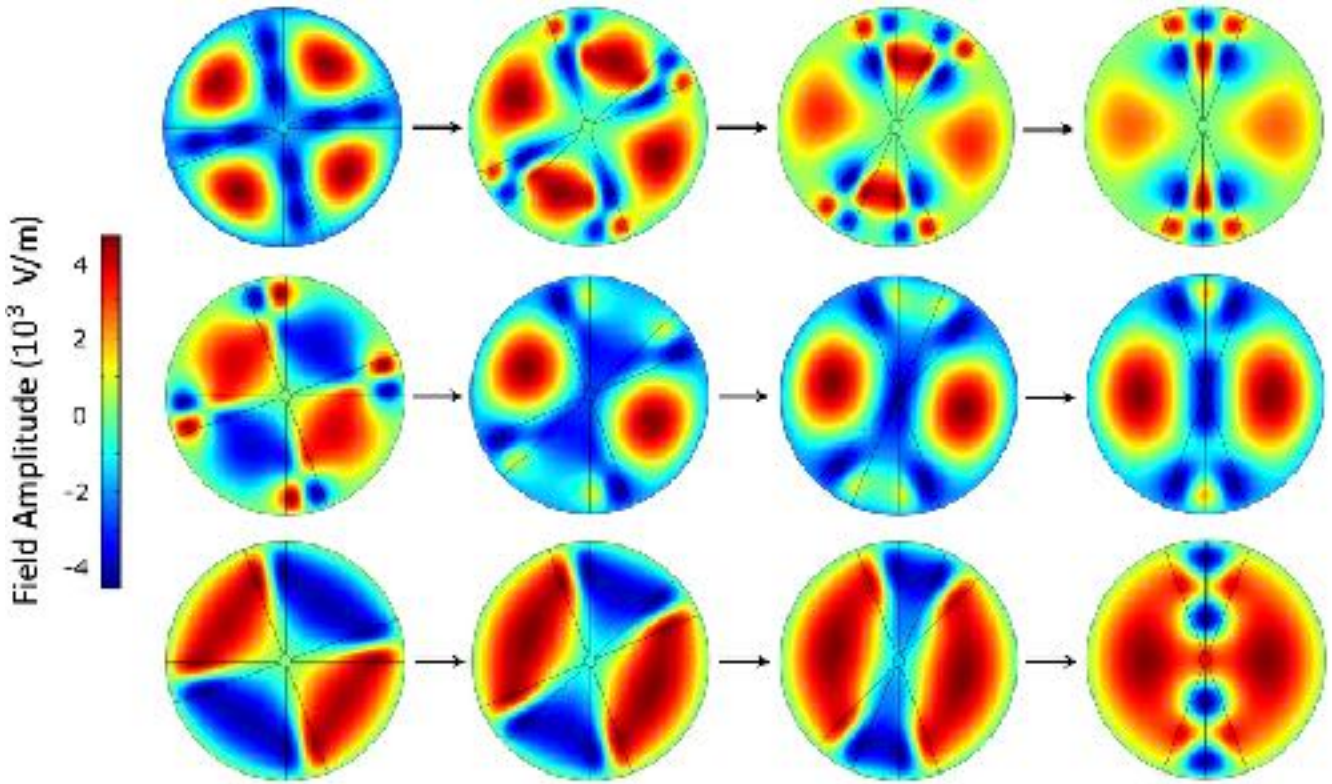


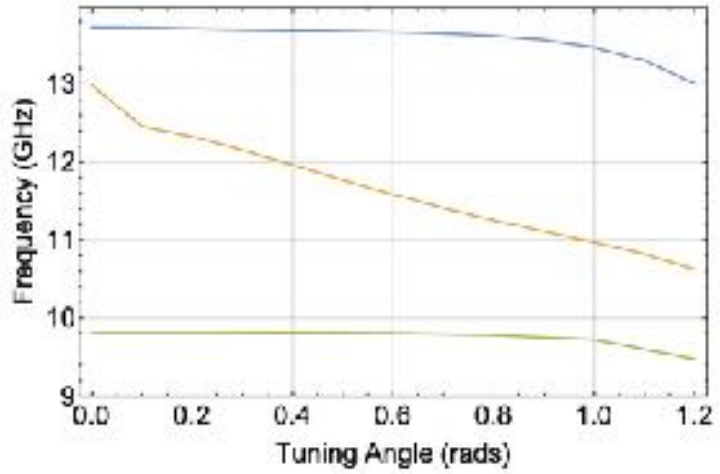


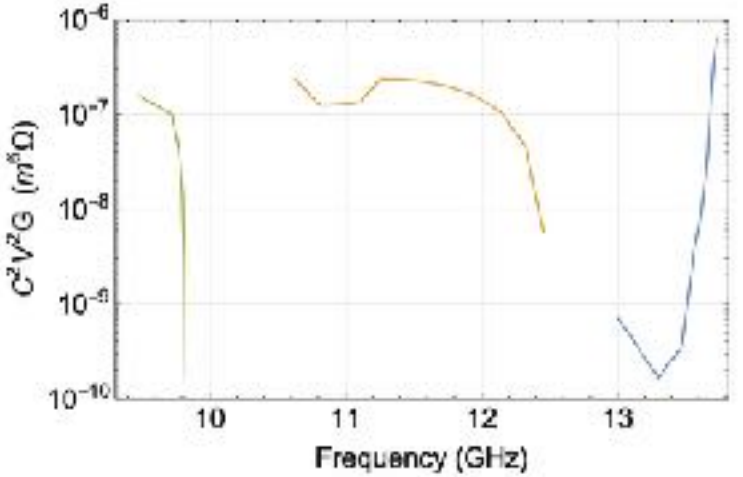


- TM410
- TM410-like
- TM210

# Improving the Amplifier

# Single Photon Counters for Axion Haloscopes

- Single Photon Detection is superior to SQL linear amplification under the right conditions
- Take ORGAN as an example
  - 100 mK
  - >15 GHz
- SQL Noise ~ 1K
- Ratio of SQL linear amp to SPD noise power:

$$\frac{P_\ell}{P_{sp}} = \frac{\bar{n}+1}{\sqrt{\bar{n}}}\sqrt{\frac{\Delta\nu_a}{\eta\Gamma}}$$

- For above parameters, with efficiency of 0.9: SQL about 50 times noisier
- If we lower the temperature this ratio can become order of thousands

# Single Photon Counters

- We want single photon counters in the ~10s of GHz range
- Not a lot…but a few options
- Currently exploring **current-biased Josephson junctions**
- Basic idea – photon kicks junction into voltage state

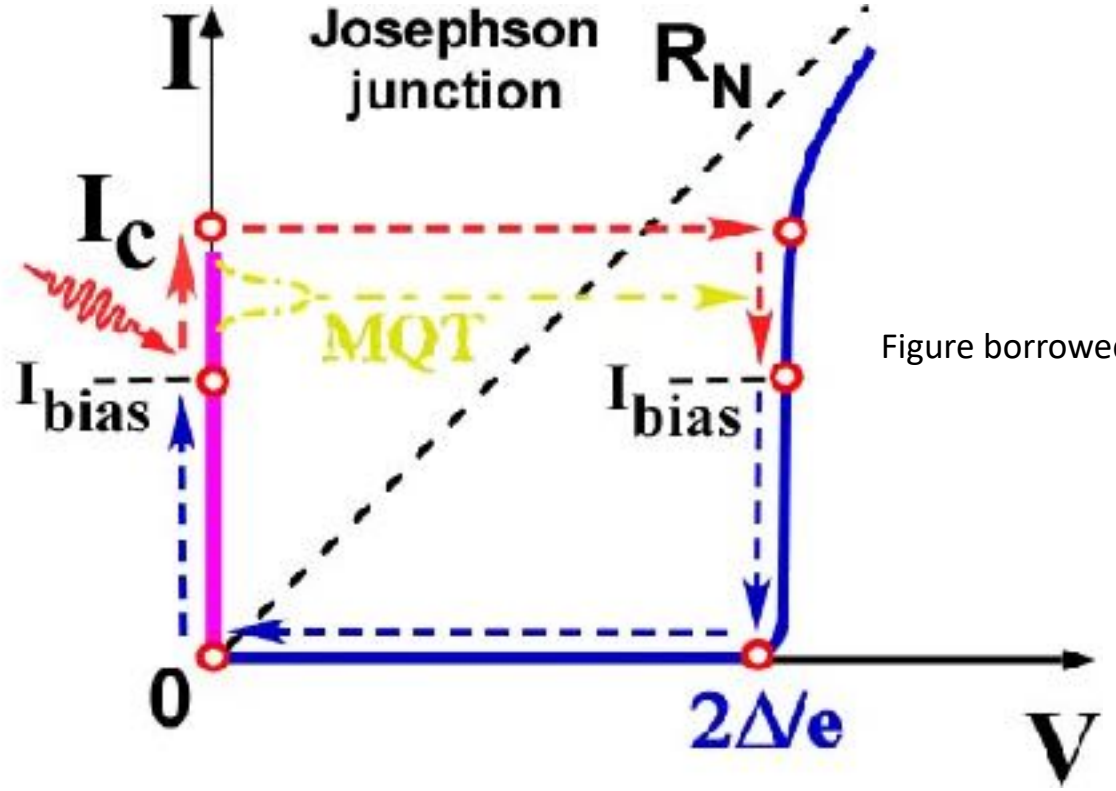


Figure borrowed from Leonid Kuzmin

# Single Photon Counters

- Have some (15 GHz) samples to test from Chalmers



- In the dilution fridge right now
- Watch this space

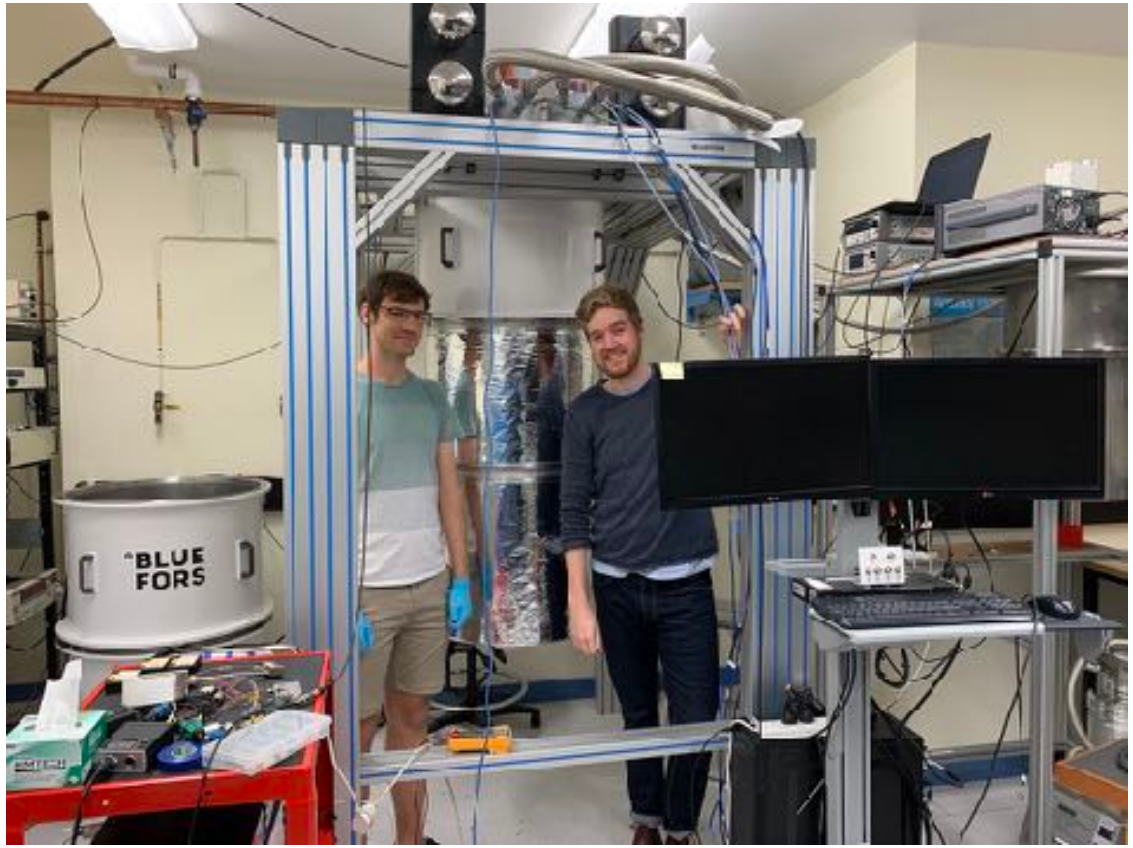

# ORGAN Run Plan Summary

- Phase 1: Narrow searches around 15-16 GHz and 26-27 GHz
- Runs 1a/1b (dark green): HEMT- amplifiers and $TM_{010}$ tuning rod resonators, form factor of 0.4. Test ALP Cogenisis
- Phase 2: Wider search (15-50GHz) building on expertise from Phase 1
- Phase 2, dark red: Quantum limited linear amplifiers (2-4 cavities)
- Light red/green: Single photon counter


PHYSICAL REVIEW LETTERS 124, 251802 (2020)

Axion Kinetic Misalignment Mechanism

Raymond T. Co, Lawrence J. Hall, and Keisuke Harigaya

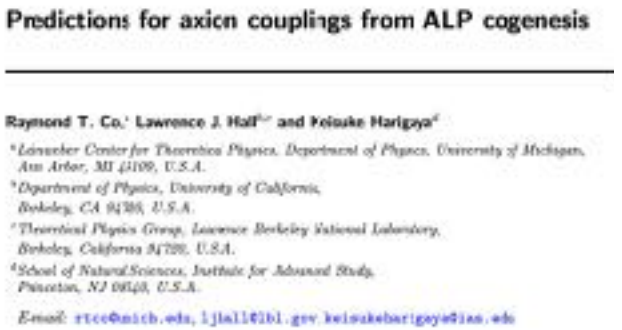
Predictions for axion couplings from ALP cogenesis

Raymond T. Co, Lawrence J. Hall and Keisuke Harigaya

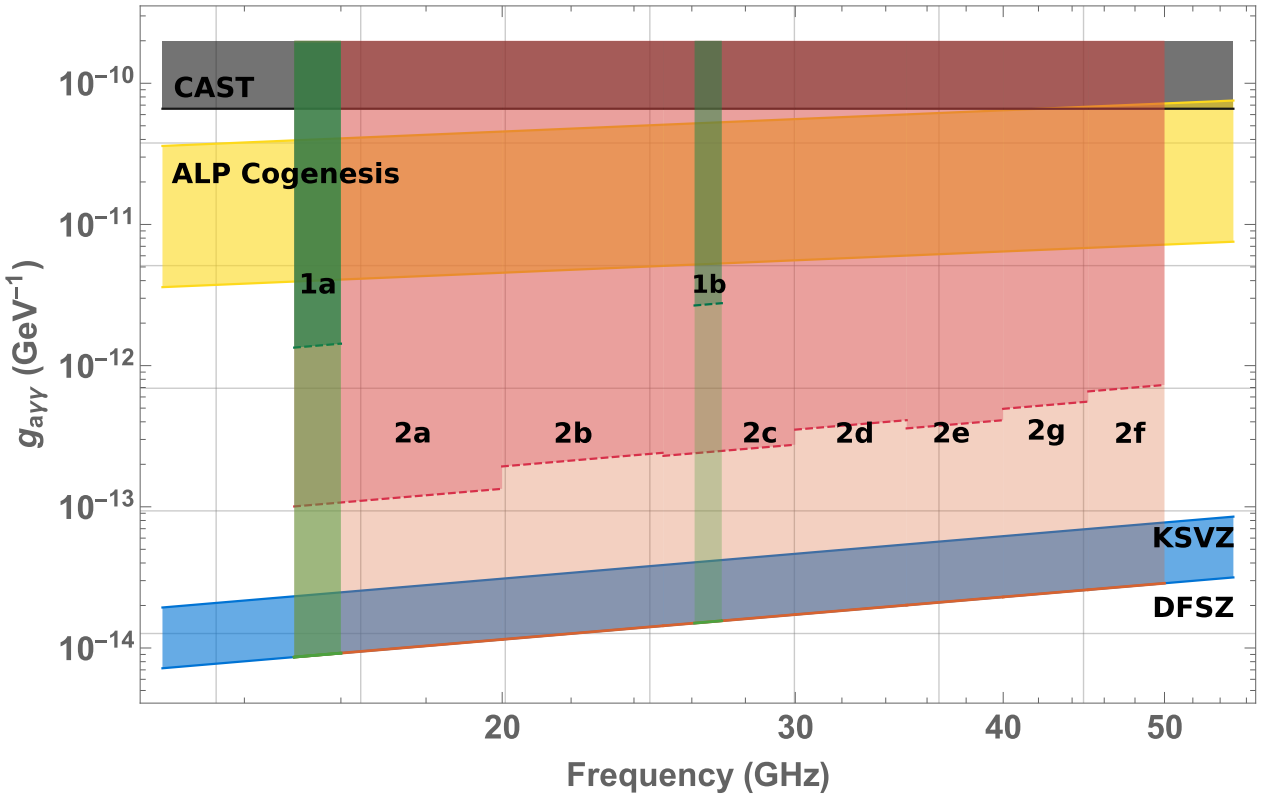

# ORGAN: Run Plans

Phase 1:
Standard TM010 Tuning
Rod Resonators

Phase 2:
Novel Dielectric Resonators
Better Amplifiers

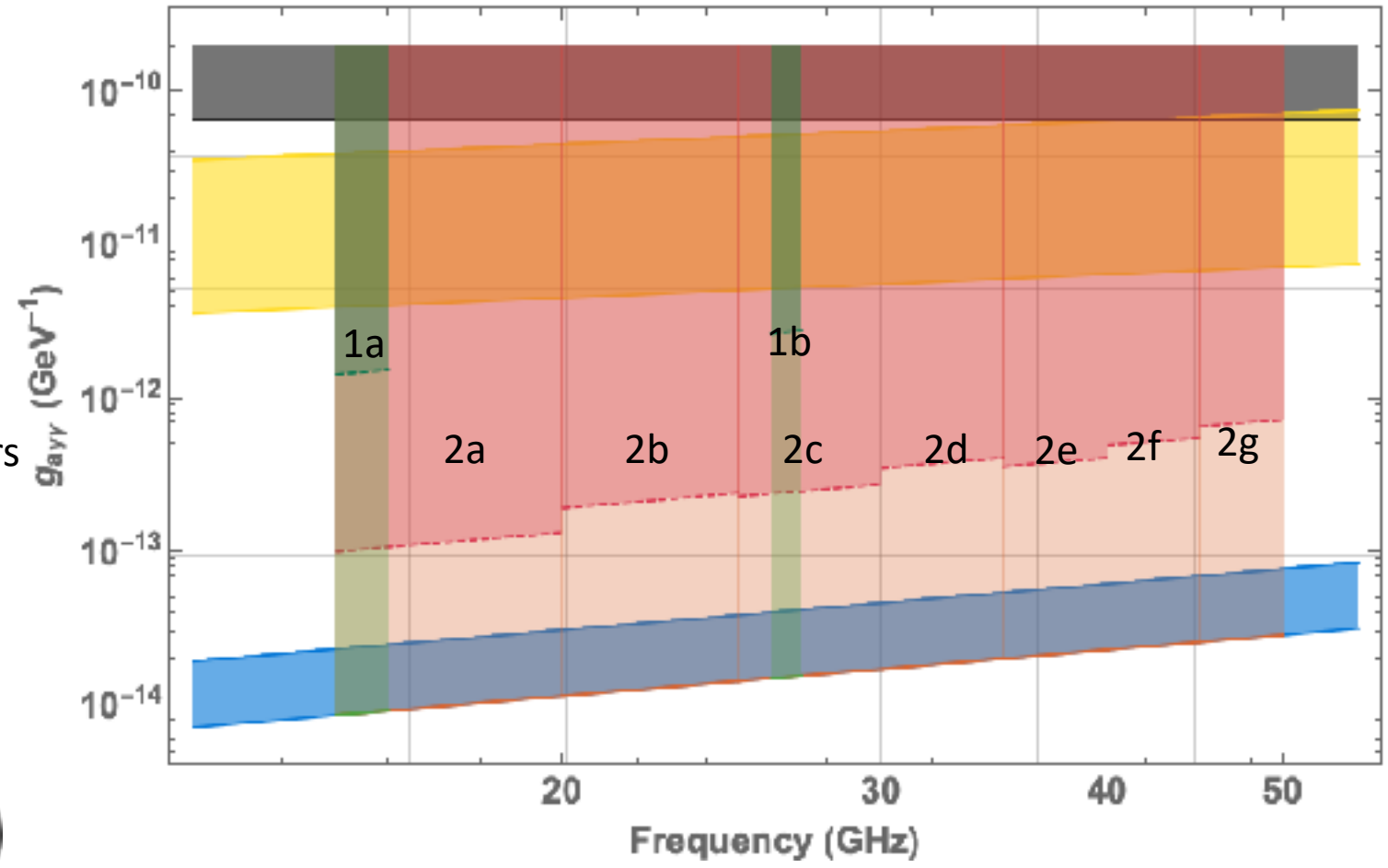


ARC CENTRE OF EXCELLENCE FOR DARK MATTER PARTICLE PHYSICS

# ORGAN: Run Plans

Phase 1:
Standard TM010 Tuning
Rod Resonators

Phase 2:
Novel Dielectric Resonators
Better Amplifiers

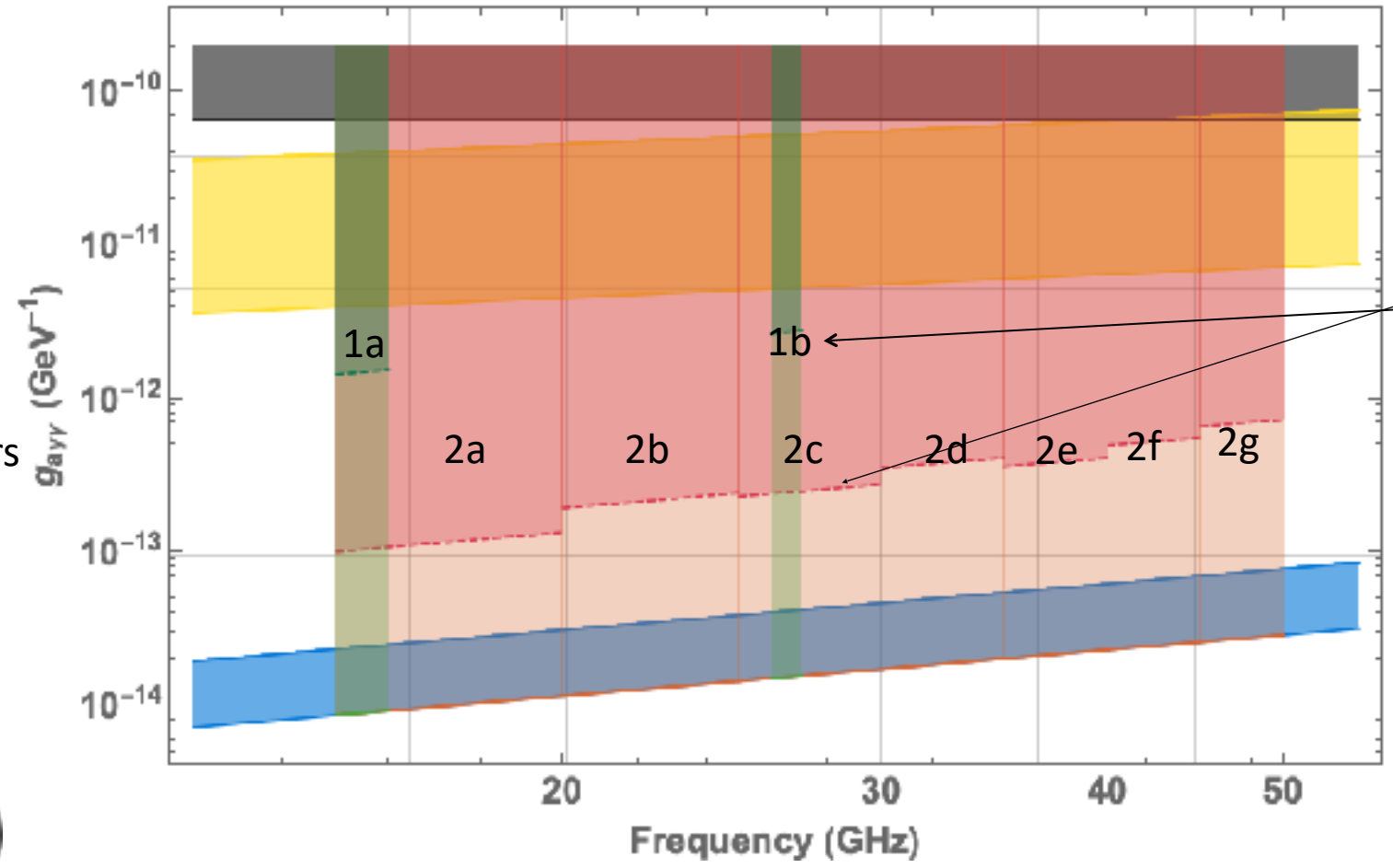


Less optimistic:
HEMT or
SQL Linear Amplifiers

ARC CENTRE OF EXCELLENCE FOR DARK MATTER PARTICLE PHYSICS

# ORGAN: Run Plans

Phase 1:
Standard TM010 Tuning
Rod Resonators

Phase 2:
Novel Dielectric Resonators
Better Amplifiers

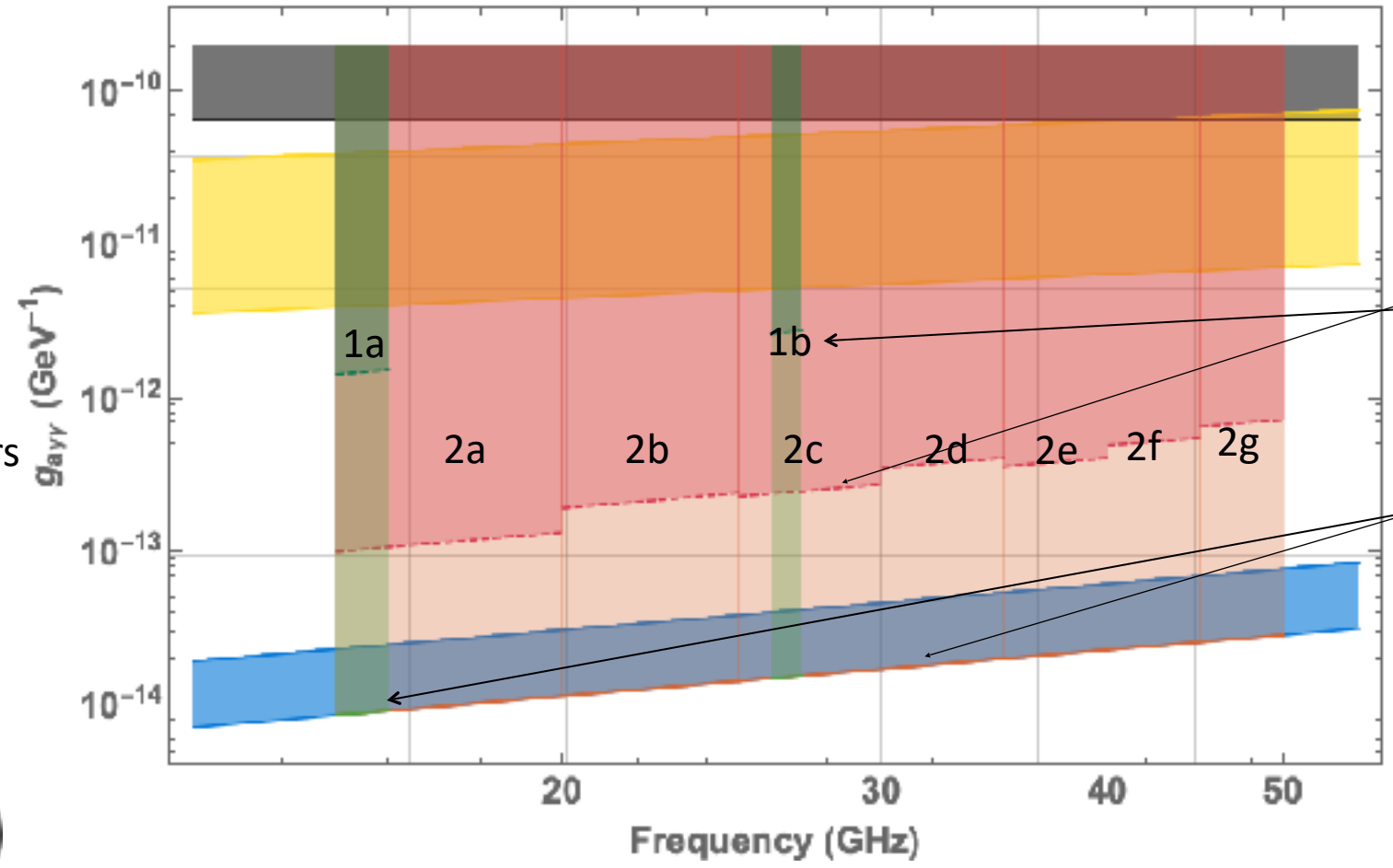


Less optimistic:
HEMT or
SQL Linear Amplifiers

More optimistic:
Efficient GHz SPC

ARC CENTRE OF EXCELLENCE FOR DARK MATTER PARTICLE PHYSICS

# ORGAN: Run Plans

- Planned runs in coming years

Phase 1a underway

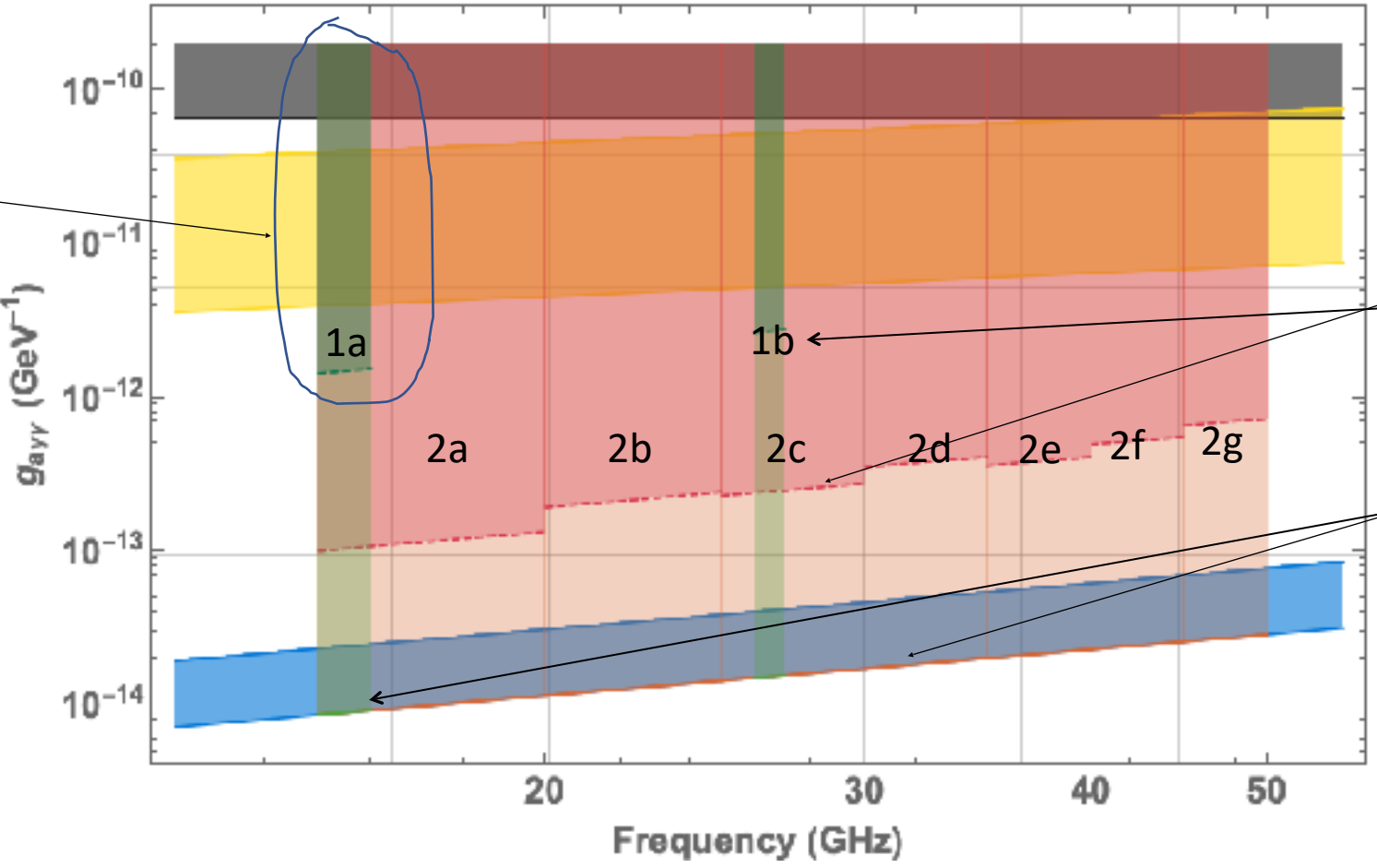


Less optimistic:
HEMT or
SQL Linear Amplifiers

More optimistic:
Efficient GHz SPC

ARC CENTRE OF EXCELLENCE FOR DARK MATTER PARTICLE PHYSICS

# Phase 1a: Taking Data Now!

- Targeting 15.3-16.5 GHz at $\sim 3 \times 10^{-12} g_{a\gamma\gamma}$ (ALP co-genesis)
- $TM_{010}$ mode with single tuning rod~15 – 16 GHz
- HEMT Amplifier
- Just fits inside 57mm diameter magnet bore
- scan rate $\propto \omega^{-14/3}$ isn't the only thing making high frequency searches difficult
- $\omega \propto R^{-1}$ and $V \propto R^{3}$
- Small cavities = Small machining tolerances







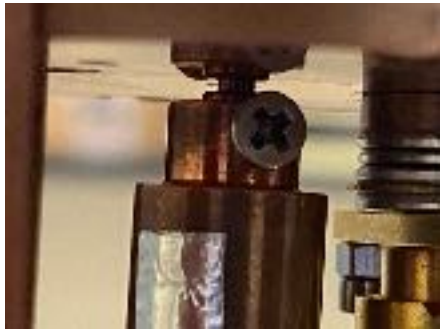

# Experimental Setup

- We've scanned for ~ 2.5 weeks so far (~600MHz)
- Use an IQ mixer and hybrid coupler for image rejection of the other sideband

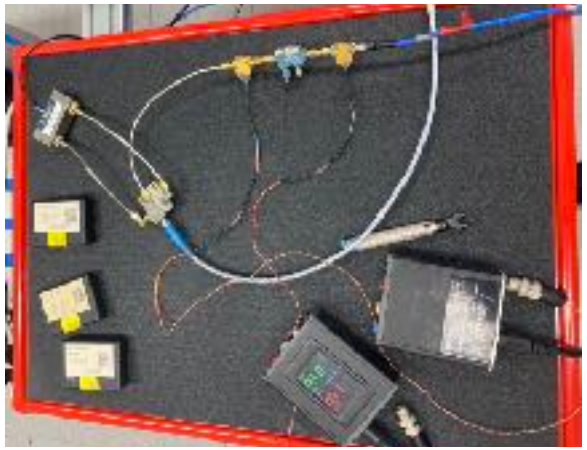





4 channel 250 MS/s
14-Bit Digitizer
Kintex-7 410T FPGA

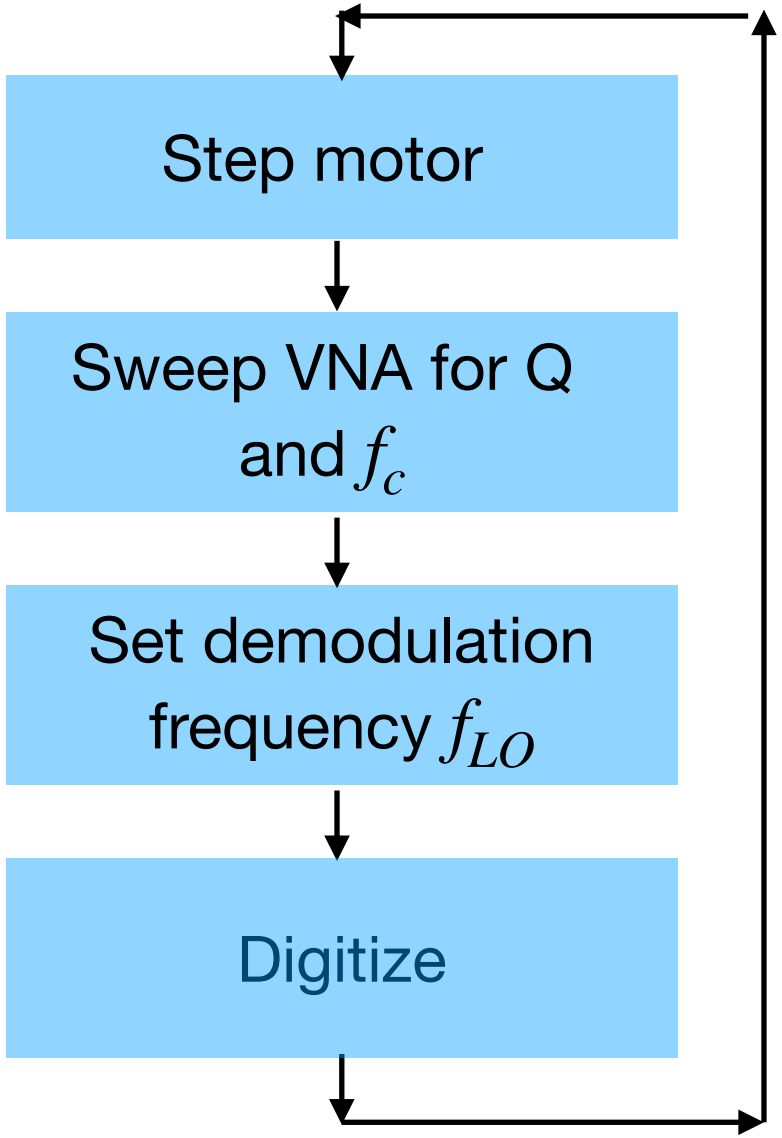


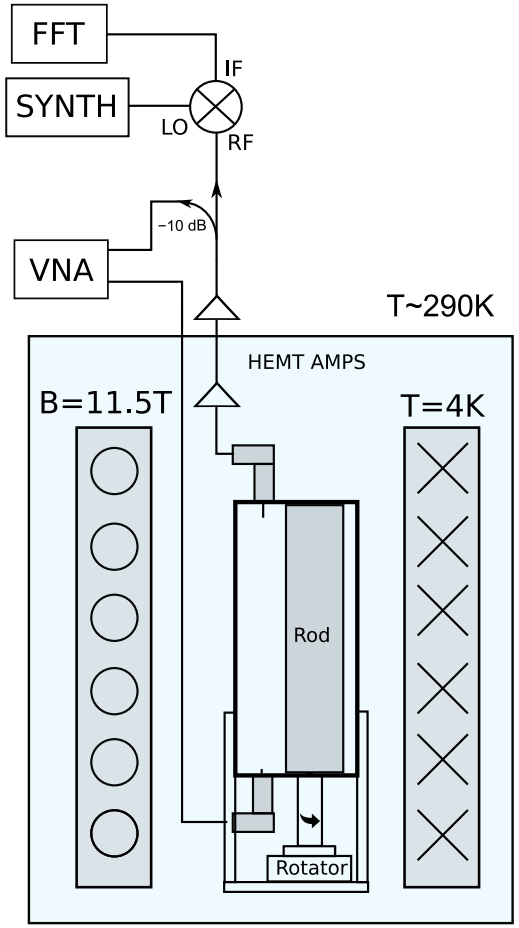

# Data Taking

- Digitizer programmed by Paul Altin (ANU)
- ~12.5 MHz, 26214 pt FFT window, cavity thermal noise
- IF bandwidth gets cropped to ~6MHz
- IF spectrum is free from contamination (45.1MHz centre)

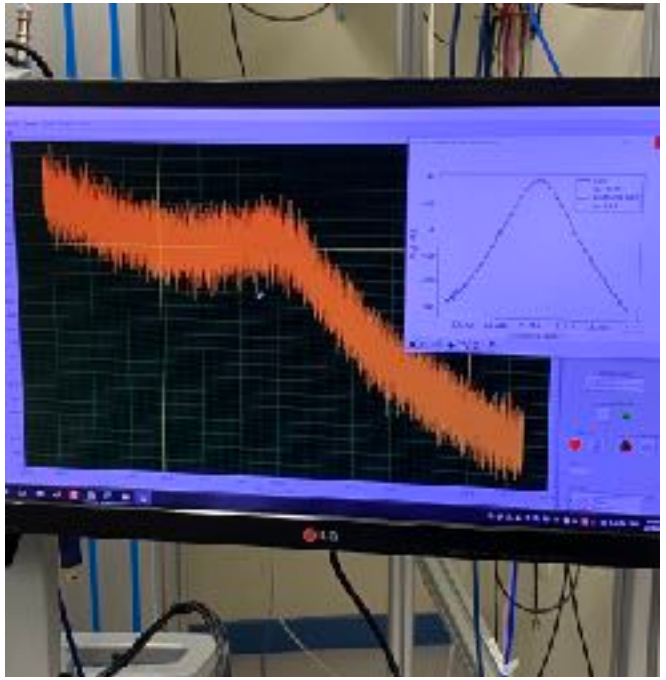

- Co-add overlapping single bins in quadrature (ML weights)
- $\Delta\nu_a \approx 32\Delta\nu_{bin}$
- Combine bins horizontally (still to come)

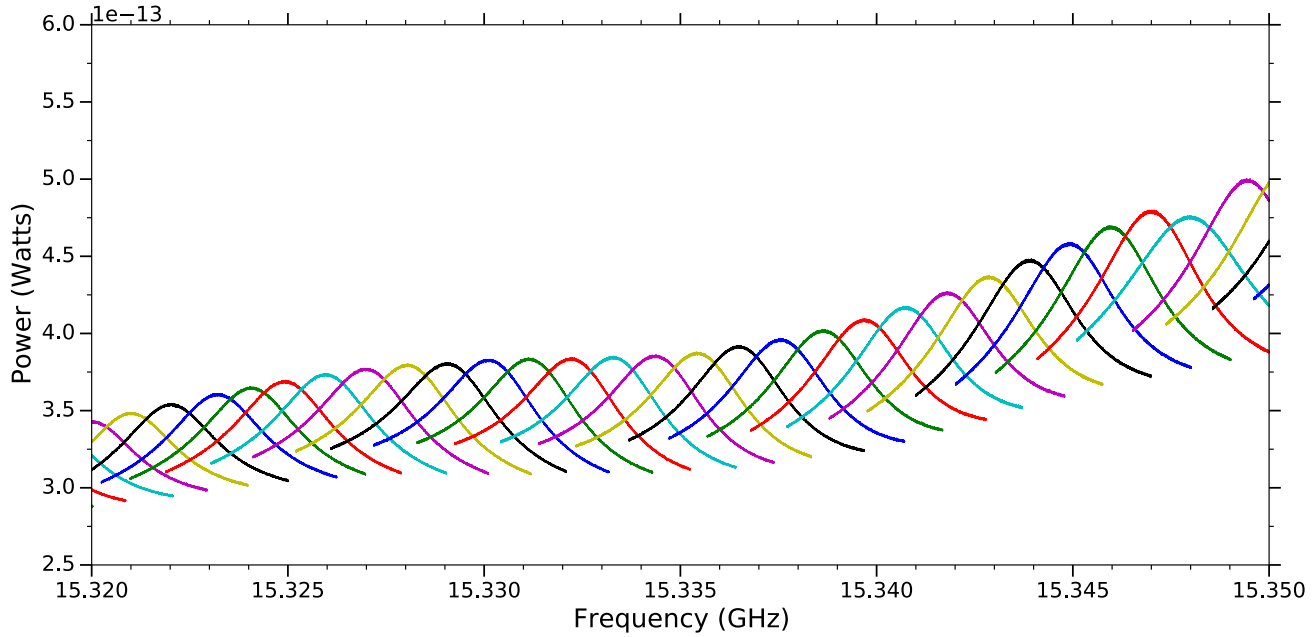

# Combined Single Bins

- Combined in quadrature
- Gaussian as one might expect
- No spurious RF noise sources detected so far

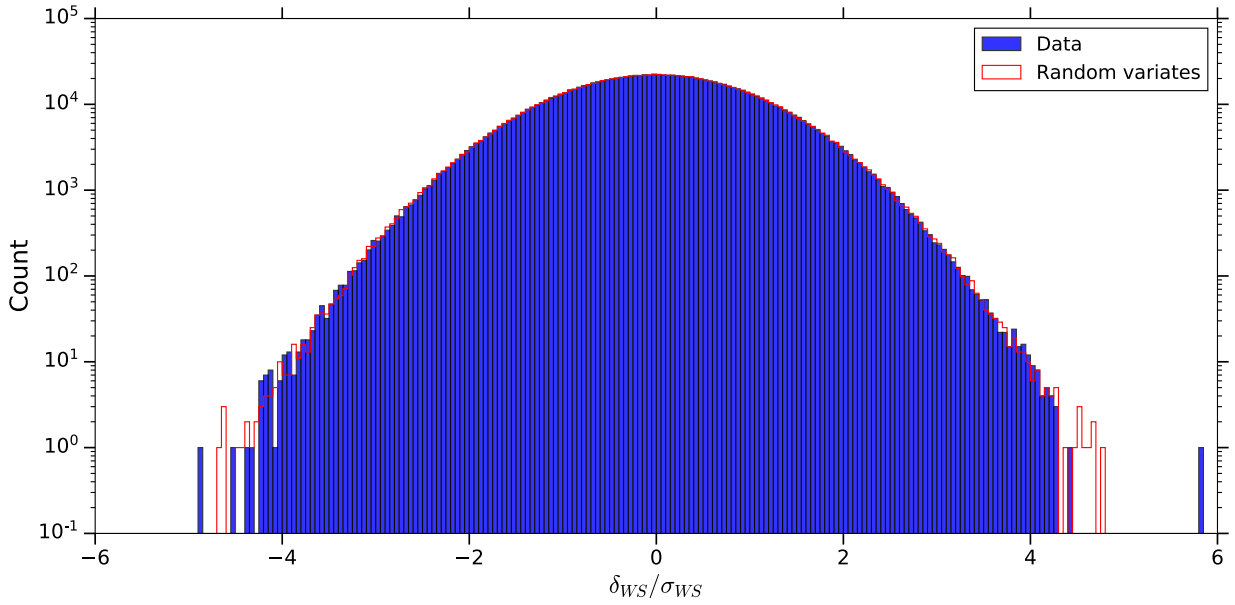


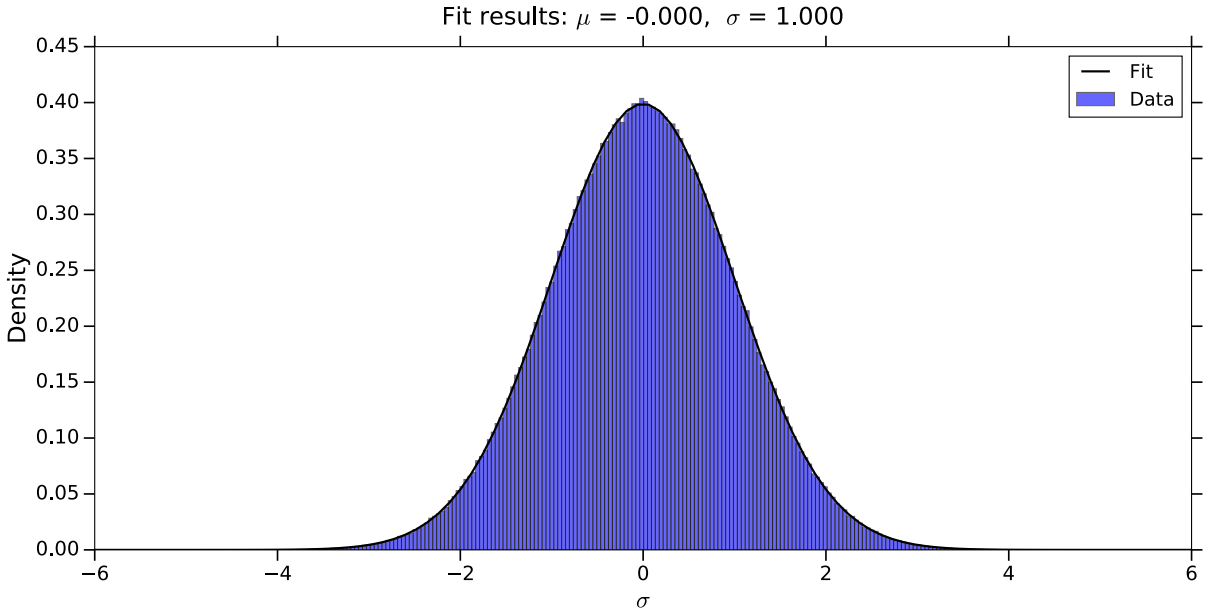

# ORGAN: Phase 1a

- On track for most sensitive limits in the region

# ORGAN: Phase 1a

- On track for most sensitive limits in the region

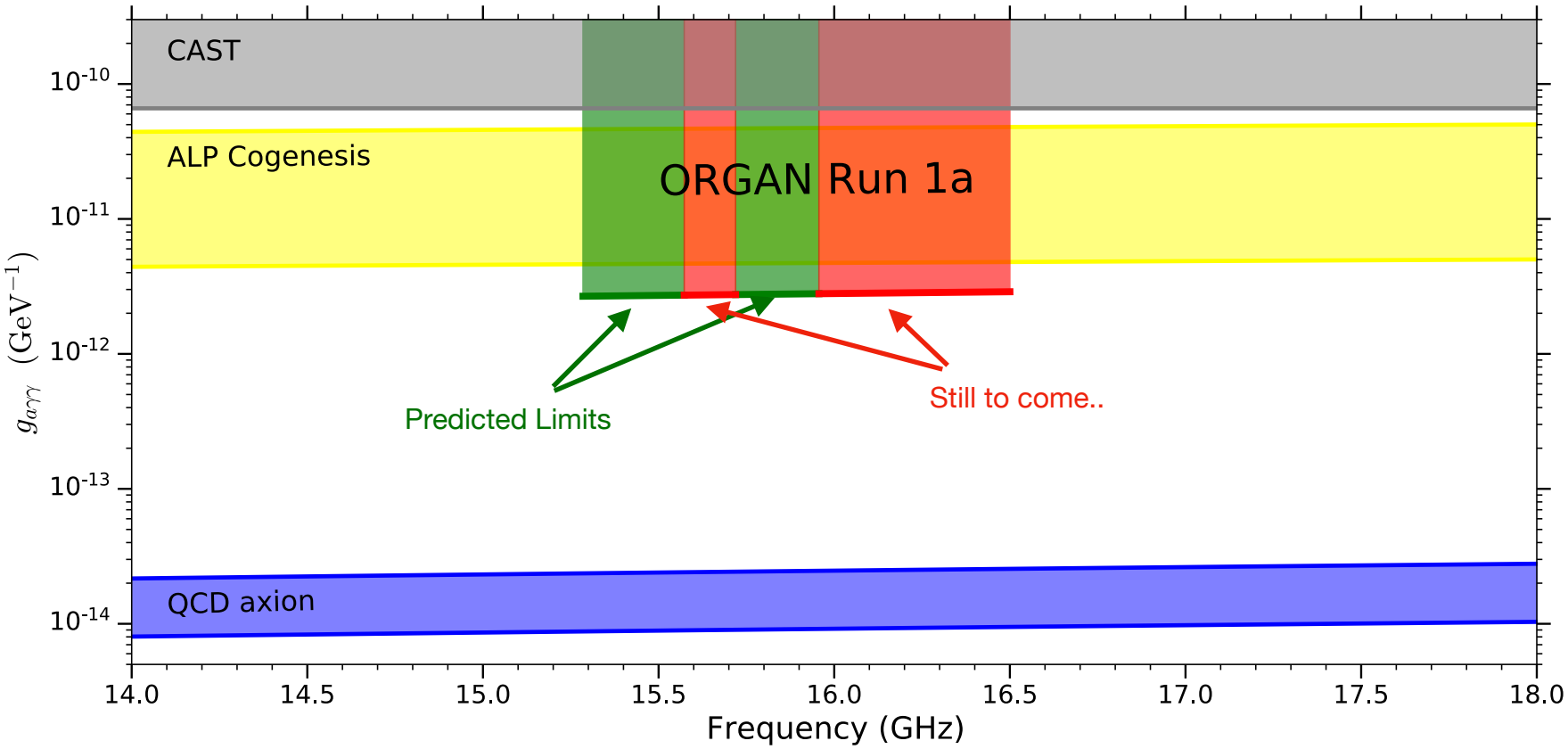

# ORGAN: Phase 1a

- On track for most sensitive limits in the region
- Green - data taken, limits based on preliminary analysis
- Red - cavity in fridge now

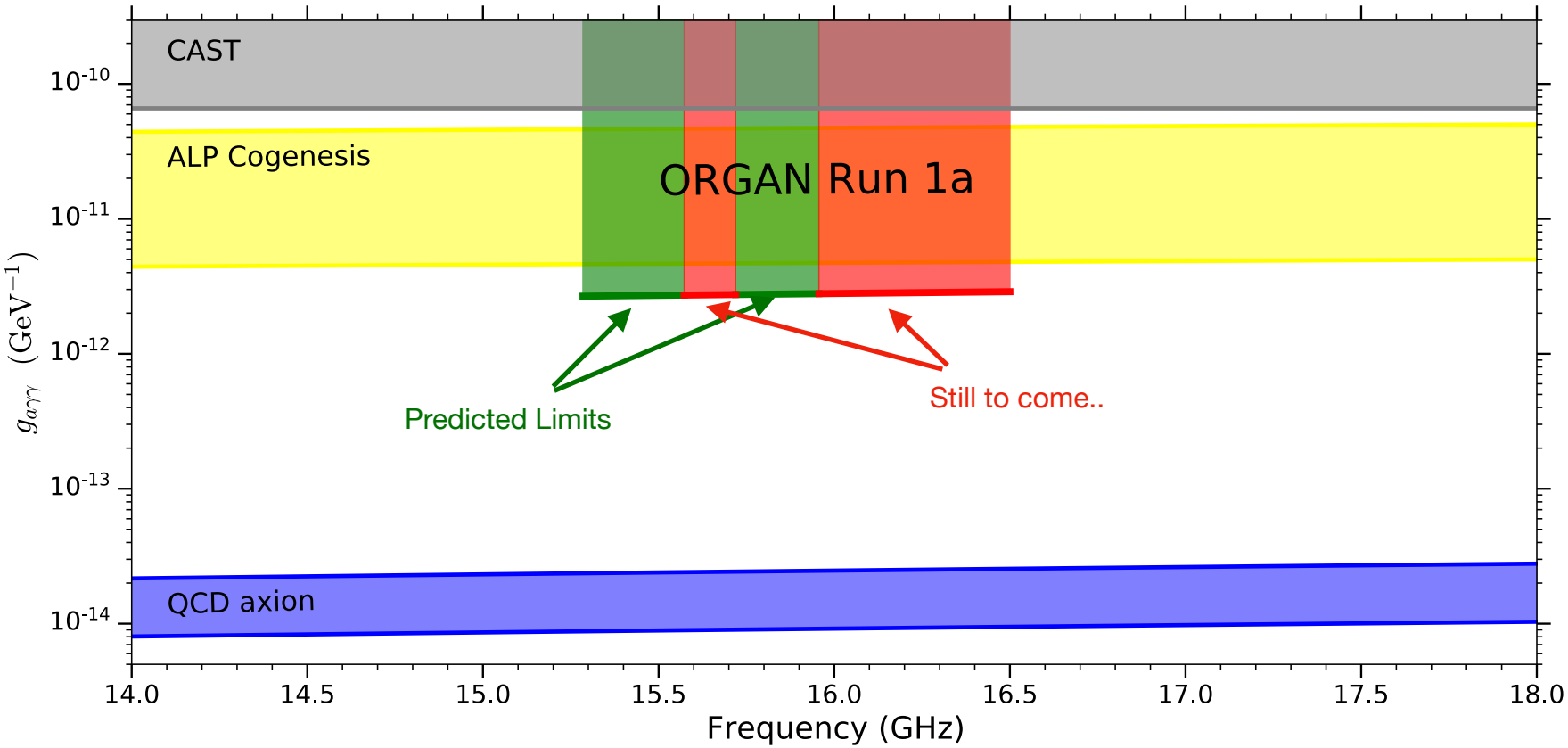


- Predicted limits using $Q_{ave} = 4000$, $T_{sys} = 10K$, $B_0 = 11.5T$

# Preliminary results from The ORGAN Experiment

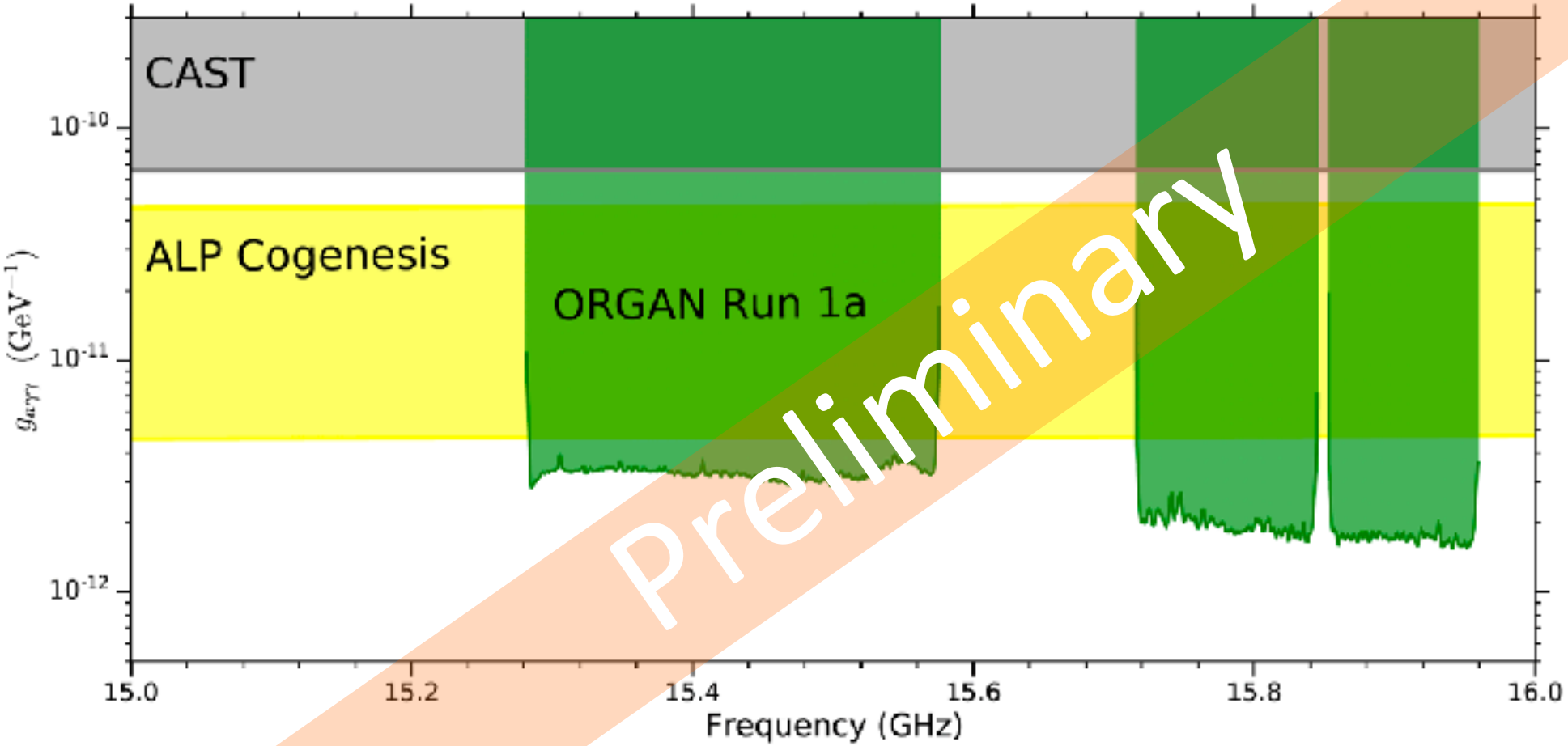

# ORGAN: Phase 1b

- Expected to commence late 2021
- Currently prototyping dielectric wedge resonator

# ORGAN: Phase 1b

- Expected to commence late 2021
- Currently prototyping dielectric wedge resonator




ARC CENTRE OF EXCELLENCE FOR DARK MATTER PARTICLE PHYSICS

# ORGAN: Phase 2

- Commencing 2022+
- Broken into 5 GHz chunks

# ORGAN: Phase 2

- Commencing 2022+
- Broken into 5 GHz chunks
- Ideally employ SPCs
- Multiple cavity arrays

# ORGAN: Phase 2

- Commencing 2022+
- Broken into 5 GHz chunks
- Ideally employ SPCs
- Multiple cavity arrays

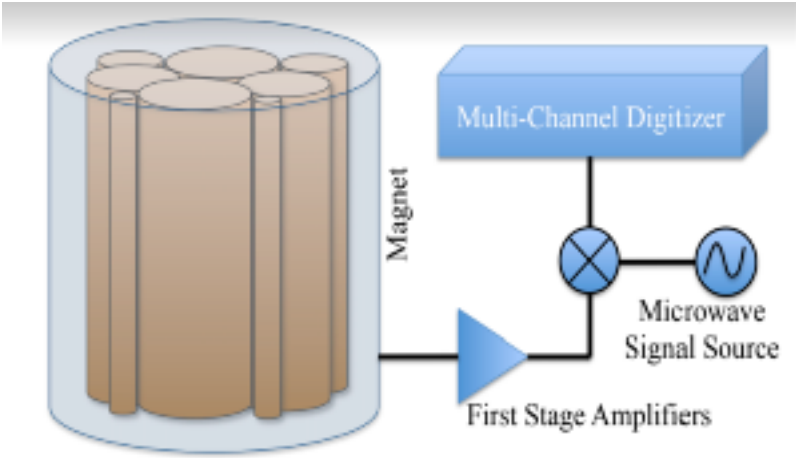




ARC CENTRE OF EXCELLENCE FOR DARK MATTER PARTICLE PHYSICS

# ORGAN Summary of Status (Coming up next UPLOAD)

- ORGAN
  - High mass axion haloscope (15+ GHz)
- Run Plans
  - Phase 1a commenced 2021
  - Limits coming soon
- Two phases
  - Short, targeted scans with existing equipment
  - Longer, broader scans with new technology
- Quantum Sensors
  - Testing a few SPC concepts for integration
  - Will be employed (if successful) during Phase 2
  - Possibility to quickly re-scan Phase 1a region

ARC CENTRE OF EXCELLENCE FOR DARK MATTER PARTICLE PHYSICS

QDm Quantum Technologies and Dark Matter Research Lab

EQUS Australian Research Council Centre of Excellence for Engineered Quantum Systems

# UPLOAD

## UPconversion Low-Noise Oscillator Axion Detection Experiment





Catriona Thomson

UWA PERTH · AUSTRALIA

# A New Technique THE AC HALOSCOPE

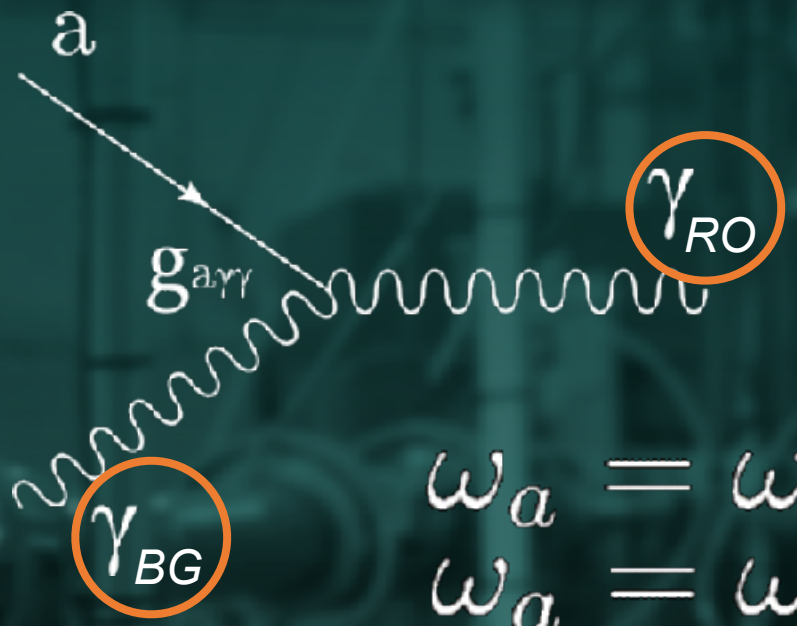


- **Two** electromagnetic modes
- **No** applied DC magnetic field
- One AC mode supplies background field (BG)
- The other is the readout mode (RO)

$$\omega_a = \omega_2 + \omega_1 \text{, axion downconversion}$$
$$\omega_a = \omega_2 - \omega_1 \text{, axion upconversion}$$

- **Up Conversion Low-Noise Oscillator Axion Detection : UPLOAD**

$$\omega_a = |\omega_1 - \omega_2| \pm \Omega \quad \textbf{where} \quad \Omega << \omega_1$$

- 1) Excite BG and RO mode to search RO Frequency Shift (Frequency technique)
- 2) Excite BG mode to search Power at RO mode frequency (Power technique)

# Sapphire Low Noise Oscillators under Development at UWA: World's best!



Cryogenic Version Under development < -180 dBc/Hz.

IEEE MICROWAVE AND WIRELESS COMPONENTS LETTERS, VOL. 31, NO. 4, APRIL 2021

## Noise Suppression With Cryogenic Resonators

Eugene N. Ivanov and Michael E. Tobar, *Fellow, IEEE*





$$Q_L = 10^9$$

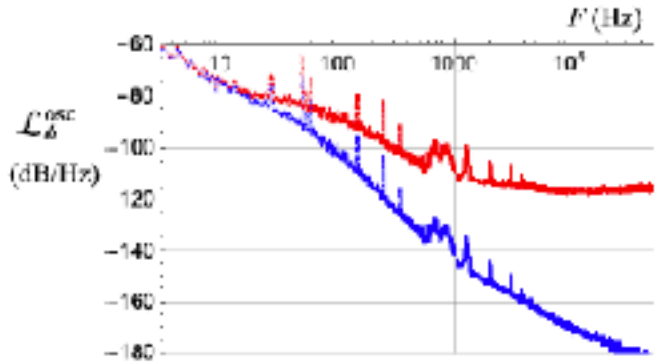


Fig. 7. SSB phase noise spectra of the E8257D at 11.2 GHz: top trace is the measured phase noise of the incident signal; bottom trace is the inferred phase noise of the transmitted signal.

IEEE TRANSACTIONS ON ULTRASONICS, FERROELECTRICS, AND FREQUENCY CONTROL, VOL. 58, NO. 2, FEBRUARY 2011 253

## Low Phase-Noise Sapphire Crystal Microwave Oscillators: Current Status

Eugene N. Ivanov and Michael E. Tobar, *Senior Member, IEEE*

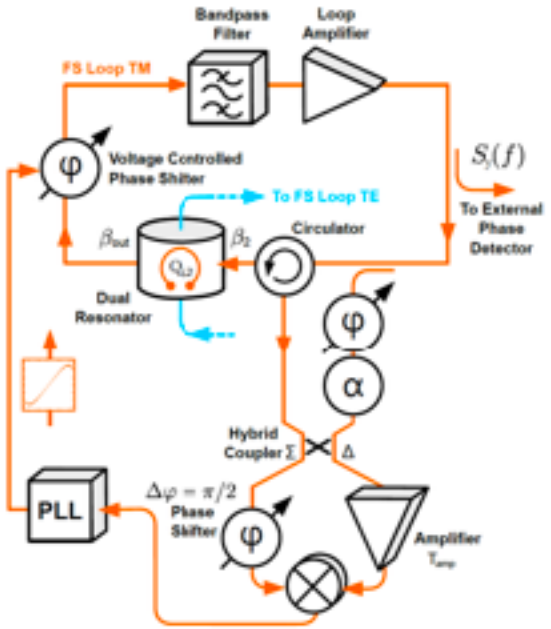


FIG. 5: Schematic of a frequency stabilized (FS) feedback oscillator with interferometric signal processing.

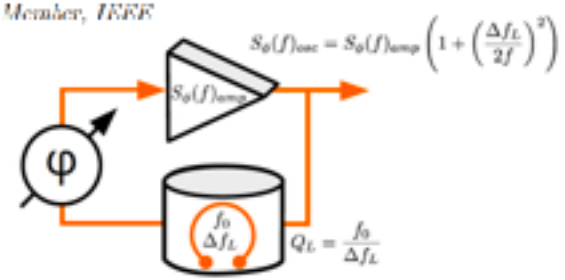


FIG. 4: Schematic of a simple feedback oscillator, with resonator loaded Q-factor $Q_L$, and amplifier phase noise of $S_\phi(f)_{amp}$. Shown is the simple relation to the oscillator phase noise, $S_\phi(f)_{osc}$.

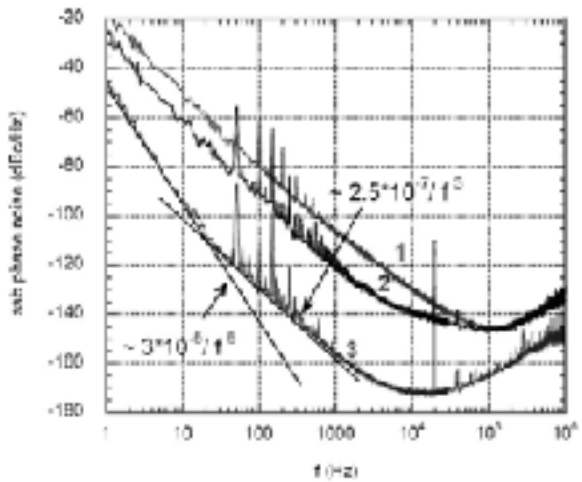


E. N. Ivanov and M. E. Tobar, "Noise Suppression with Cryogenic Resonators," in

CA Thomson, BT McAllister, M Goryachev, EN Ivanov, ME Tobar, "Upconversion Loop Oscillator Axion Detection Experiment: A Precision Frequency Interferometric Axion Dark Matter Search with a Cylindrical Microwave Cavity," Phys. Rev. Lett., vol. 126, 081803, 2021.

arXiv.org > physics > arXiv:2102.11065

Search...

Help | Advanced

Physics > Instrumentation and Detectors

[submitted on 19 Feb 2021]

# Low Noise Microwaves for Testing Fundamental Physics

Eugene Ivanov, Michael Tobar

We studied noise properties of microwave signals transmitted through the cryogenic resonator. The experiments were performed with the 11.342 GHz sapphire loaded cavity resonator cooled to 6.2 K. Based on the measured transmission coefficient of the cryogenic resonator we computed its noise suppression function. This was done via Monte-Carlo simulations some details of which are discussed in this letter. Next, we measured technical fluctuations of a signal incident on the cryogenic resonator. Having processed these data with the previously computed noise filtering "template" we inferred noise spectra of the transmitted signal. We found that spectral densities of both phase and amplitude fluctuations of the transmitted signal were close to the thermal noise limit of −180 dB/Hz at Fourier frequencies $F \geq 10$ kHz. Such thermal noise limited microwaves allow more precise tests of special relativity and could be useful at some stages of quantum signal processing.

Comments: 4 pages
Subjects: Instrumentation and Detectors (physics.ins-det); Applied Physics (physics.app-ph)
ACM classes: J.6
Cite as: arXiv:2102.11065 [physics.ins-det]
(or arXiv:2102.11065v1 [physics.ins-det] for this version)

**In general both low AM and PM noise required**

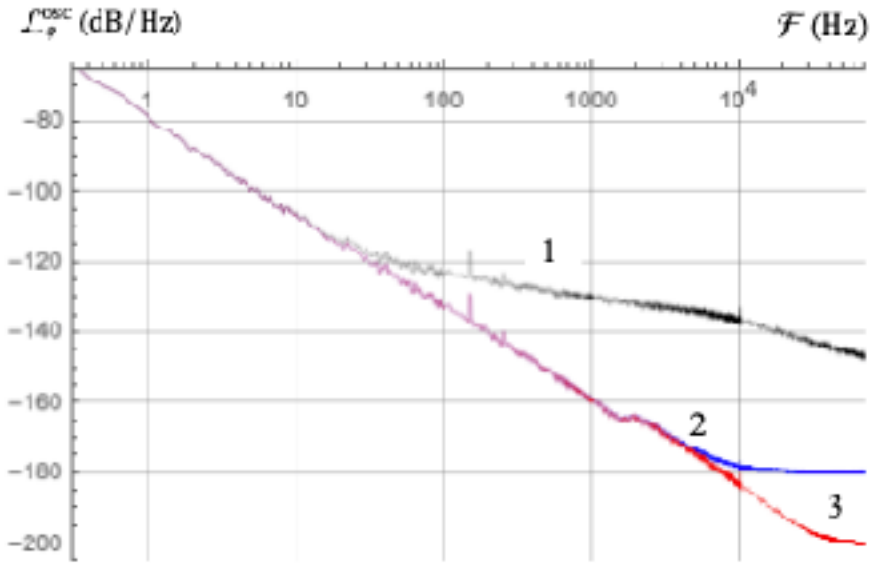


Fig. 5. SSB PM-noise spectra of the 11.343 GHz cryogenic loop oscillator. Trace 1 corresponds to signal incident on resonator. Traces 2 and 3 correspond to the transmitted signals at T = 296 K and 6.2 K respectively.

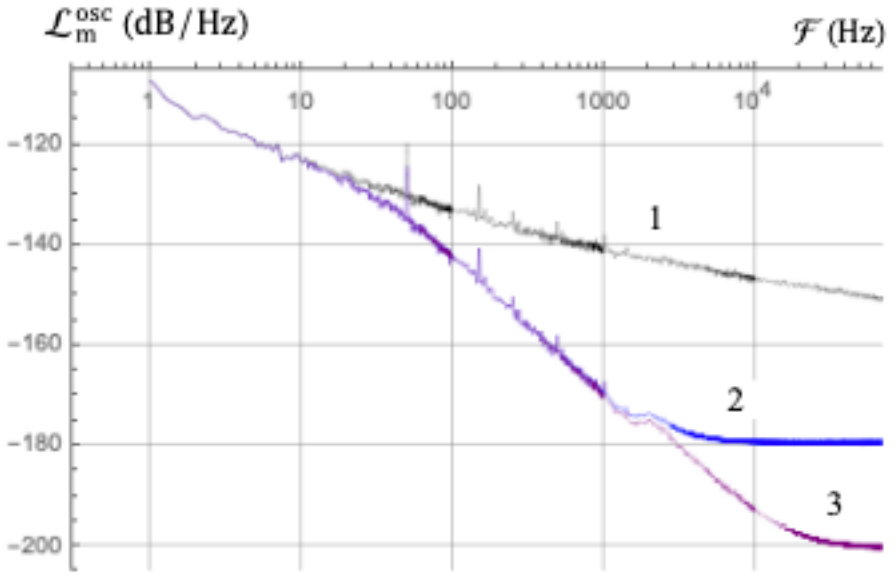


Fig. 6. SSB AM-noise spectra of the 11.343 GHz cryogenic loop oscillator. Trace 1 corresponds to signal incident on resonator. Traces 2 and 3 correspond to transmitted signal at T = 296 K and 6.2 K respectively.

# The World's Lowest Noise Oscillators







# UPLOAD: Previous Work->First Experiment and Theory



PHYSICAL REVIEW LETTERS 126, 081803 (2021)

## Upconversion Loop Oscillator Axion Detection Experiment: A Precision Frequency Interferometric Axion Dark Matter Search with a Cylindrical Microwave Cavity

Catriona A. Thomson, Ben T. McAllister, Maxim Goryachev, Eugene N. Ivanov, and Michael E. Tobar
*ARC Centre of Excellence for Engineered Quantum Systems and ARC Centre of Excellence for Dark Matter Particle Physics, Department of Physics, University of Western Australia, 35 Stirling Highway, Crawley, Western Australia 6009, Australia*



Physics of the Dark Universe 26 (2019) 100345

Contents lists available at ScienceDirect

Physics of the Dark Universe

journal homepage: www.elsevier.com/locate/dark



## Axion detection with precision frequency metrology

Maxim Goryachev, Ben T. McAllister *, Michael E. Tobar
*ARC Centre of Excellence for Engineered Quantum Systems, School of Physics, University of Western Australia, 35 Stirling Highway, Crawley, WA 6009, Australia*

## Corrigendum to "Axion detection with precision frequency metrology" [Phys. Dark Universe 26 (2019) 100345]

Catriona Thomson, Maxim Goryachev, Ben T. McAllister *, Michael E. Tobar
*ARC Centre of Excellence for Engineered Quantum Systems, School of Physics, University of Western Australia, 35 Stirling Highway, Crawley, WA 6009, Australia*

**First Proposed in 2018 arXiv:1806.07141 [physics.ins-det]: Proposal Published in 2019**

We are very grateful to Kevin Zhou for meticulously going through our paper and finding our mistake and for reading this correction to make sure of its validity. This work was funded by the ARC Centre of Excellence for Engineered Quantum Systems, CE170100009, and Dark Matter Particle Physics, CE200100008.

PHYSICAL REVIEW LETTERS 127, 019901(E) (2021)

## Erratum: Upconversion Loop Oscillator Axion Detection Experiment: A Precision Frequency Interferometric Axion Dark Matter Search with a Cylindrical Microwave Cavity [Phys. Rev. Lett. 126, 081803 (2021)]

Catriona A. Thomson, Ben T. McAllister, Maxim Goryachev, Eugene N. Ivanov, and Michael E. Tobar

(Received 10 May 2021; published 2 July 2021)



**Corrected versions consistent with**
1) **Optical phase experiments,**
2) **AC Microwave Power Techniques and**
3) **Total Derivative = 0**

# UPLOAD: Looking to the future

- 1) Phase 2 Room Temperature Experiment Underway (Preliminary results shown in this talk)
  - Frequency Stabilised Sources: 7-5 Orders of magnitude improvement in Phase noise
  - Under Vacuum: Eliminate frequency drift over measurement time: Increase sensitivity by order of magnitude
  - Noise measurements and characterisation completed, Conservative estimate ~ 6 orders of improvement
  - Discussion on trying to detect ultra-light axions with frequency and power technique
  - Discussion on Cryogenic UPLOAD

- 2) New Calculations (Not shown in this talk)
  - Frequency Technique: Electromagnetic perturbation analysis -> consistent with prior corrected frequency analysis
  - Power Technique: Poynting Theorem -> consistent with prior calculations (Sikivie, Lasenby, Berlin et al)
  - Comparison of Power and Frequency techniques experimentally and theoretically being undertaken now
  - Determine which technique is best for a) ultra-light axions and b) 1 MHz to 300 MHz mass range

- Axion Electrodynamics: Poynting vector analysis of AC and DC Haloscope (DC on ArXiv)
- Two possible choices (Abraham / Minkowski Controversy) Abraham consistent with prior calculations
  - Frequency Technique: Perturbation analysis with Minkowski Poynting vector -> predicts enhanced sensitivity
  - Power Technique: Poynting Theorem analysis with Minkowski Poynting vector -> predicts enhanced sensitivity

# How to choose mode pair?

$TE_{0,1,1} - TM_{0,2,0}$

## Overlap function

$$C_{01} = \left( \frac{1}{V} \int (\mathbf{e}_1 \cdot c\mathbf{b}_0) dV \right)^2$$

$$\mathbf{e}_1 = \frac{J_0\left(\frac{\chi_{02}}{a} r\right)}{J_1(\chi_{02})} \hat{z}$$

$$\mathbf{b}_0 = \frac{\sqrt{2}\frac{a\pi}{L\chi'_{01}} J_1\left(\frac{\chi'_{01}}{a} r\right) \cos\left(\frac{\pi z}{L}\right)}{\sqrt{1 + \left(\frac{a\pi}{L\chi'_{01}}\right)^2} J_0(\chi'_{01})} \hat{r} - \frac{\sqrt{2} J_0\left(\frac{\chi'_{01}}{a} r\right) \sin\left(\frac{\pi z}{L}\right)}{\sqrt{1 + \left(\frac{a\pi}{L\chi'_{01}}\right)^2} J_0(\chi'_{01})} \hat{z},$$




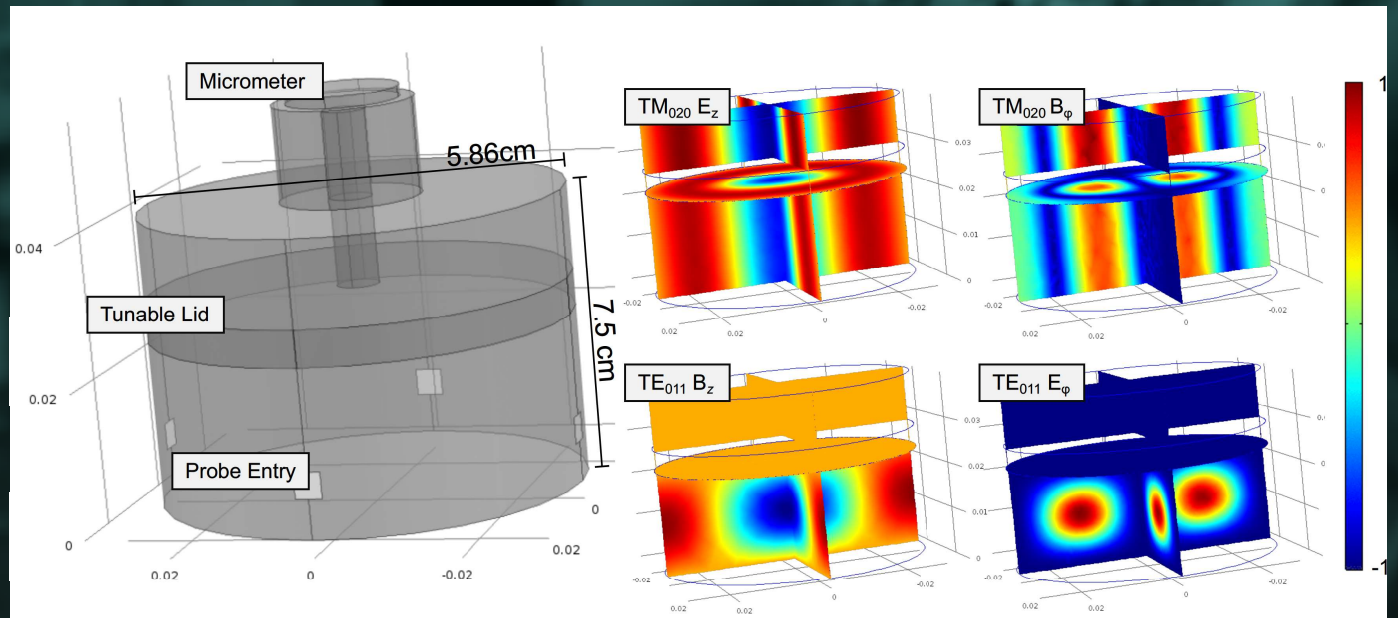

# SENSITIVE TUNED MODE PAIRS

$m_1 = m_2$

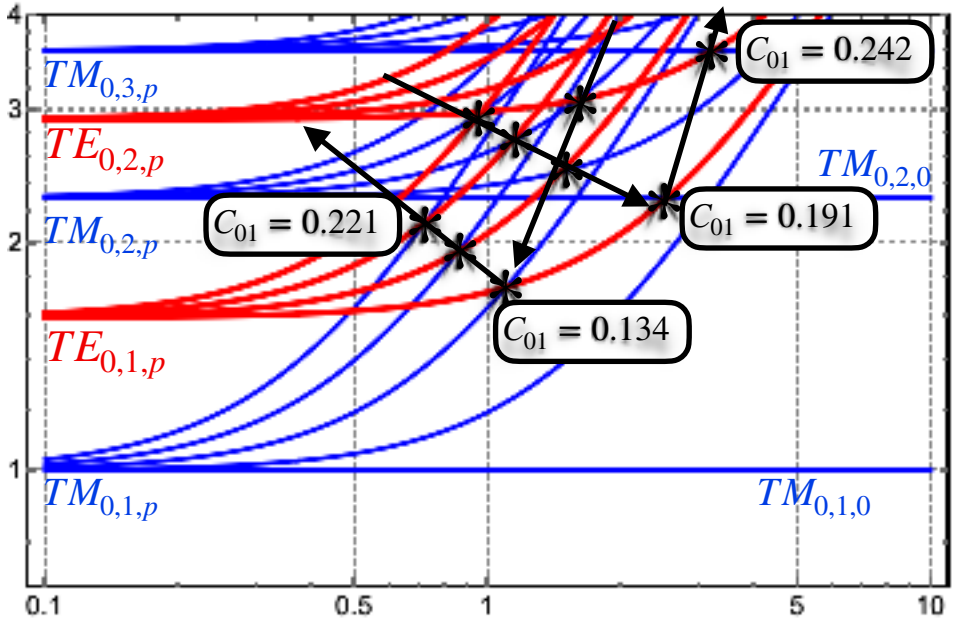


$AR = \frac{2a}{L}$

$\frac{f_{mode}}{f_{TM_{0,1,0}}}$

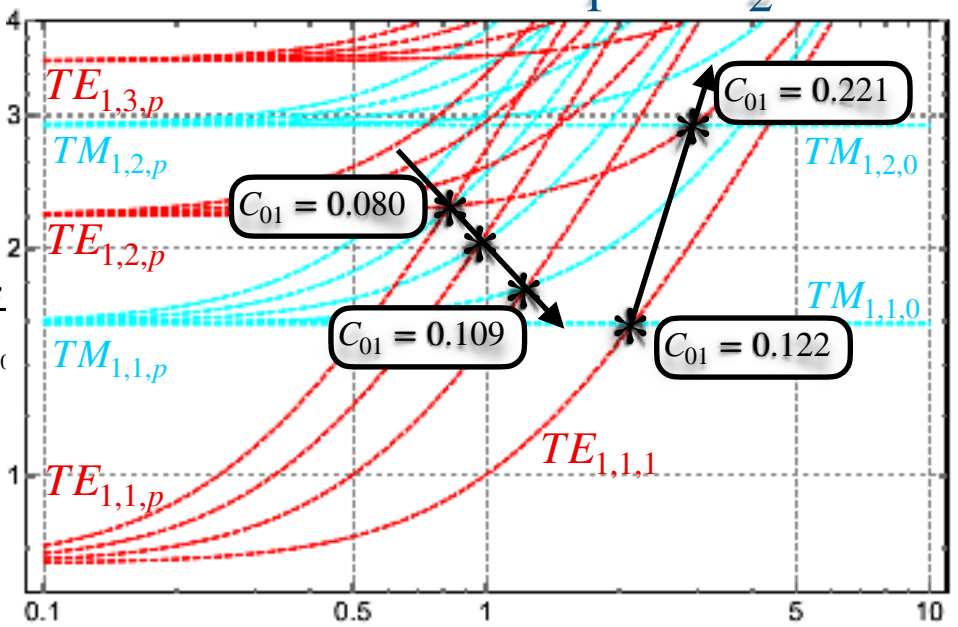


$AR = \frac{2a}{L}$

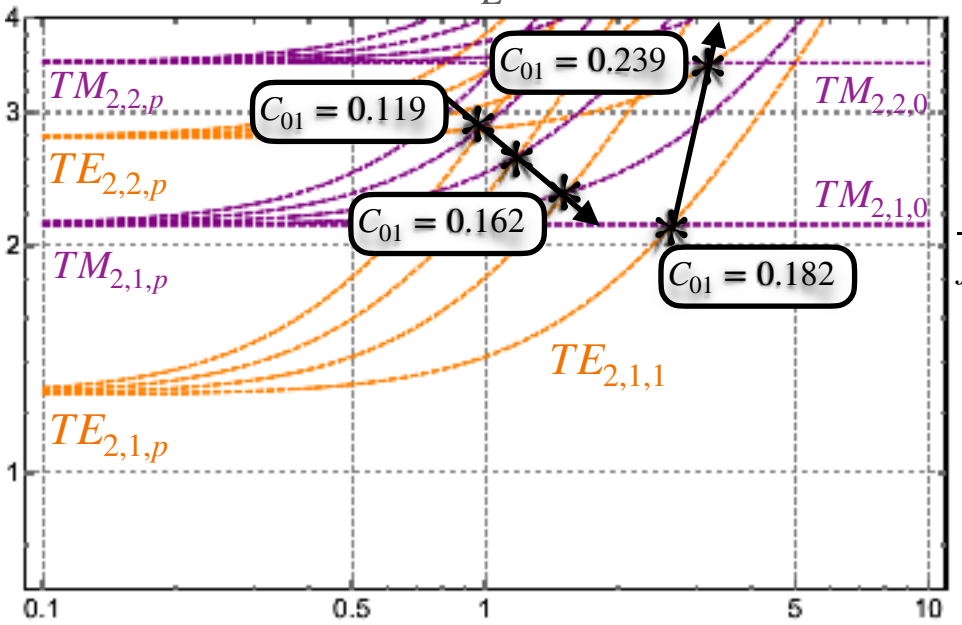


$\frac{f_{mode}}{f_{TM_{0,1,0}}}$

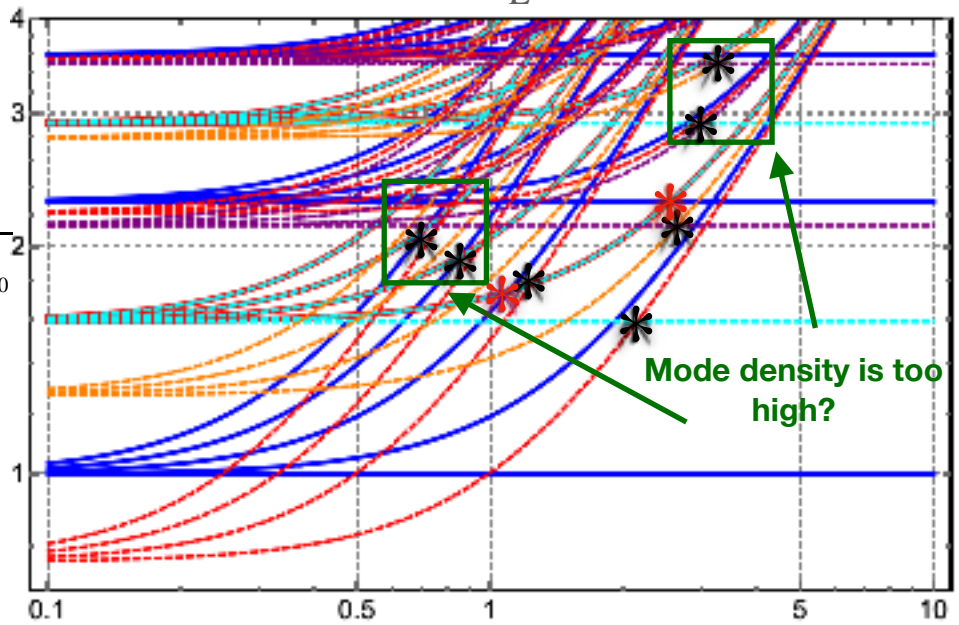


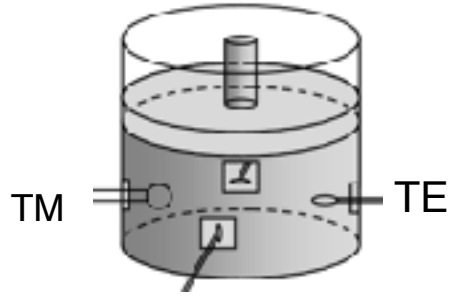


Possible Mode Pairs

when $f_0 = f_1$

$TE_{0,1,1} - TM_{0,2,0}$

$C_{01} = 0.191$

$TE_{0,1,1} - TM_{0,1,2}$

$C_{01} = 0.134$

$TE_{1,1,1} - TM_{1,1,0}$

$C_{01} = 0.122$

$TE_{1,1,2} - TM_{1,1,1}$

$C_{01} = 0.109$

$TE_{2,1,1} - TM_{2,1,0}$

$C_{01} = 0.182$

$m \neq 0$ Maybe too complicated experimentally

# The Axion Limits

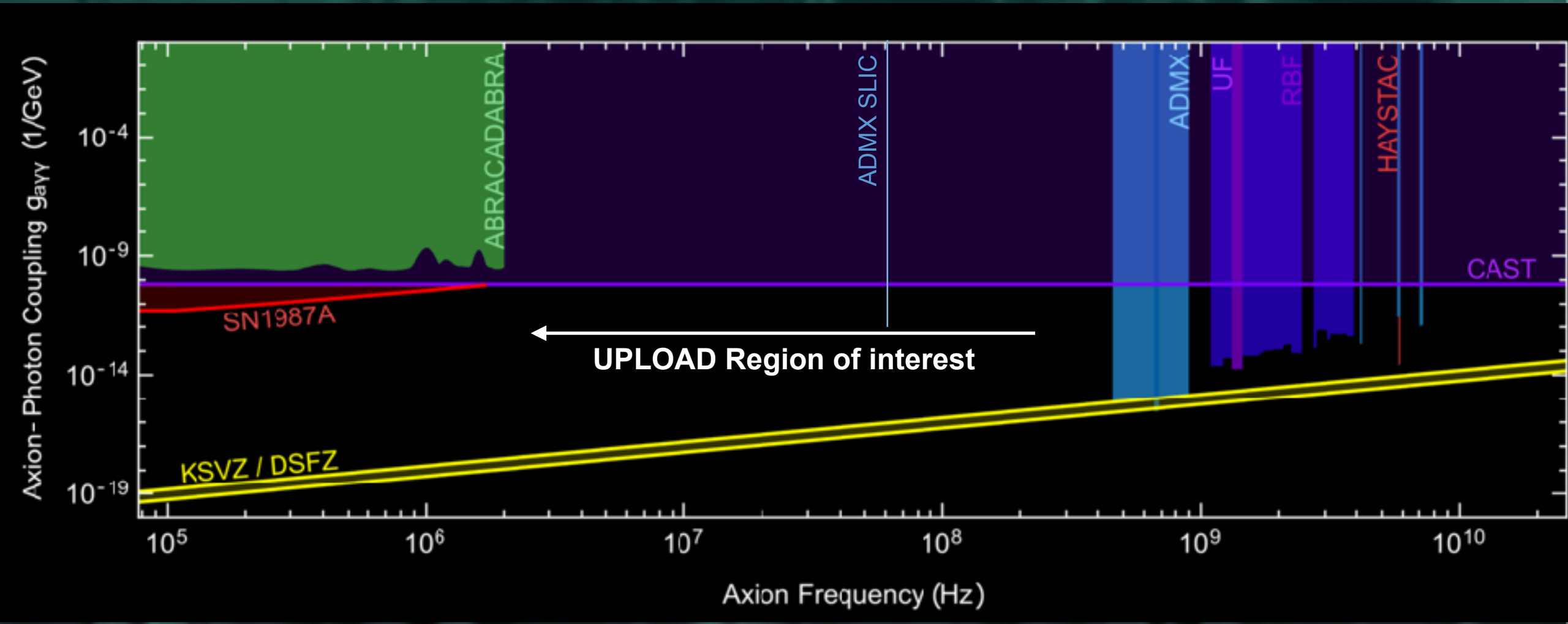

# Recap Phase 1 UPLOAD: UPCONVERSION LOOP OSCILLATOR AXION DETECTION





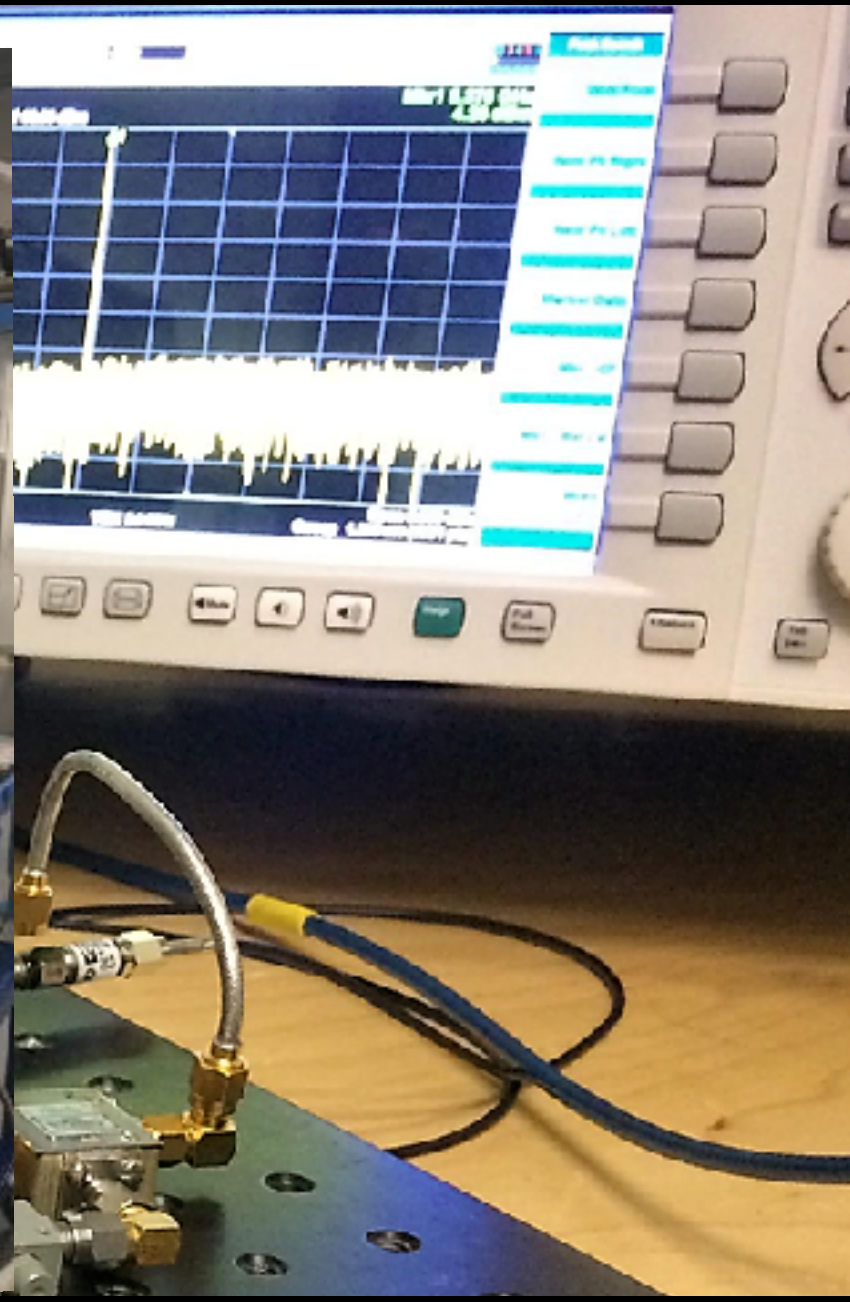

# Experimental Design

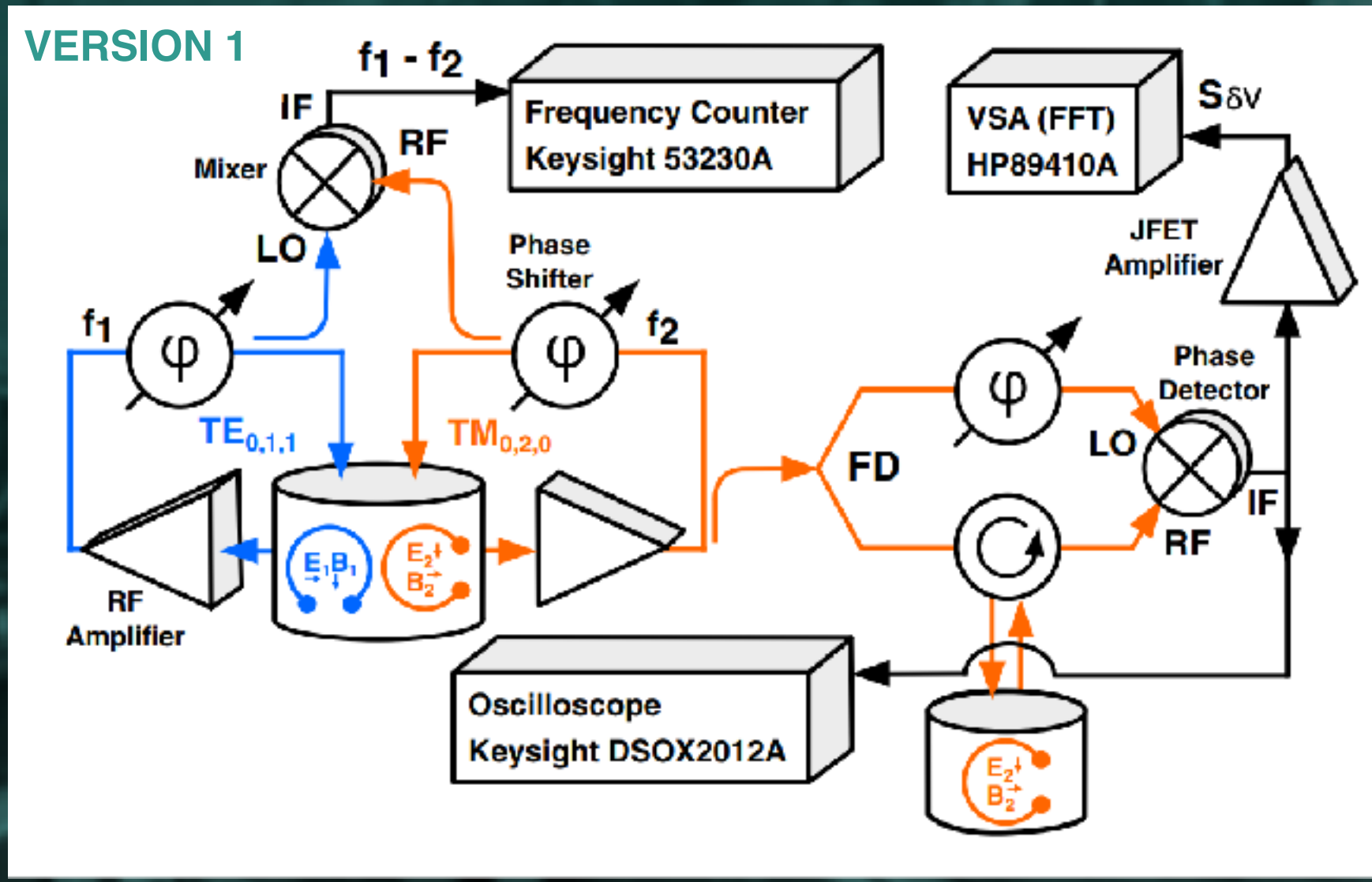


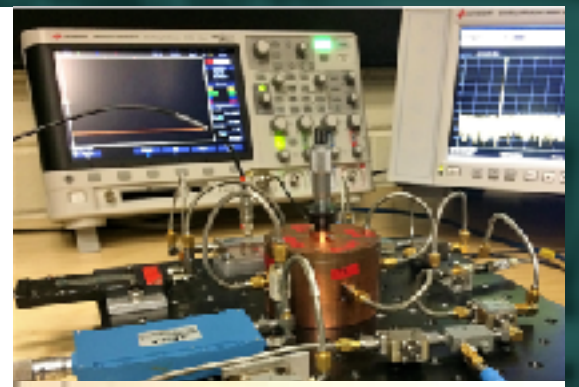

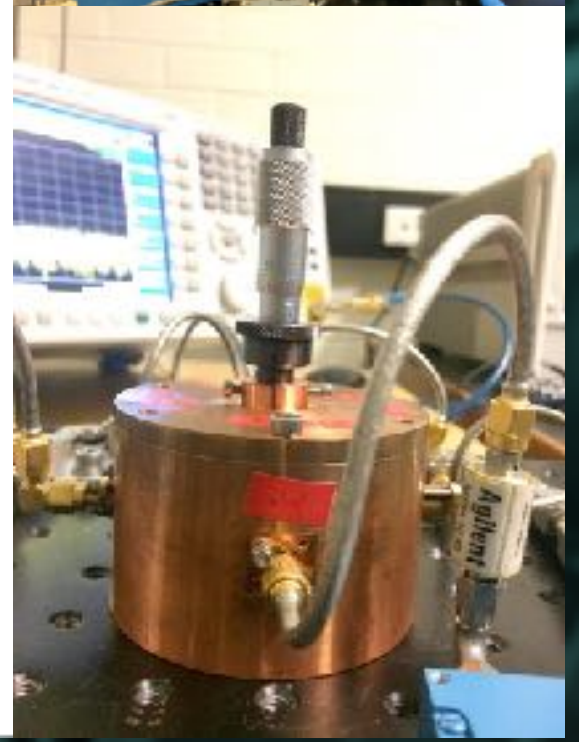

# Results IDENTIFYING AN AXION SIGNAL

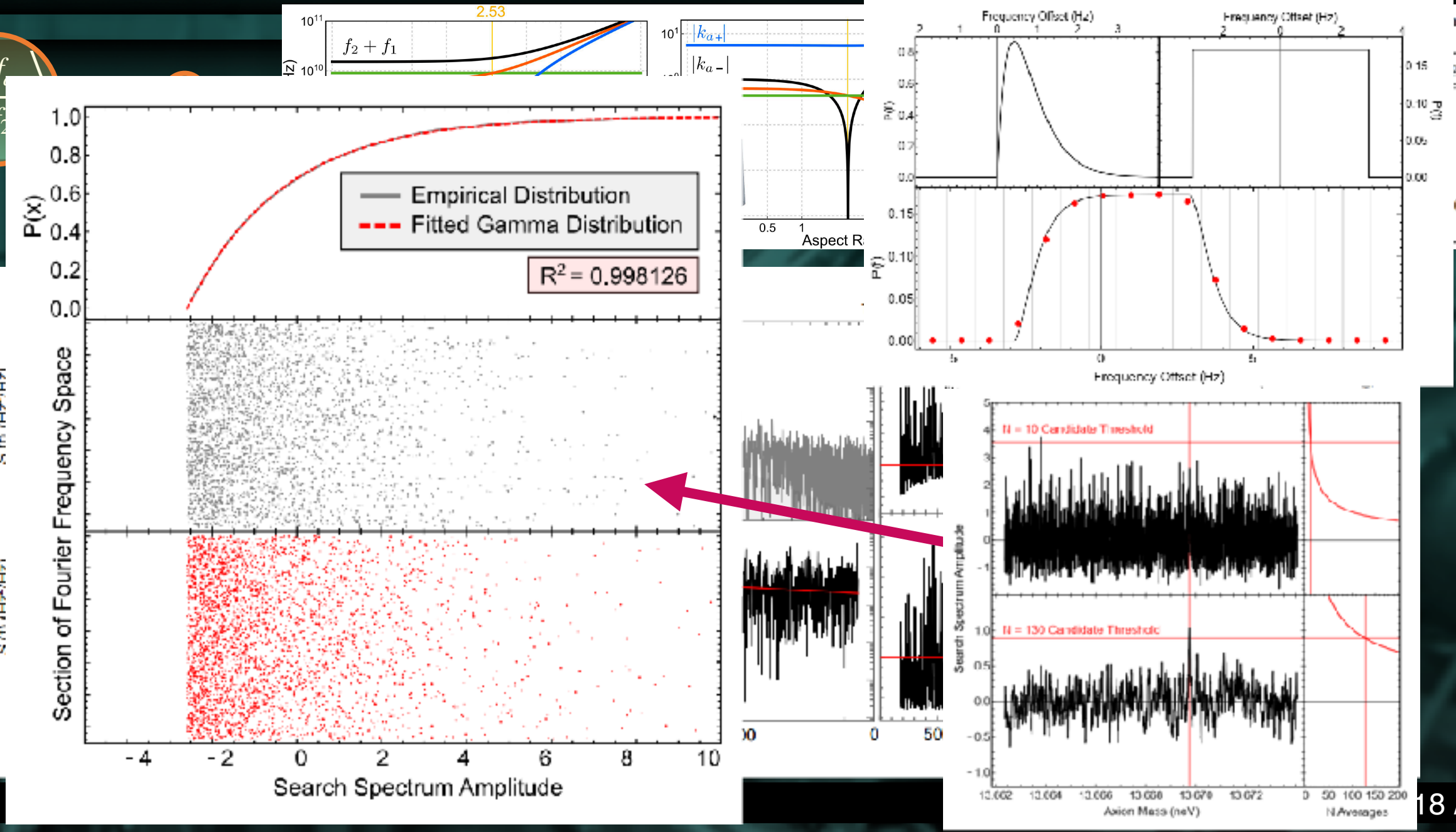

# Phase 1 FIRST LIMITS

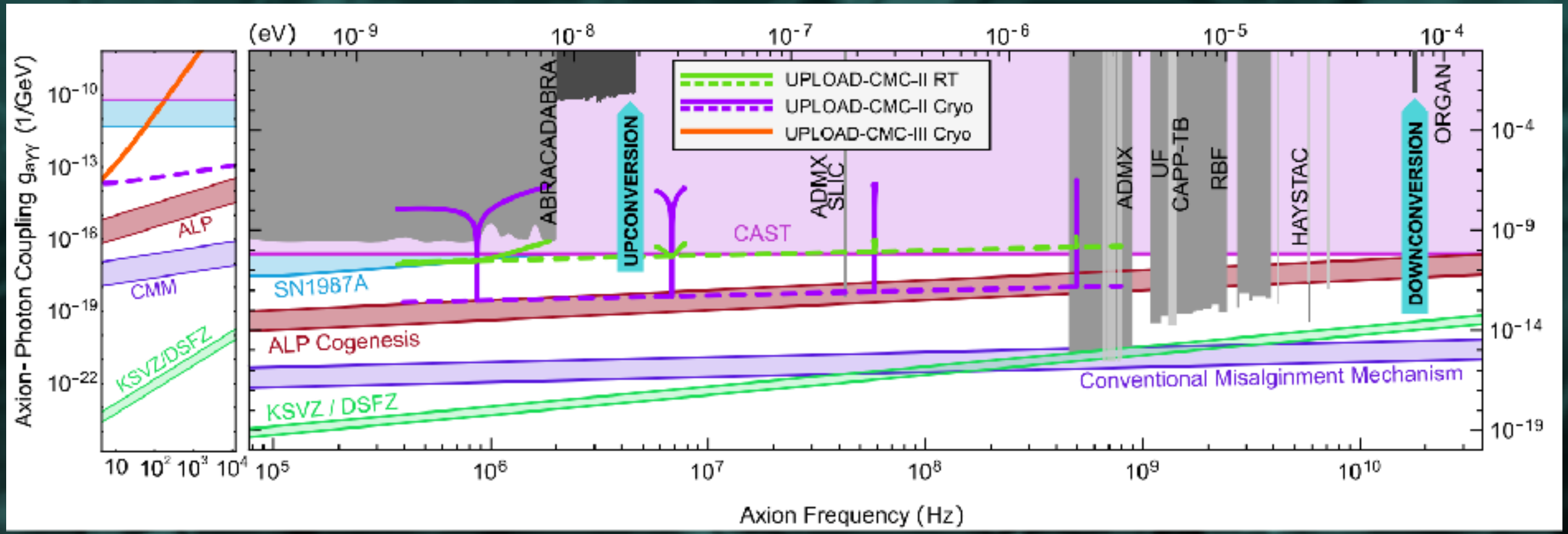

# Add noise suppression and vacuum

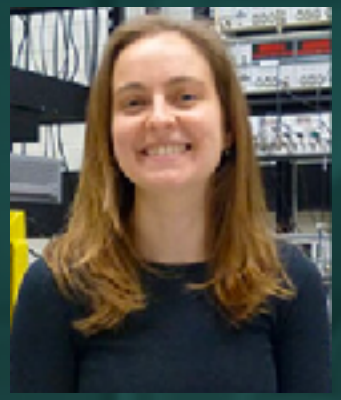

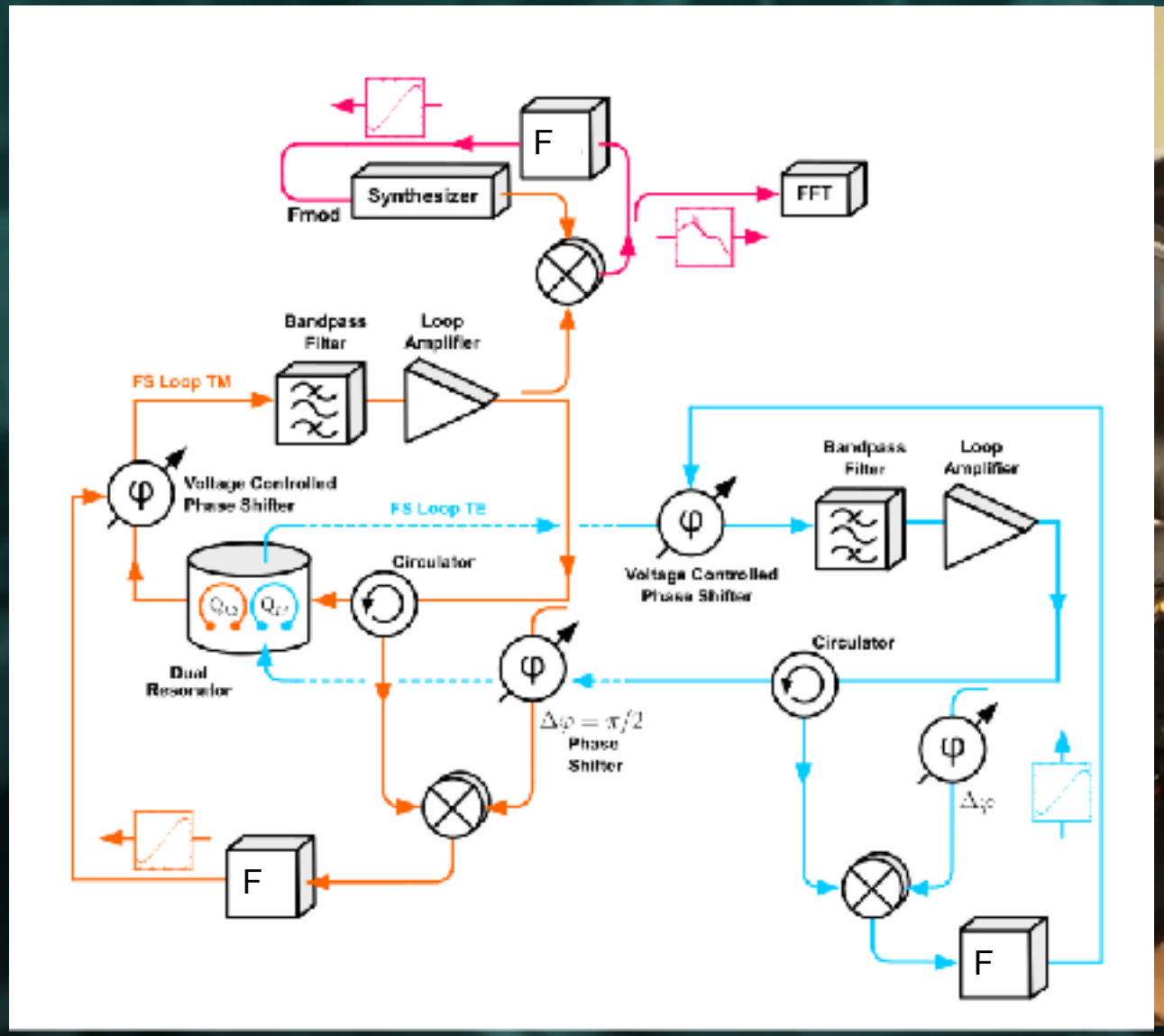




# Results

# FREQUENCY NOISE PSD

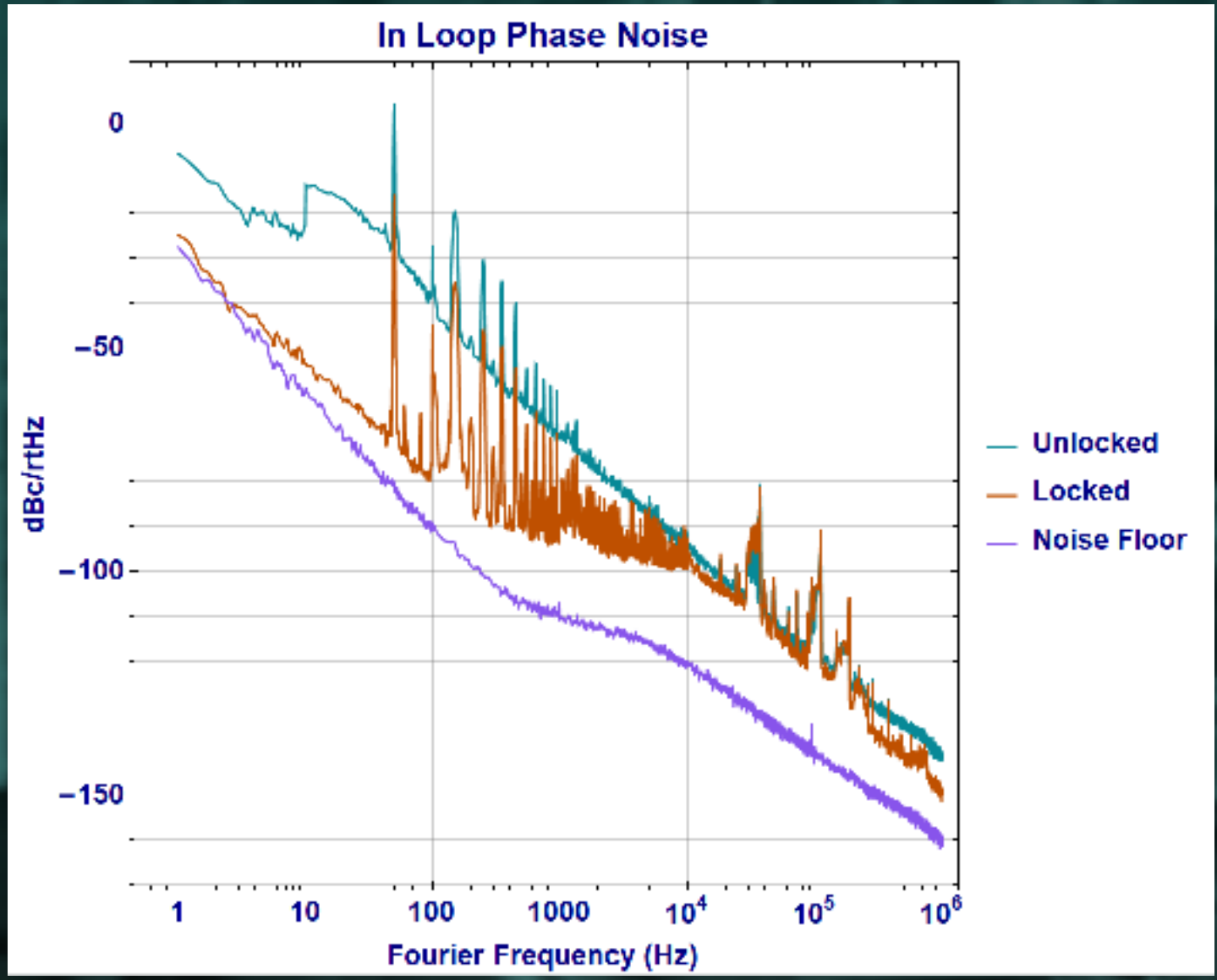

# Results IDENTIFYING AN AXION SIGNAL

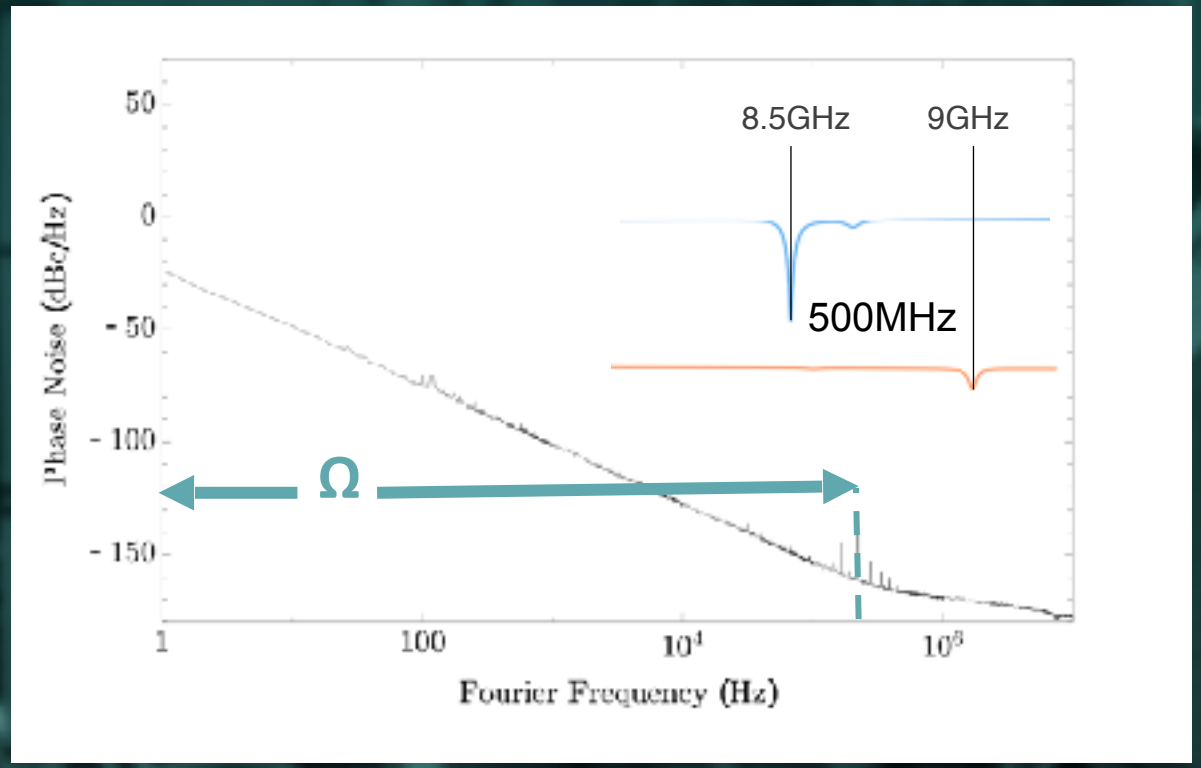


Can Search multiple spectra, while mode tunes

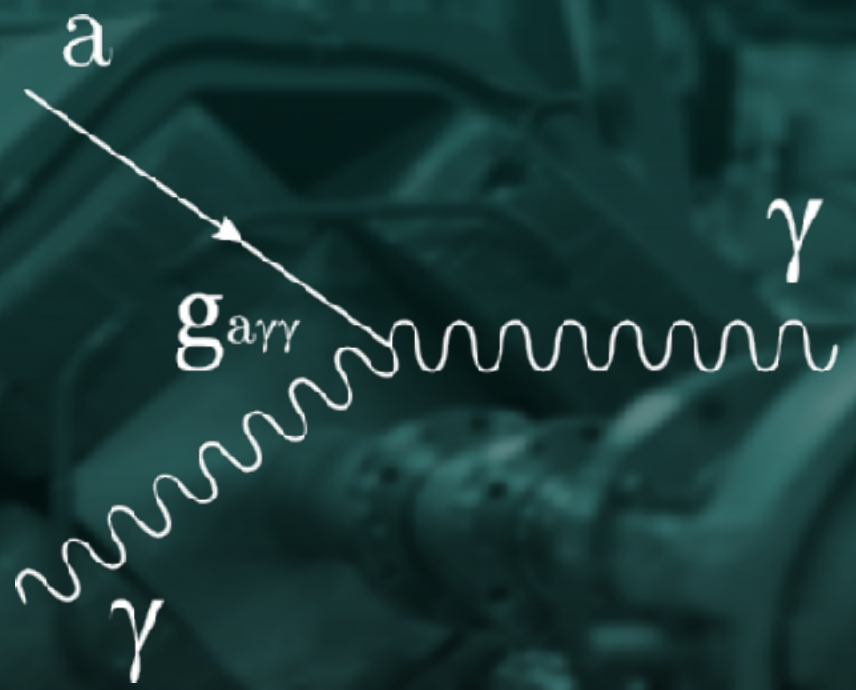


$$\omega_a = |\omega_1 - \omega_2| \pm \Omega \quad \textbf{where} \quad \Omega << \omega_1$$

# THE PUMPED EXPERIMENT

## Experimental Design



# THE PUMPED EXPERIMENT

## Experimental Design

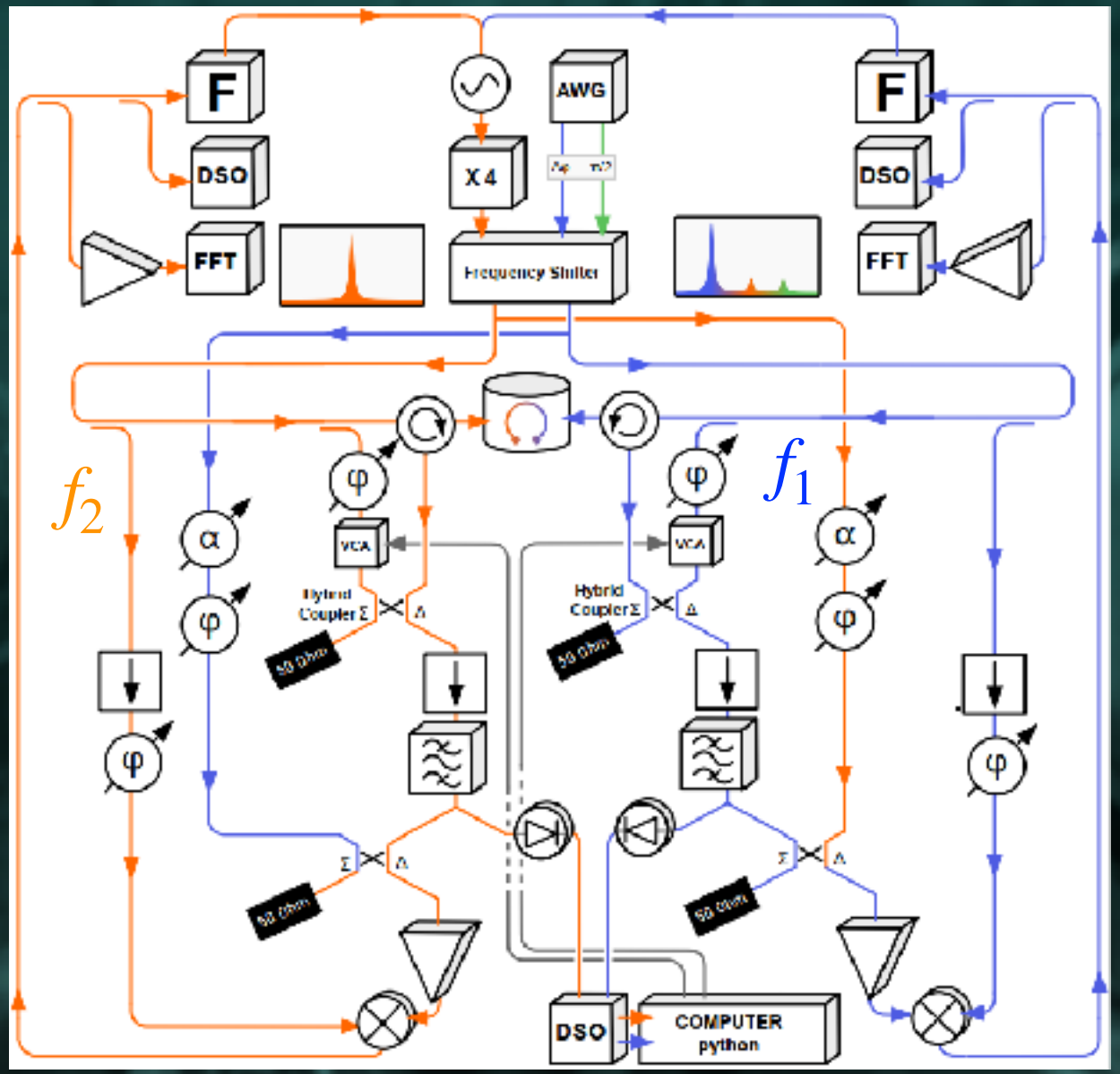


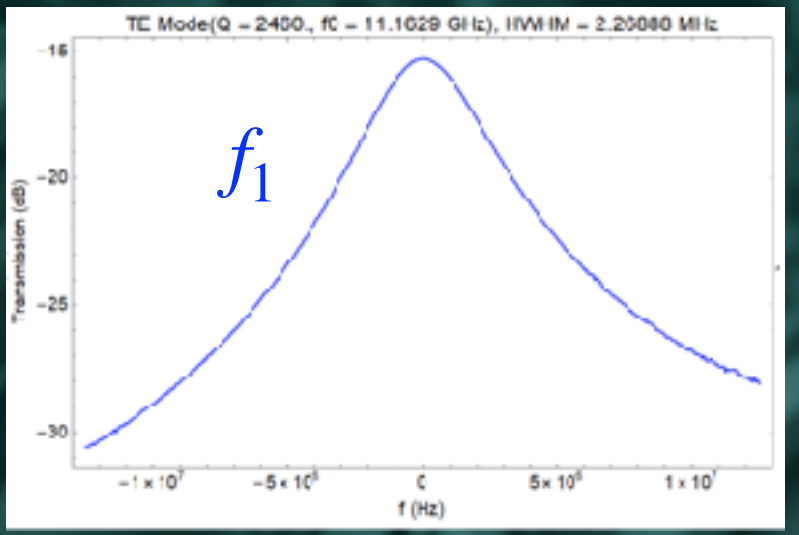


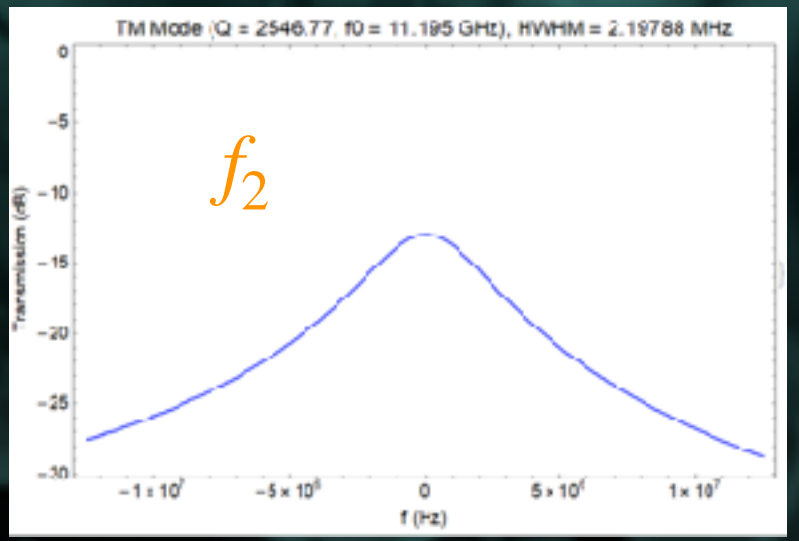

# THE PUMPED EXPERIMENT

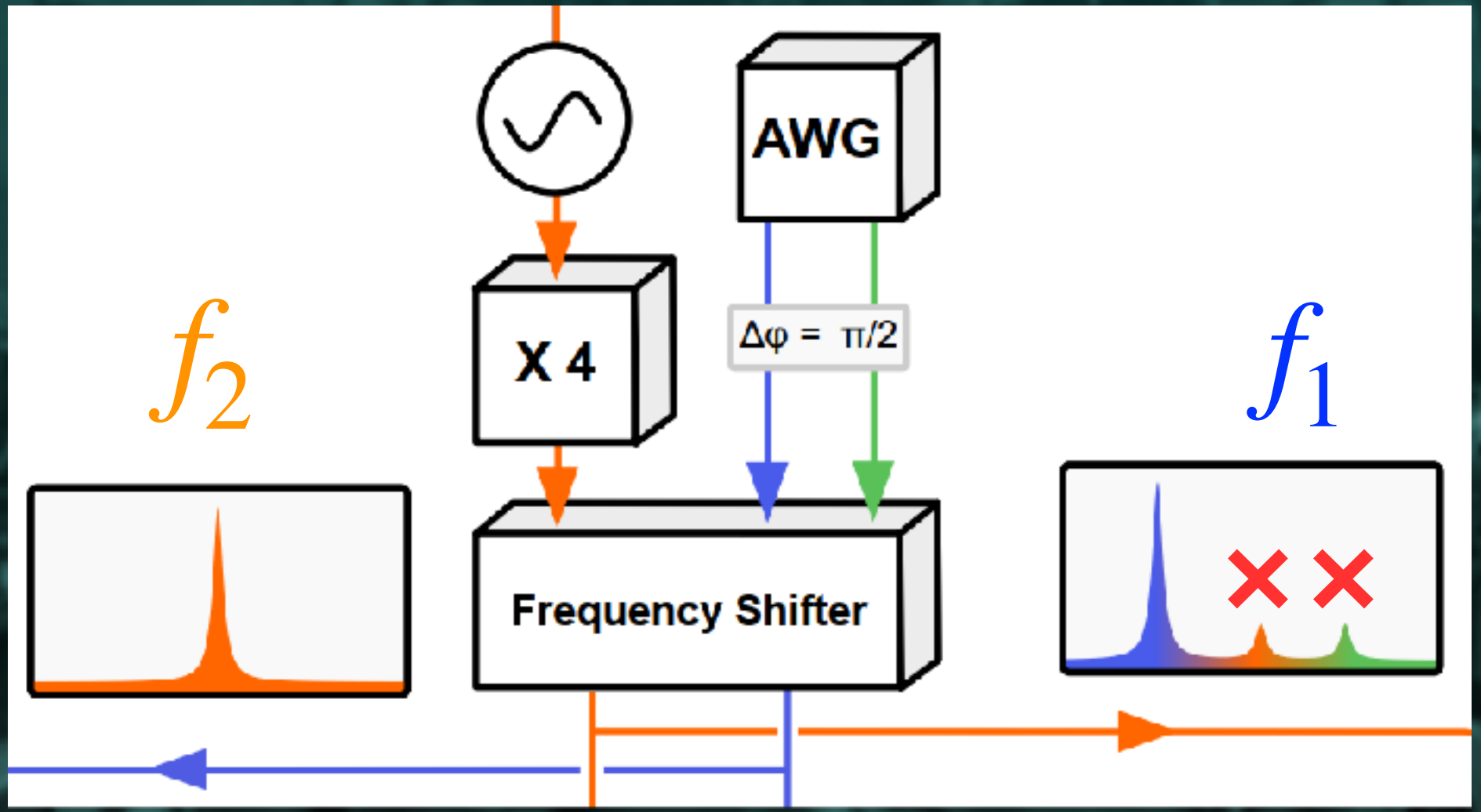




# THE PUMPED EXPERIMENT

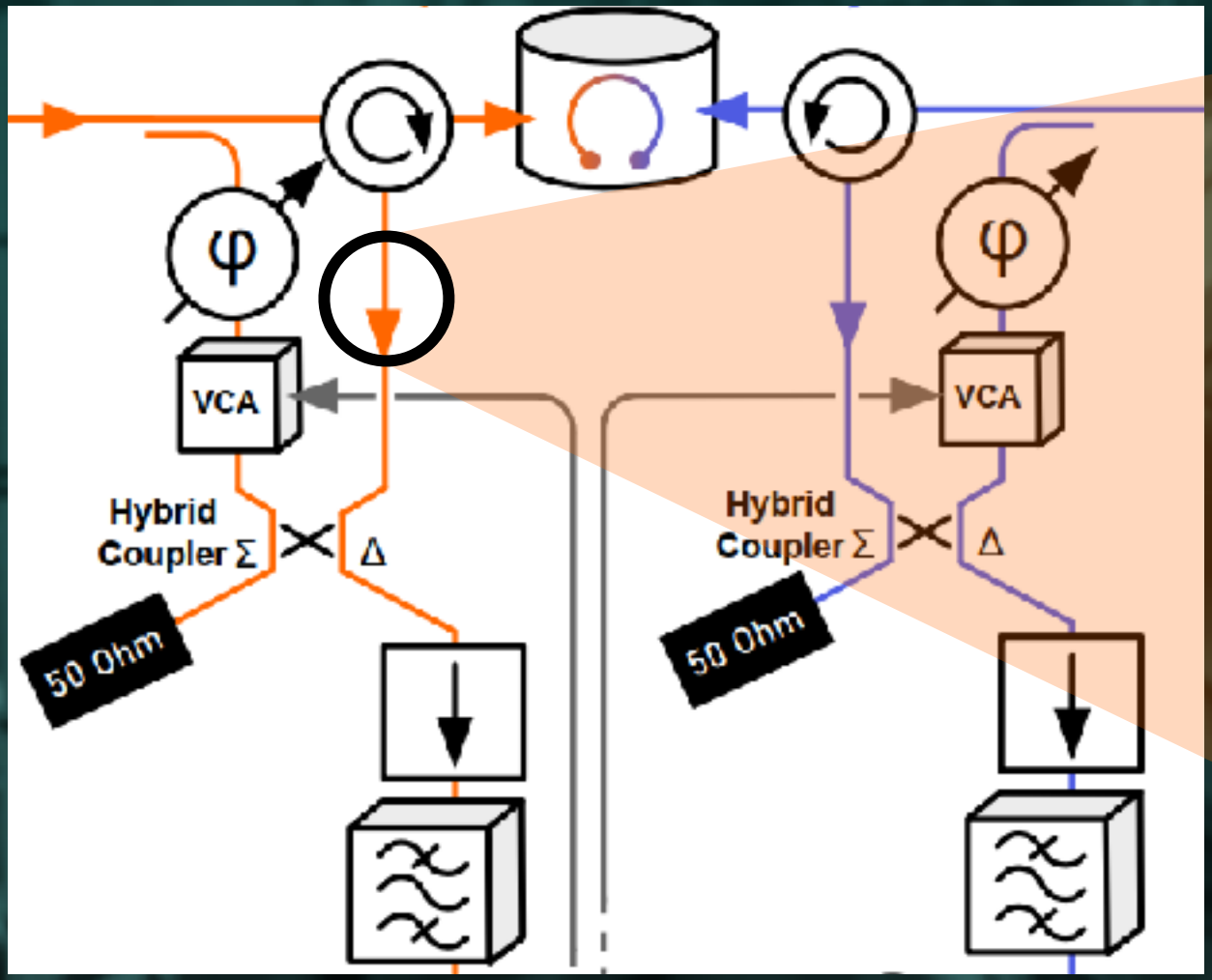




# THE PUMPED EXPERIMENT

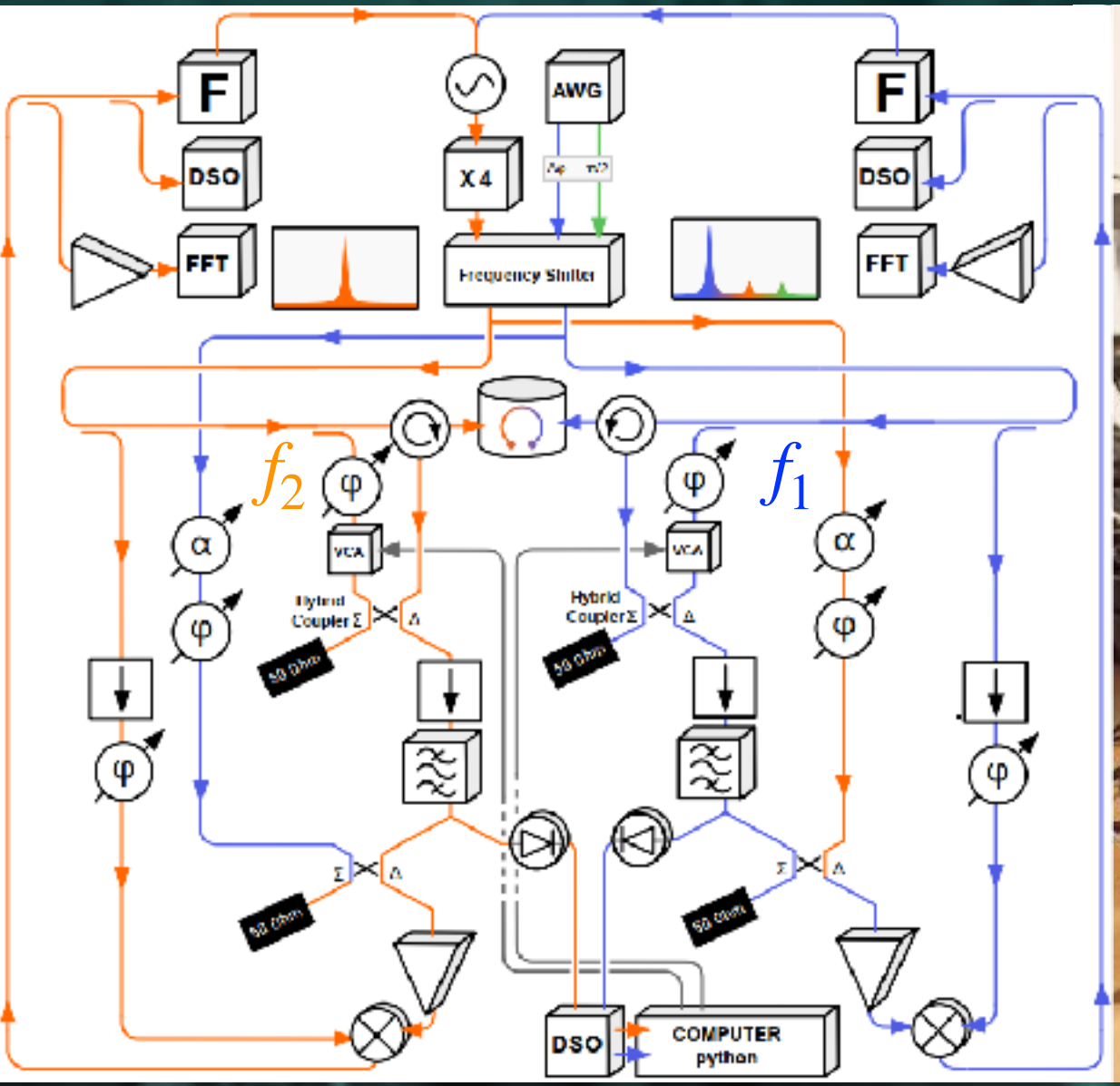


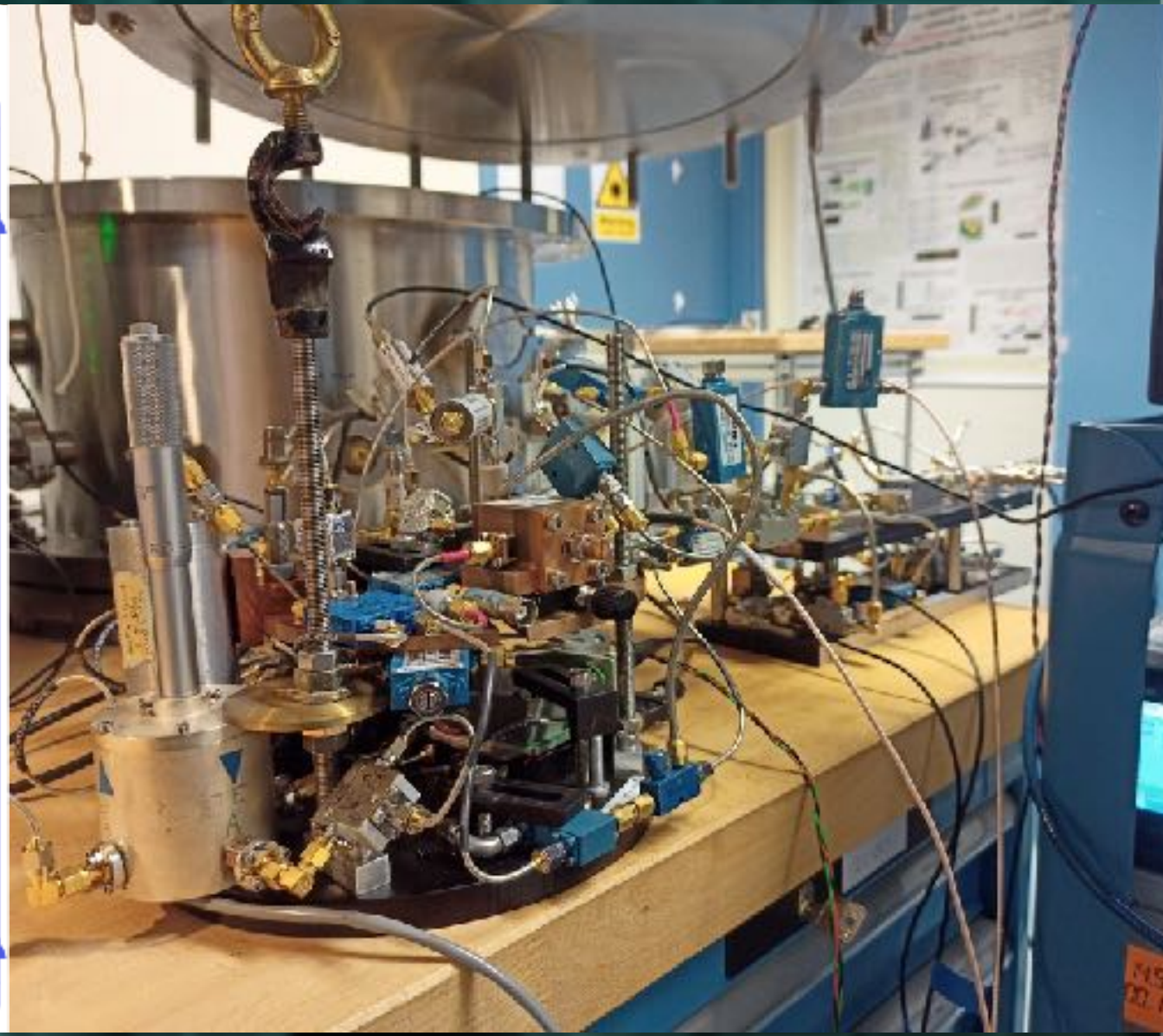

# Results

# THE PUMPED EXPERIMENT

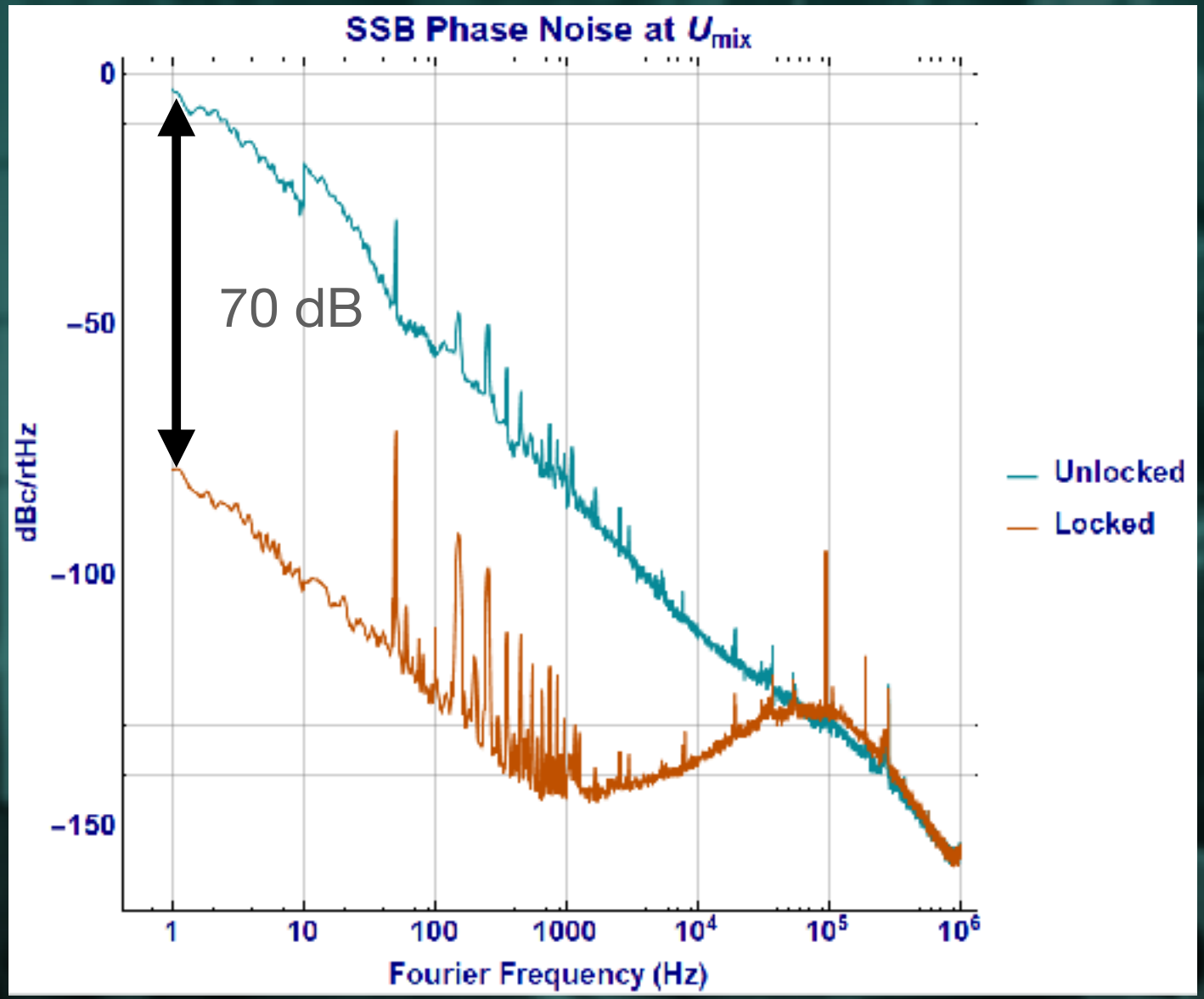

# Results

# THE PUMPED EXPERIMENT

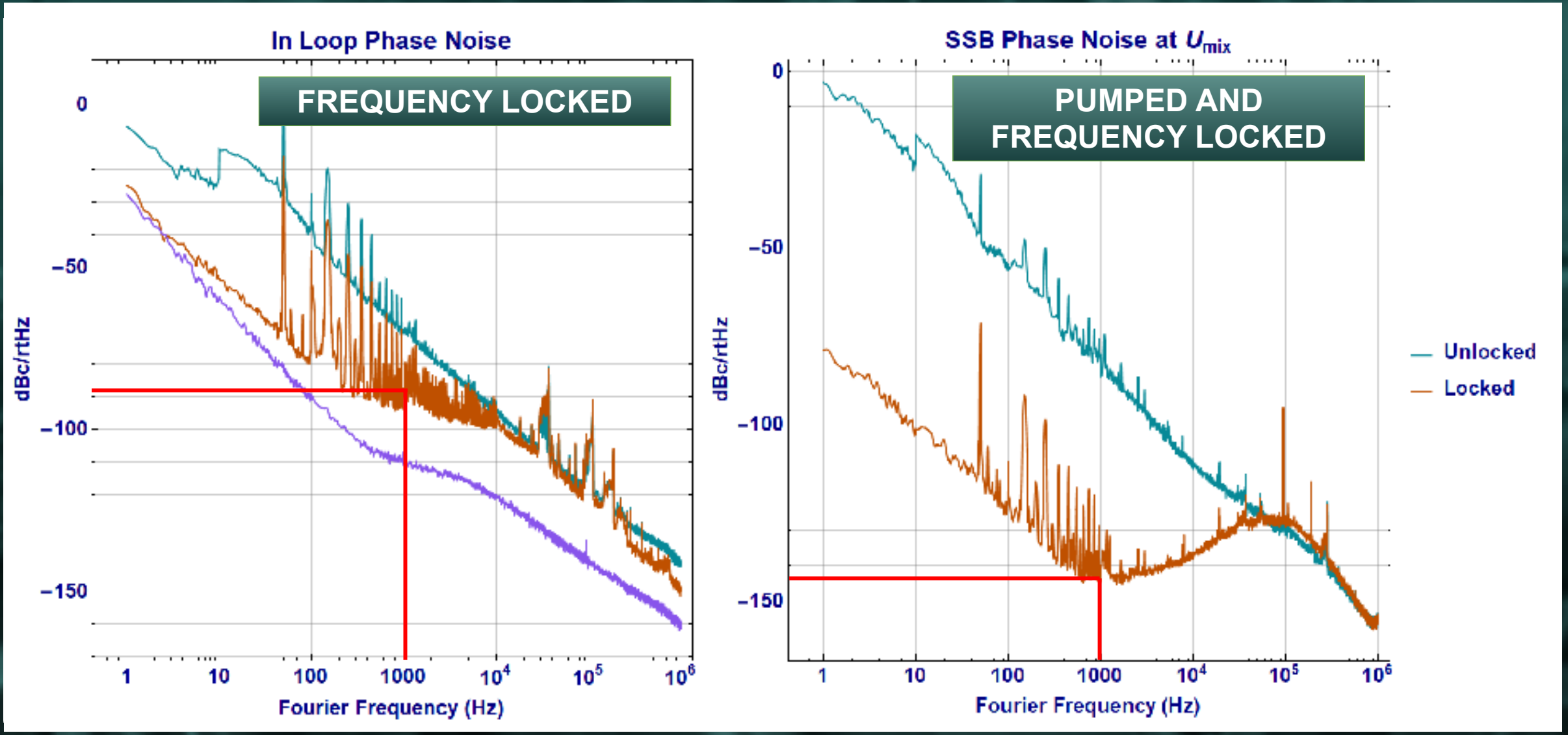

# Results

# THE PUMPED EXPERIMENT

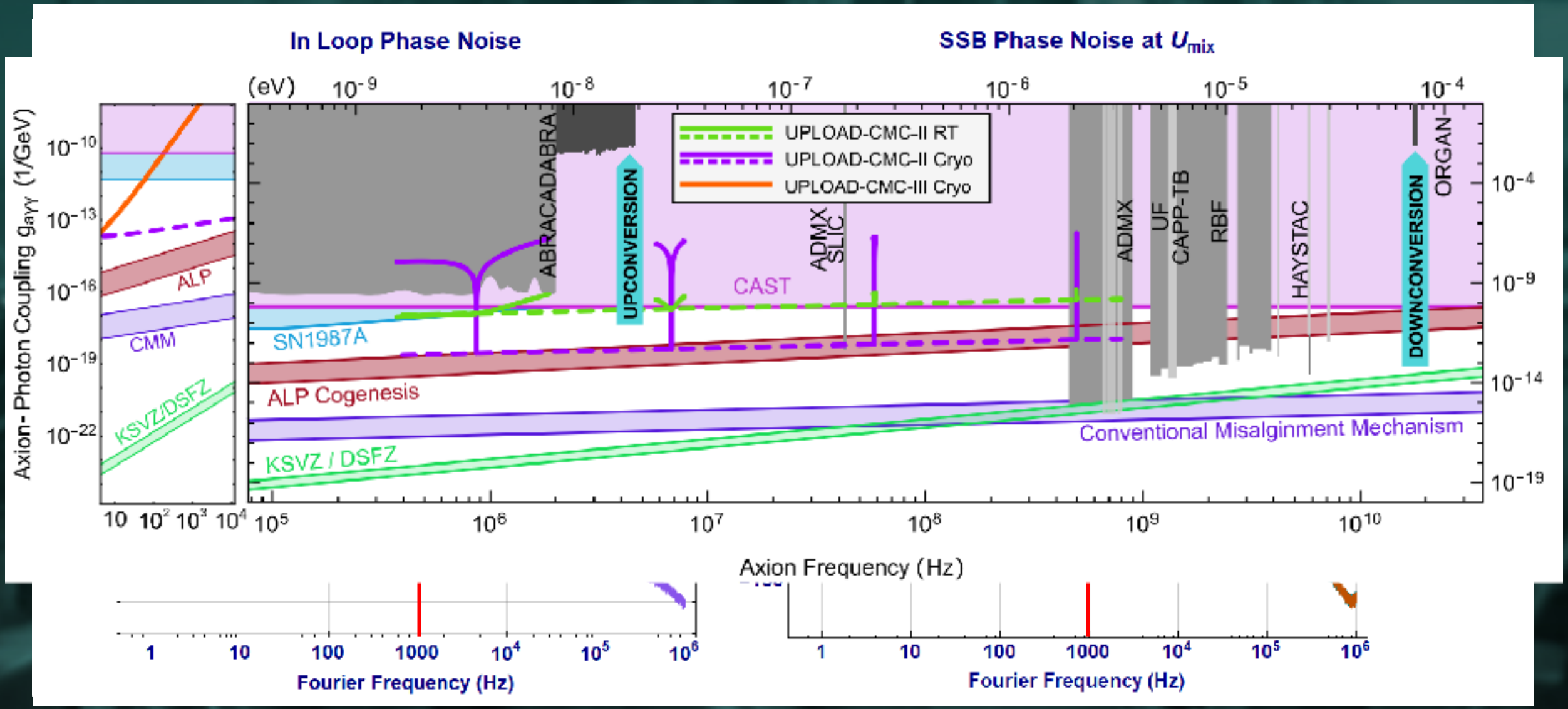

# Ultralight Axions: Frequency and Power technique

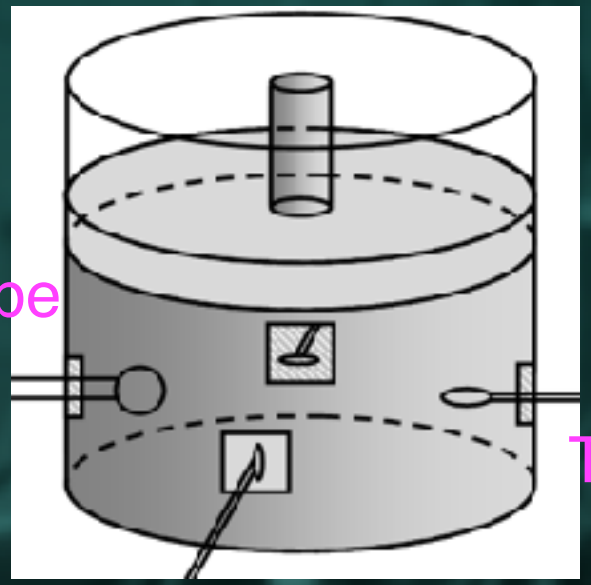


- Tuneable cavity height (lid attached to micrometer)
- $TM_{020}$ mode frequency fixed by cavity radius
- $TE_{011}$ mode frequency tuned by cavity height

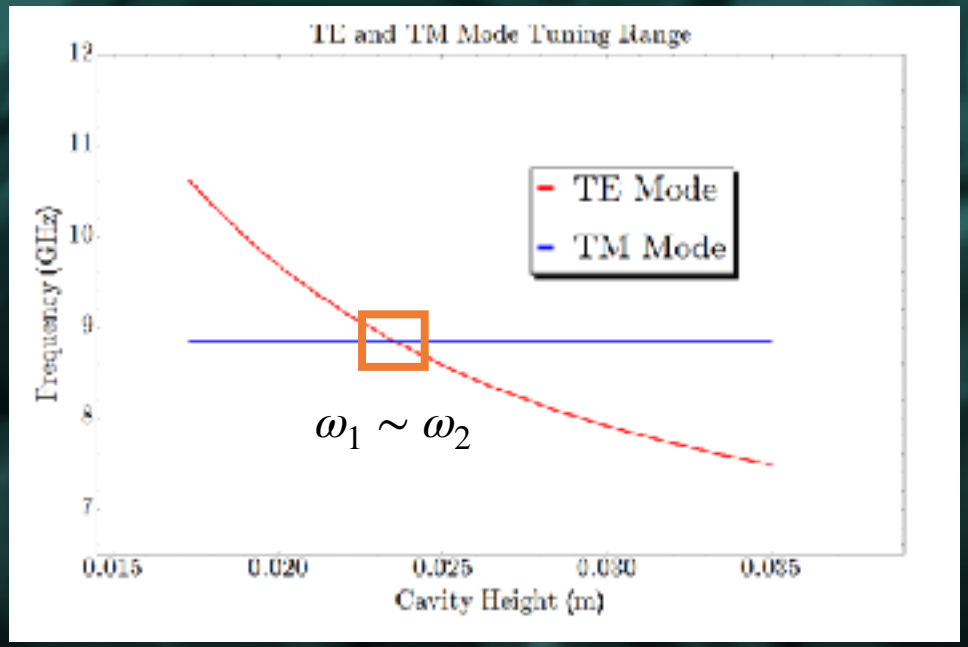


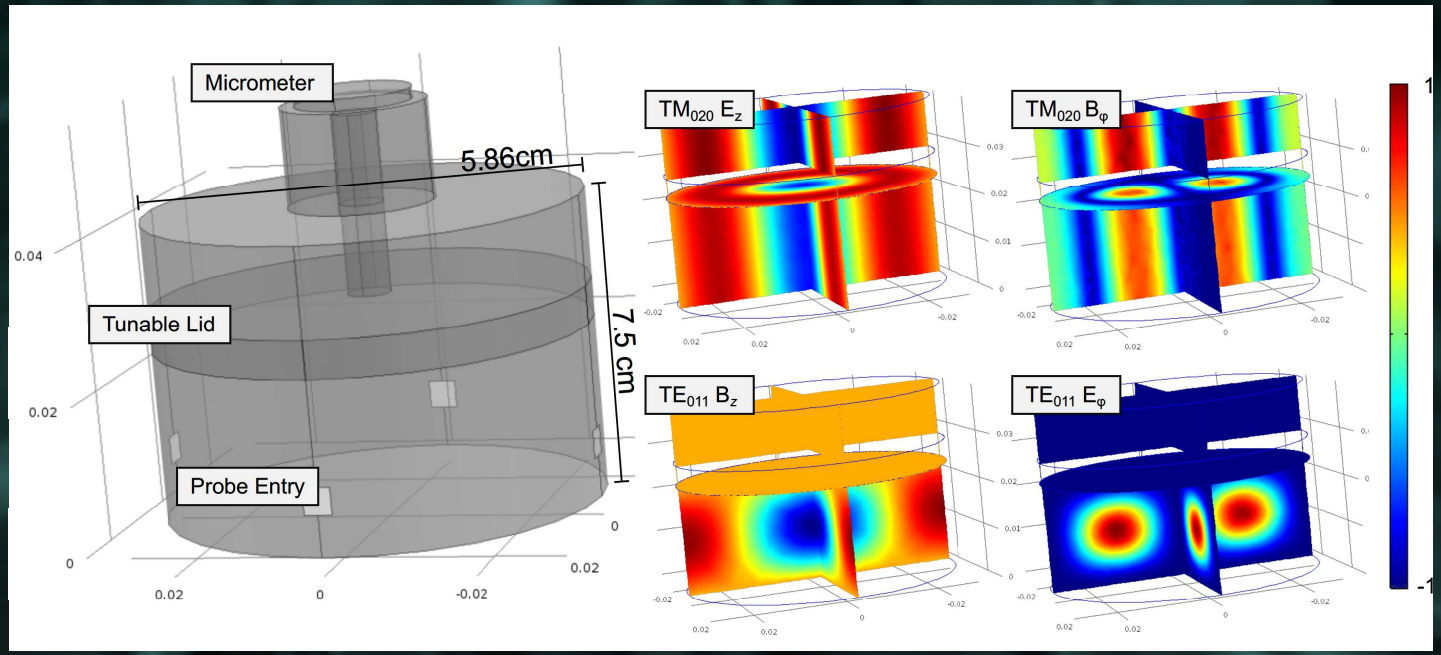


$$\omega_a = \delta\omega \pm \Omega$$

Detuning  Fourier Frequency

# Problems for Ultralight Axions

$\delta f = 2MHz$

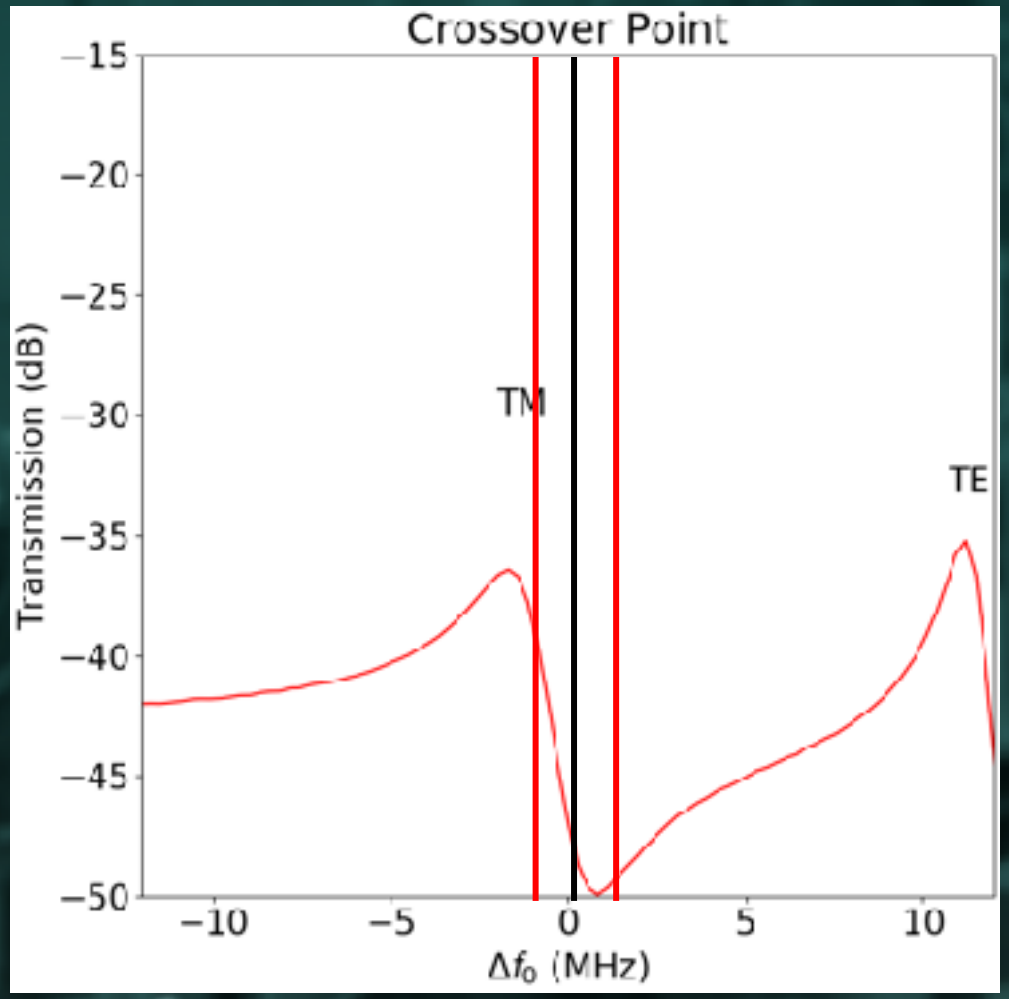


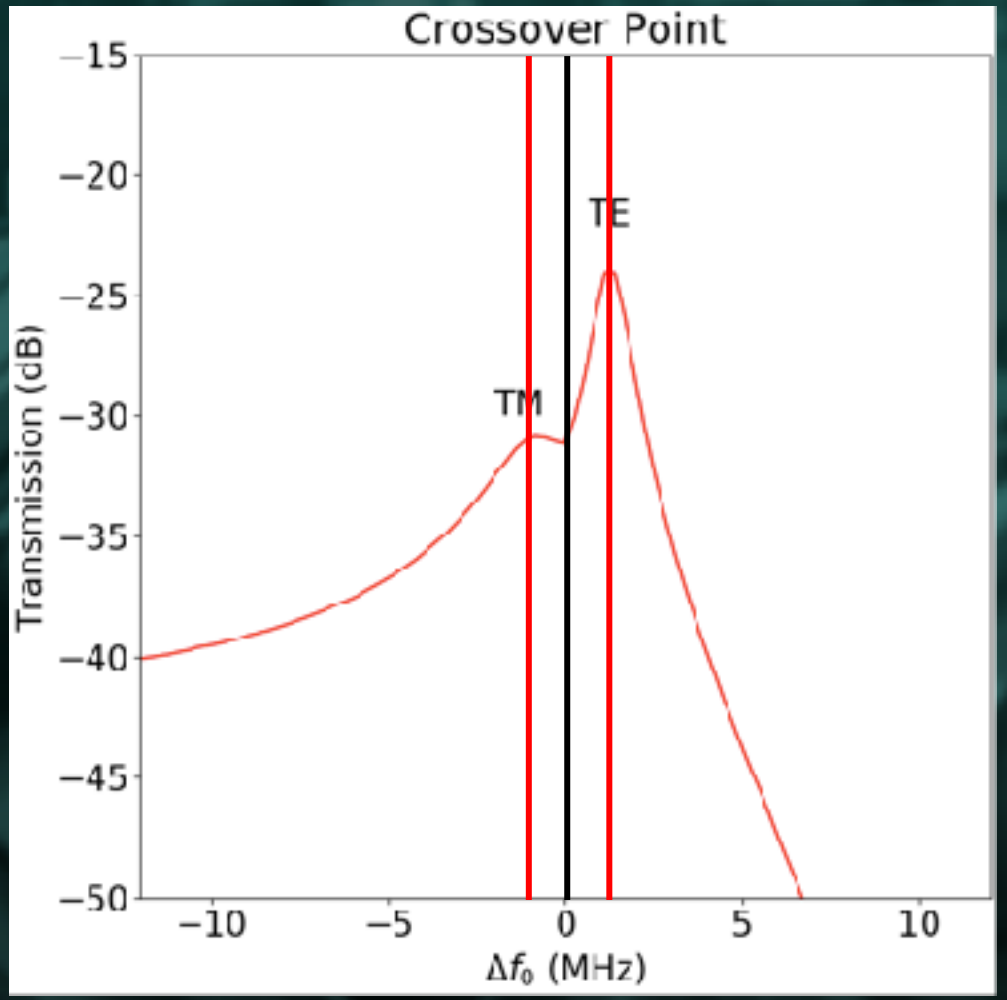


$\delta f$ and Mode Orthogonality? Calculate overlap v tuning

$-1 \quad 1$

Non Lorentzian line shape distorts phase noise

# Ultralight Axions: Frequency and Power technique

$$f_a = \delta f \pm f$$

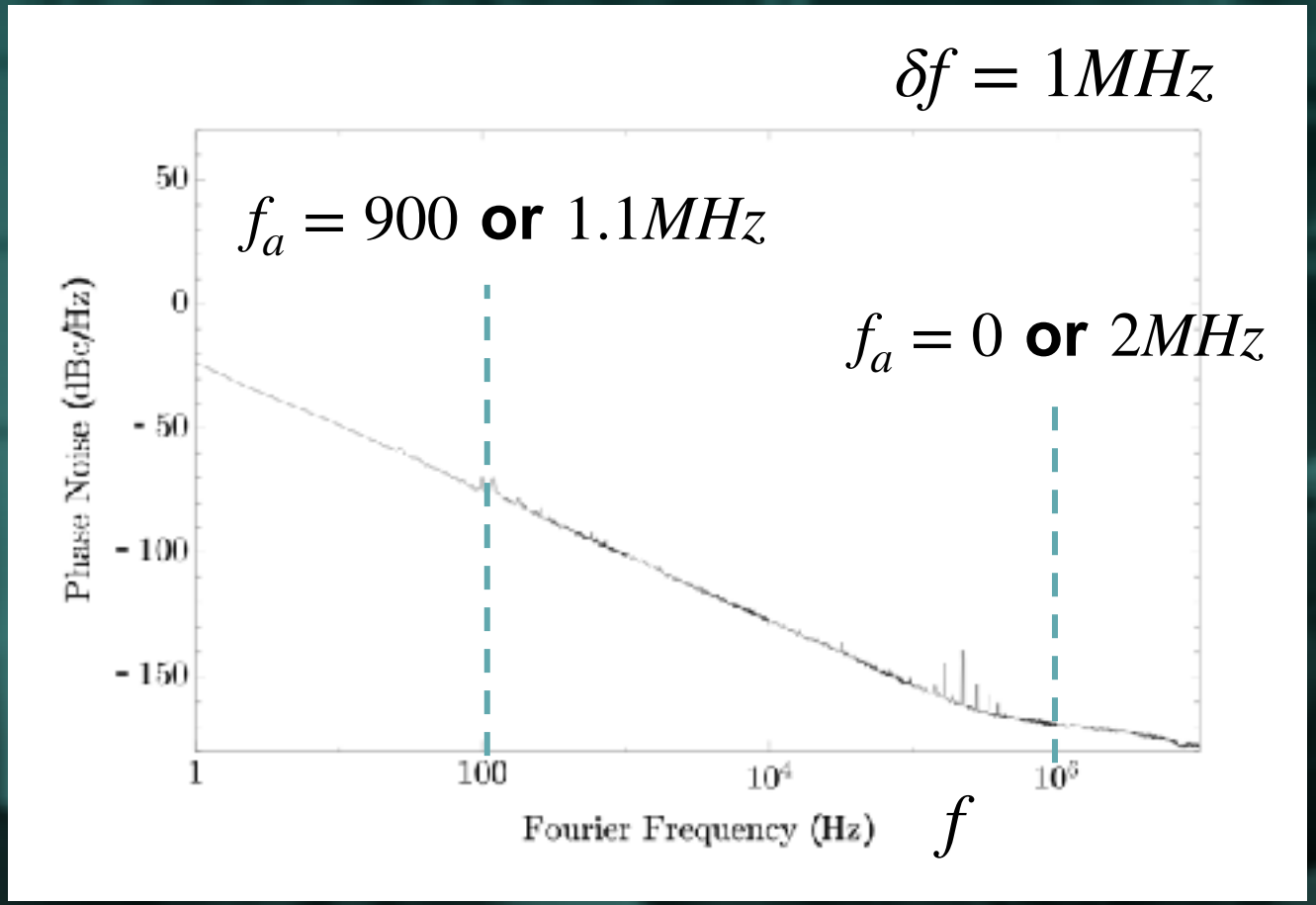

# Interferometric Phase Noise Measurements Syste

$$\delta f = 0$$

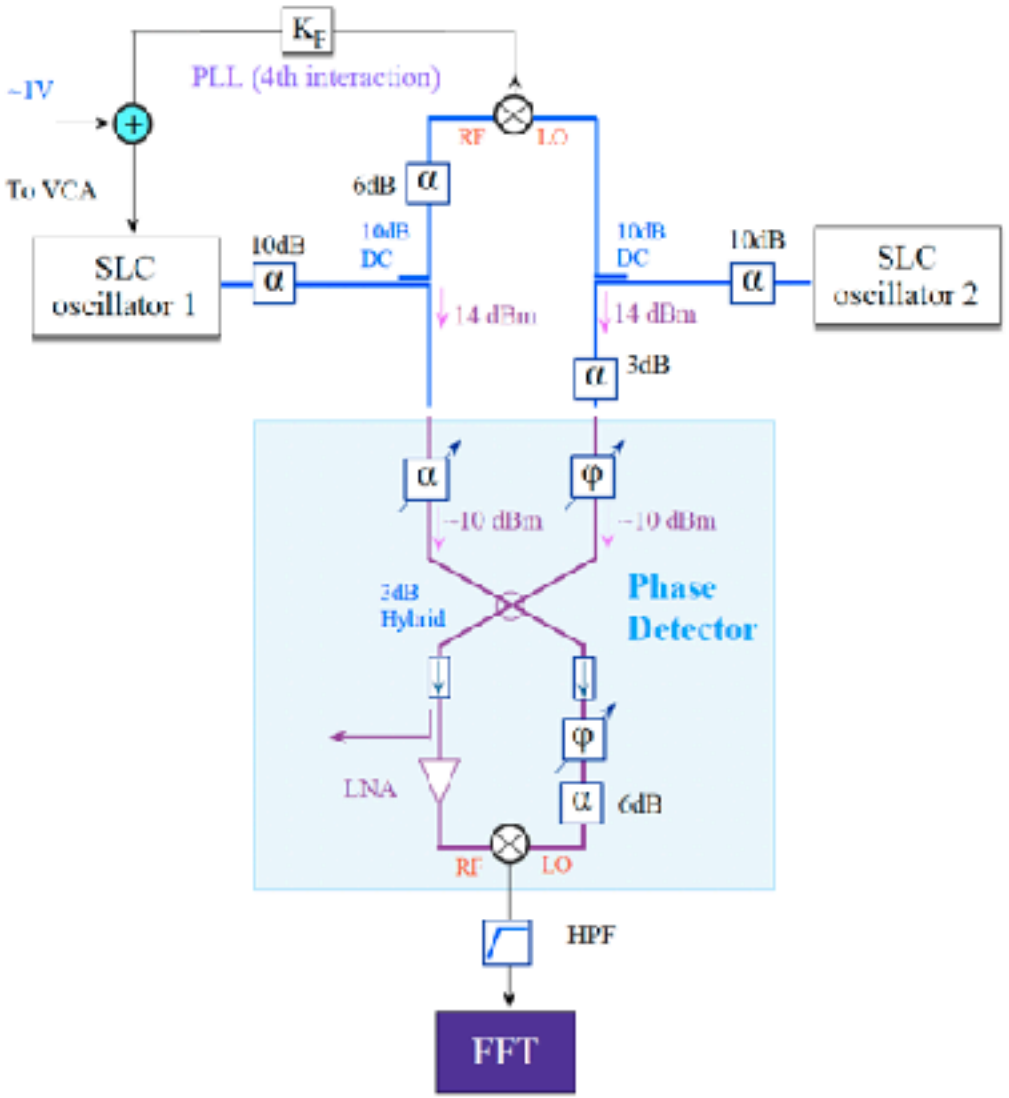


## Results of Phase Noise Measurements

$$\delta f = 2MHz$$

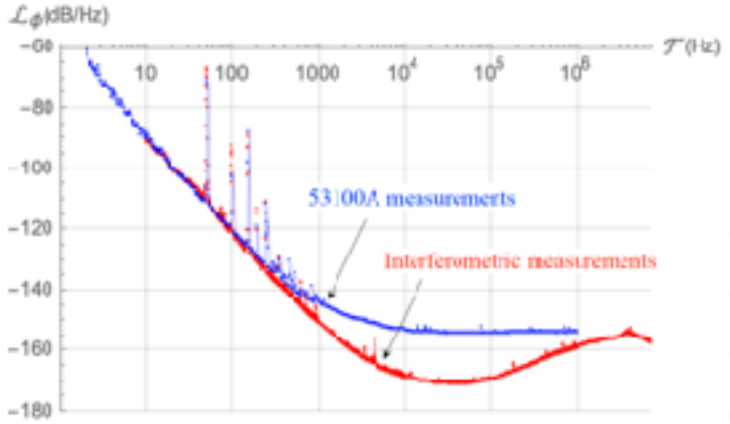


*SSB phase noise of an individual 9 GHz oscillator: 53100A ($f_{beat}$ ~ 2 MHz) vs Interferometric detection*

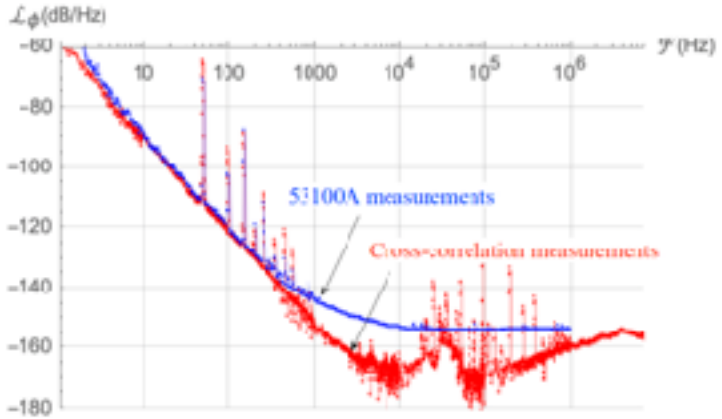


*SSB phase noise of an individual 9 GHz oscillator: 53100A ($f_{beat}$ ~ 2 MHz) vs Cross-correlation detection*



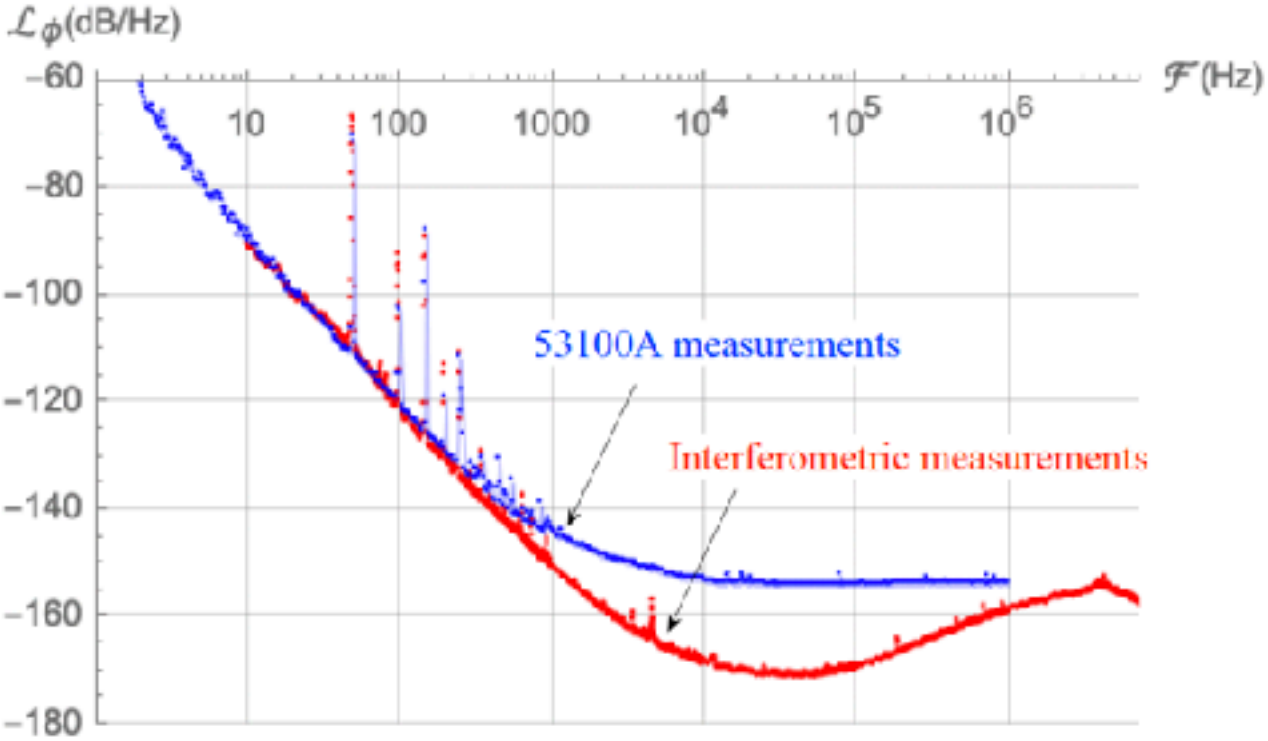


*SSB phase noise of an individual 9 GHz oscillator: 53100A ($f_{beat}$ ~ 2 MHz) vs Interferometric detection*



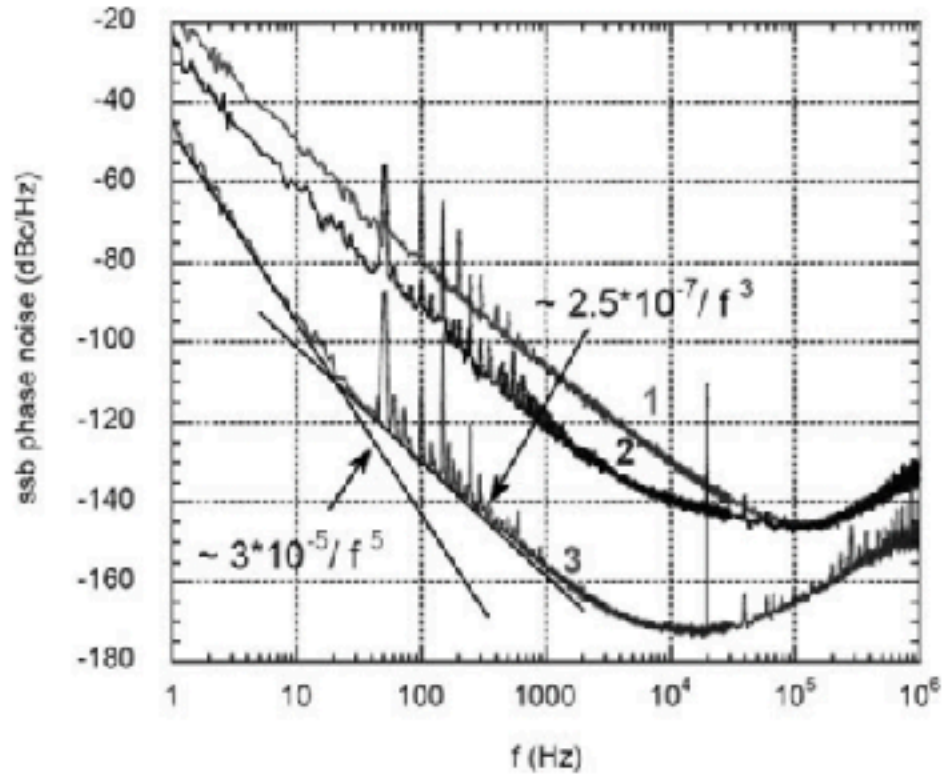


Fig. 9. The SSB phase-noise spectra of a high-power microwave oscillator in different modes of operation: (a) free-running oscillator, (b) free-running oscillator with an additional phase control system, and (c) frequency-stabilized oscillator.

IEEE TRANSACTIONS ON ULTRASONICS, FERROELECTRICS, AND FREQUENCY CONTROL, VOL. 56, NO. 2, FEBRUARY 2009 253

# Low Phase-Noise Sapphire Crystal Microwave Oscillators: Current Status

Eugene N. Ivanov and Michael E. Tobar, *Senior Member, IEEE*

# Proposal for Power Technique

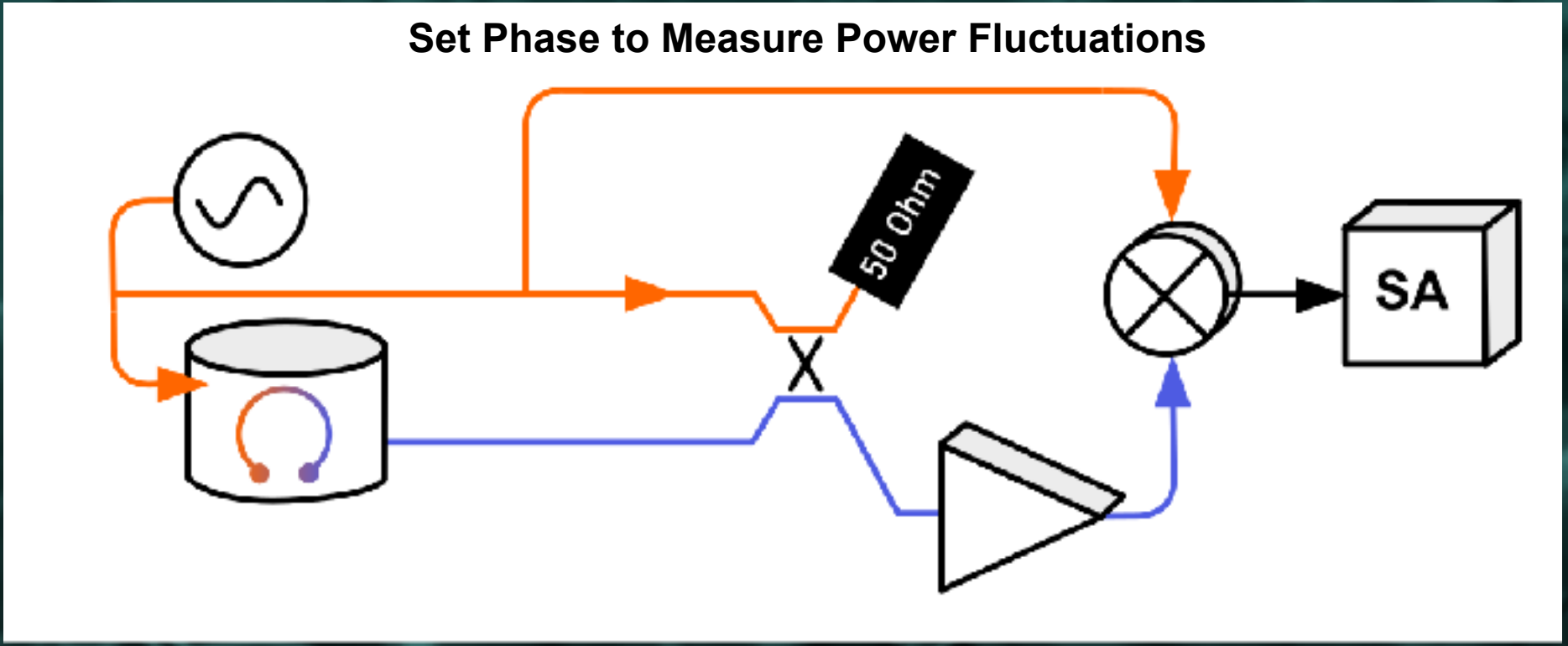


1. Dispersive System
2. AM and PM Noise Important
3. PM-> AM Conversions important
4. Non-trivial calculations, we know how to do it

$$\omega_a = |\omega_1 - \omega_2| \pm \Omega \quad \textbf{where} \quad \Omega << \omega_1$$

# Cryogenic UPLOAD Experiment

## Nb Tesla Cavities

TE 011 MODE, 2.5 GHz

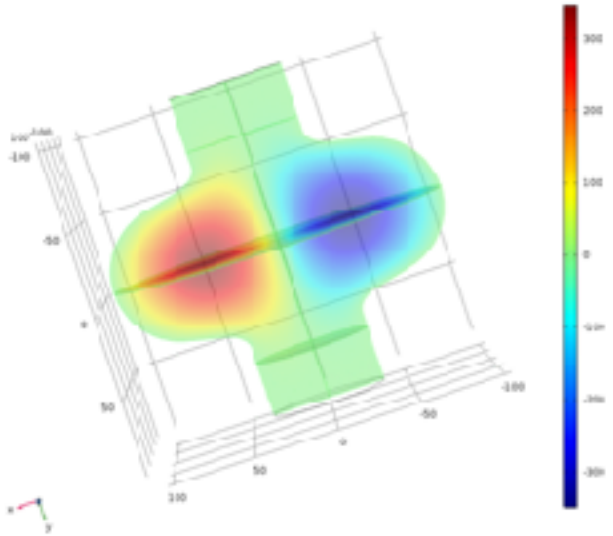

TM 010 MODE, 1.3 GHz

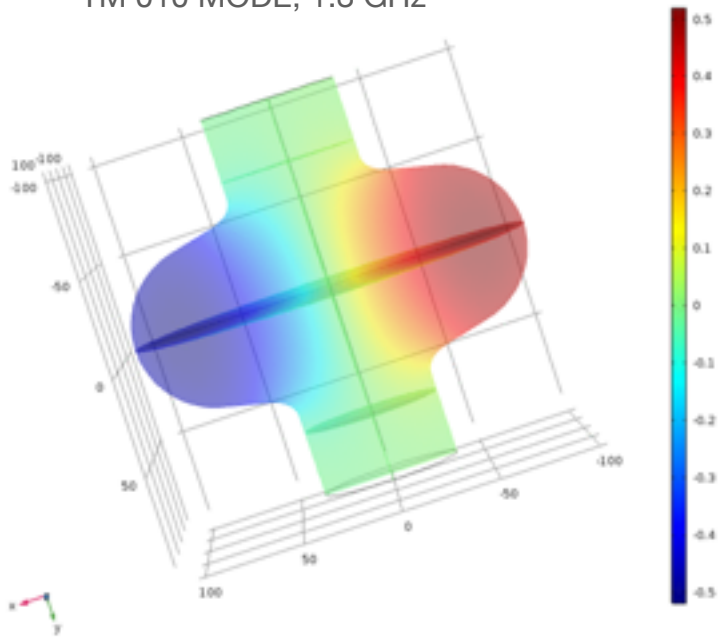

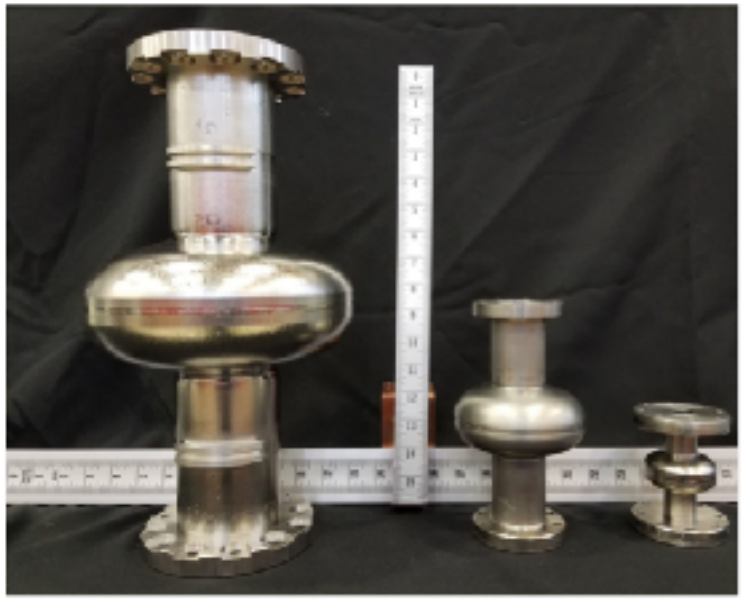

Snowmass2021 - Letter of Interest

*UP-conversion Loop Oscillator Axion Detector using a Microwave Cavity (UPLOAD-MC)*

**Thematic Areas:** (check all that apply ☐/■)
☐ (CF1) Dark Matter: Particle Like
■ (CF2) Dark Matter: Wavelike
☐ (CF3) Dark Matter: Cosmic Probes
☐ (CF4) Dark Energy and Cosmic Acceleration: The Modern Universe
☐ (CF5) Dark Energy and Cosmic Acceleration: Cosmic Dawn and Before
☐ (CF6) Dark Energy and Cosmic Acceleration: Complementarity of Probes and New Facilities
☐ (CF7) Cosmic Probes of Fundamental Physics

**Contact Information:** Michael E Tobar (University of Western Australia) [michael.tobar@uwa.edu.au]:

**Authors:**
Michael E Tobar[1], Maxim Goryachev[1], Eugene Ivanov[1], Ben McAllister[1], Catriona Thomson[1], Paul Altin[2], Alexander Romanenko[2], Anna Grassellino[2], Sam Posen[2], Yanhei Chen[4]

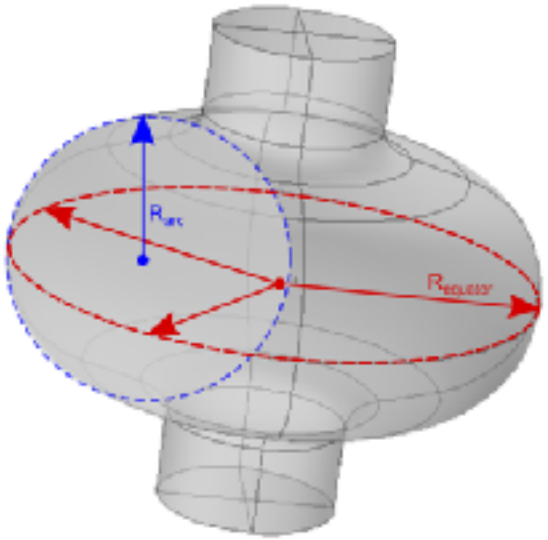
R_arc
R_EQUATOR

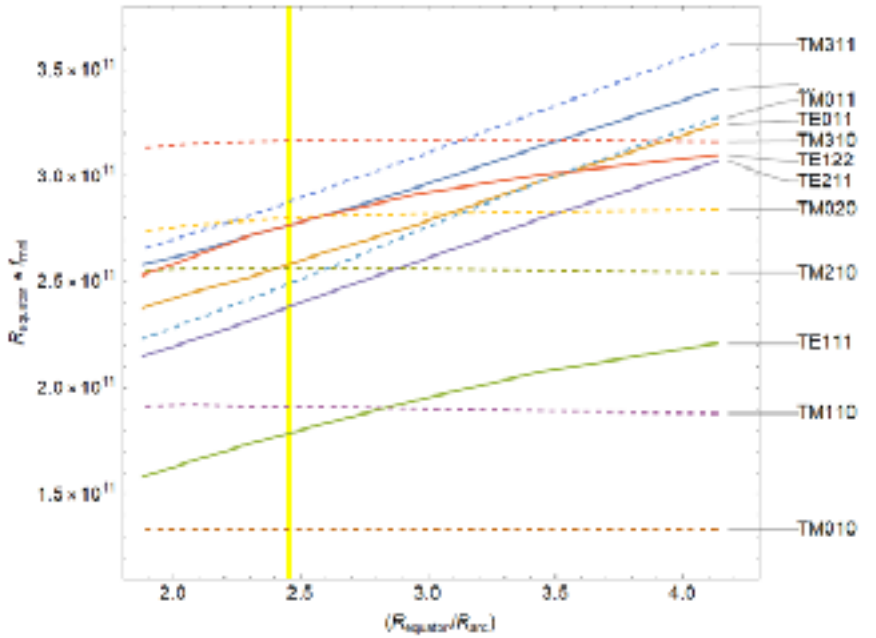
TM311
TM011
TE011
TM310
TE122
TE211
TM020
TM210
TE111
TM110
TM010
(R_equator/R_arc)



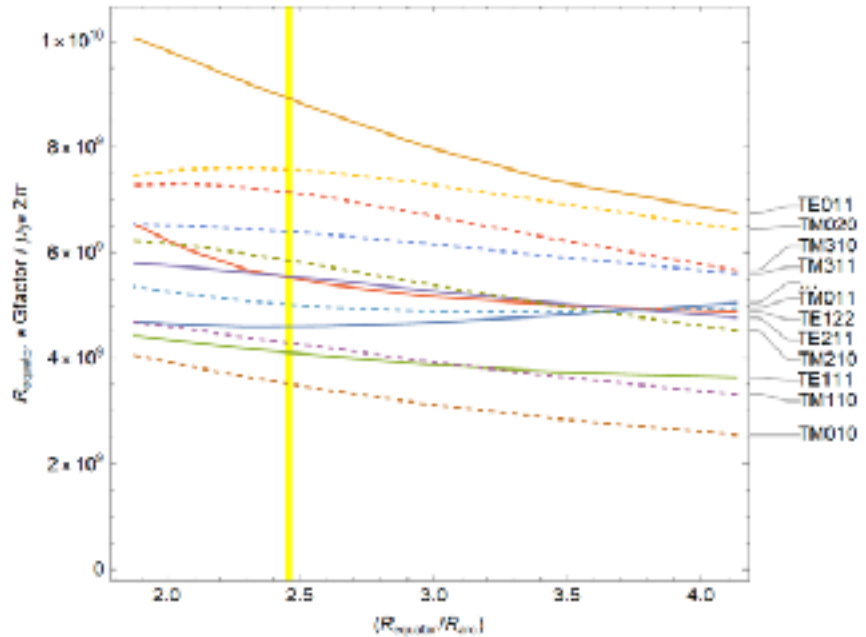
TE011
TM020
TM310
TM311
TM011
TE122
TE211
TM210
TE111
TM110
TM010
(R_equator/R_arc)

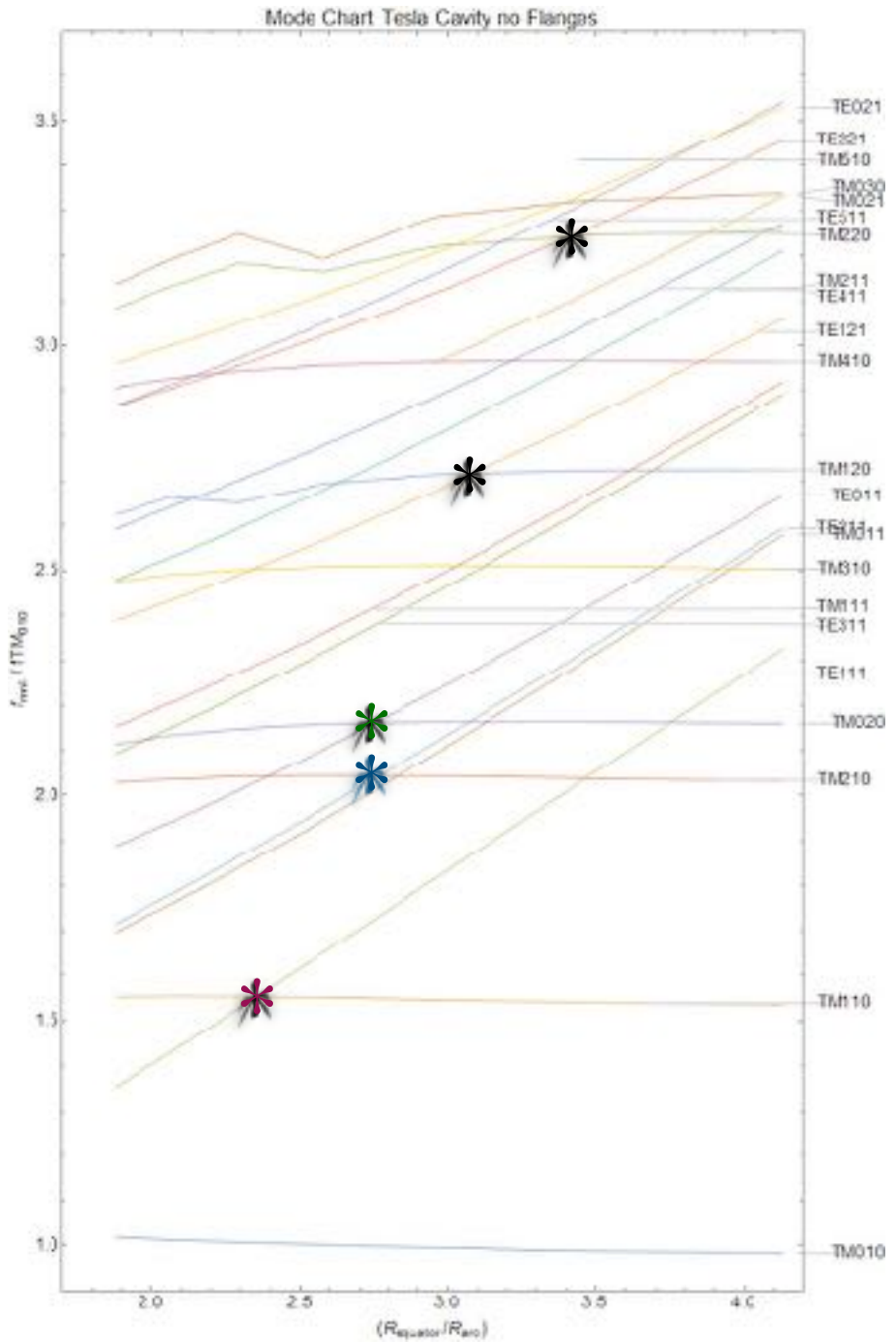
Mode Chart Tesla Cavity no Flanges
TE021
TE321
TM510
TM030
TM021
TE511
TM220
TM211
TE411
TE121
TM410
TM120
TE011
TM011
TM310
TM111
TE311
TE111
TM020
TM210
TM110
TM010
(R_equator/R_arc)

# SUMMARY UPLOAD

## (Coming up next Poynting vector haloscope analysis)

- First Table-Top Two-Photon Oscillator Experiment
- Cylindrical Microwave Cavity with $TE_{011}$ and $TM_{020}$ Modes close in Frequency
- Limits set with basic Loop Oscillator Set-up
- Large Improvement underway with external stabilised Sythesizer
- Sensitive Enough to put Limits on known Axion Models
- Next version under construction

# POYNTING VECTOR ANALYSIS OF PHOTONIC CONVERSION OF THE DARK MATTER AXION MIXING WITH A BACKGROUND DC MAGNETIC FIELD

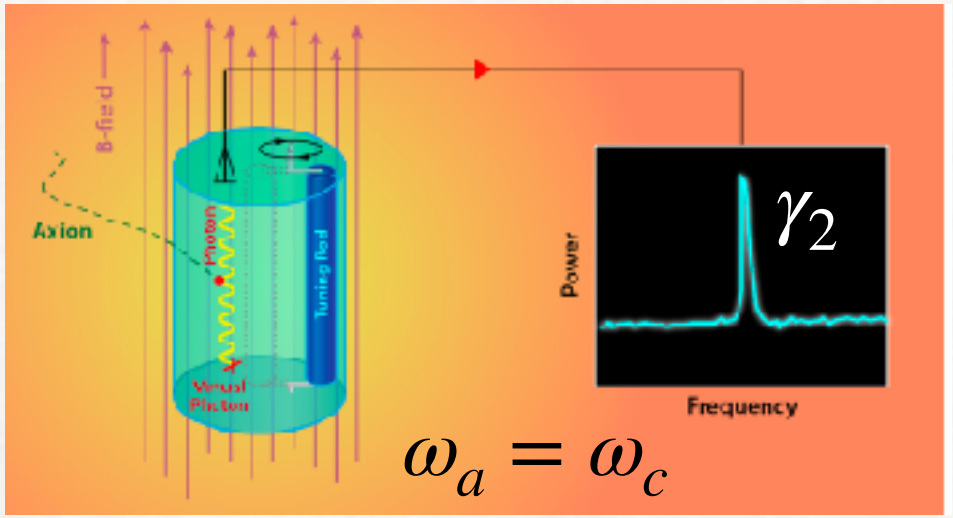


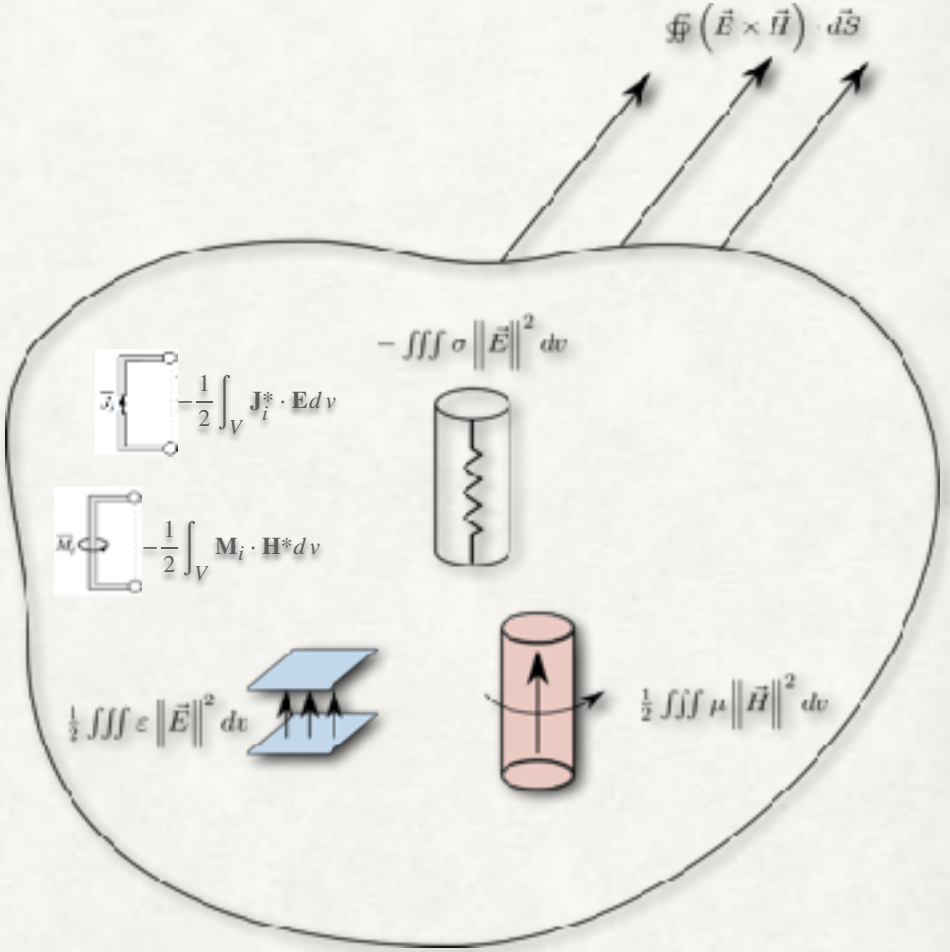




arXiv.org > hep-ph > arXiv:2109.04056

High Energy Physics - Phenomenology

**Abraham and Minkowski Poynting vector controversy in axion modified electrodynamics**

Michael F Tobar, Ben T McAllister, Maxim Goryachev

The most sensitive haloscopes that search for axion dark matter through the two photon electromagnetic anomaly, convert axions into photons through the mixing of axions with a large DC magnetic field. In this work we apply Poynting theorem to the resulting axion modified electrodynamics and identify two possible Poynting vectors, one similar to the Abraham Poynting vector and the other to the Minkowski Poynting vector in electrodynamics. The latter picks up the extra non-conservative terms while the former does not. To understand the source of energy conversion and power flow in the detection systems, we apply the two Poynting theorems to axion modified electrodynamics, for both the resonant cavity and broadband low-mass axion detectors. We show that both Poynting theorems give the same sensitivity for a resonant cavity axion haloscope, but predict markedly different sensitivity for a low-mass broadband capacitive haloscope. Hence we ask the question, can understanding which one is the correct one for axion dark matter detection, be considered under the framework of the Abraham-Minkowski controversy? In reality, this should be confirmed by experiment when the axion is detected. However, many electrodynamic experiments have ruled in favour of the Minkowski Poynting vector when considering the canonical momentum in dielectric media. In light of this, we show that the axion modified Minkowski Poynting vector should indeed be taken seriously for sensitivity calculation for low-mass axion haloscope detectors in the quasi-static limit, and predict orders of magnitude better sensitivity than the Abraham Poynting vector equivalent.

Subjects: High Energy Physics - Phenomenology (hep-ph); Instrumentation and Methods for Astrophysics (astro-ph.IM); General Relativity and Quantum Cosmology (gr-qc); High Energy Physics - Experiment (hep-ex)

Cite as: arXiv:2109.04056 [hep-ph]

or arXiv:2109.04056v1 [hep-ph] (for this version)

arXiv:2109.04056 [hep-ph]

# DC Magnetic Haloscopes

- Axions convert into photons in presence of strong magnetic field
- Mass is unknown
- So: narrowband photon signal of an unknown frequency is generated (need to scan frequency)
- Three regimes of haloscope detector

$$\lambda_a = \frac{h}{m_a c}$$

$\lambda_a > d_{exp}$ $\qquad$ $\lambda_a \sim d_{exp}$ $\qquad$ $\lambda_a < d_{exp}$



$m_a$ $\qquad$ $\omega_a \approx \frac{m_a c^2}{\hbar}$

- Lumped Element Reactive
- Resonant
- Propagative

$$m_a[eV] \equiv \frac{m_a[kg]c^2}{q_e} \qquad 1eV = 1.8 \times 10^{-36}[kg]$$

Resonant: $\lambda_a \sim d_{exp} \sim 1cm \rightarrow 1m$ $\qquad$ $\frac{\omega_a}{2\pi} \sim 300\ MHz \rightarrow 30\ GHz$ $\qquad$ $m_a \sim 1\ \mu eV \rightarrow 100\ \mu eV$

# DC Magnetic Haloscopes

Low Mass: Lumped Element
Reactive

Middle Mass: Resonant Cavity
Reactive and Dissipative

High Mass: Propagating

$300\ MHz$ $30\ GHz$ $\frac{\omega_a}{2\pi}\ Hz$

$1.25 \times 10^{-6}$ $1.25 \times 10^{-4}$ $m_a\ eV$

$\lambda_a > d_{exp}$ $\lambda_a \sim d_{exp}$ $\lambda_a < d_{exp}$

ADMX SLIC
RE-ENTRANT CAVITY
ABRACADABRA
SHAFT
DM RADIO
BEAST

ADMX
CULTASK
ORGAN
QUAX
RADES

MADMAX
BREAD

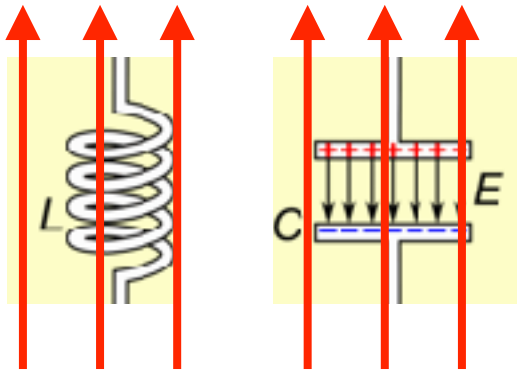


$\vec{B} = B_{DC}\hat{z}$

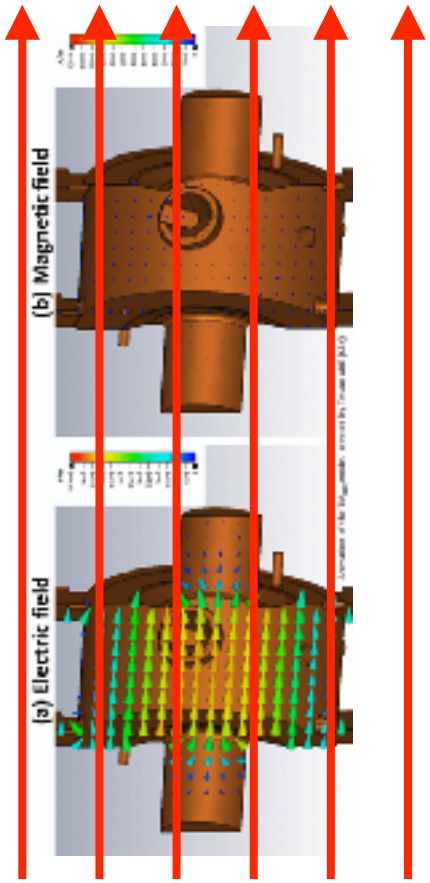


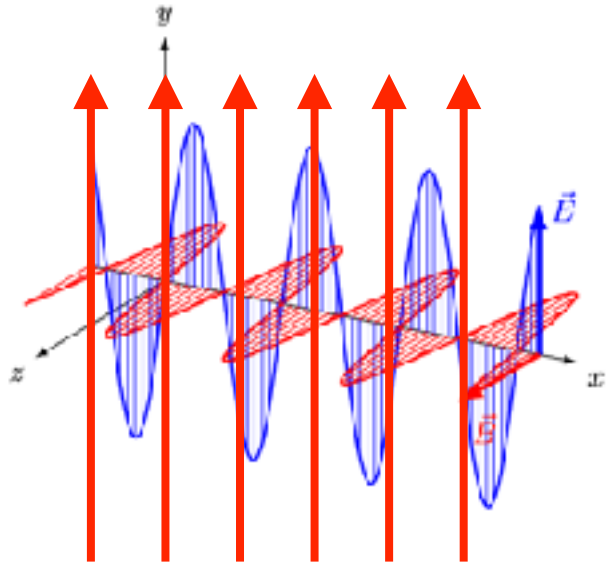

# REMEMBERING POYNTING THEOREM

- Basic conservation law for electromagnetic energy for AC system
- Describes complex power flow (phasors) in a volume, considering: 1) Sources, 2) Storage, 3) Dissipation, 4) Radiation
- The direction and density of power flow at a point is defined by the instantaneous Poynting vector, $\vec{S}(t)$ [W/m²]

## Instantaneous Poynting vector in vacuum

$$\vec{S}_1(t) = \frac{1}{\mu_0}\vec{E}_1(t) \times \vec{B}_1(t) = \frac{1}{2}\left(\mathbf{E}_1 e^{-j\omega_1 t} + \mathbf{E}_1^* e^{j\omega_1 t}\right) \times \frac{1}{2\mu_0}\left(\mathbf{B}_1 e^{-j\omega_1 t} + \mathbf{B}_1^* e^{j\omega_1 t}\right)$$

$$= \frac{1}{2\mu_0}\mathrm{Re}\left(\mathbf{E}_1 \times \mathbf{B}_1^*\right) + \frac{1}{2\mu_0}\mathrm{Re}\left(\mathbf{E}_1 \times \mathbf{B}_1\, e^{-j2\omega_1 t}\right),$$

$$\langle \vec{S}_1 \rangle = \frac{1}{T}\int_0^T \vec{S}_1(t)dt = \frac{1}{T}\int_0^T \left[\frac{1}{2\mu_0}\mathrm{Re}\left(\mathbf{E}_1 \times \mathbf{B}_1^*\right) + \frac{1}{2\mu_0}\mathrm{Re}\left(\mathbf{E}_1 \times \mathbf{B}_1 e^{-2j\omega t}\right)\right] dt = \frac{1}{2\mu_0}\mathrm{Re}\left(\mathbf{E}_1 \times \mathbf{B}_1^*\right)$$

## Complex Poynting vector in vacuum

- The corresponding phasor form of the Poynting vector

$$\mathbf{S}_1 = \frac{1}{2\mu_0}\mathbf{E}_1 \times \mathbf{B}_1^* \quad \text{and} \quad \mathbf{S}_1^* = \frac{1}{2\mu_0}\mathbf{E}_1^* \times \mathbf{B}_1,$$

$$\mathrm{Re}\left(\mathbf{S}_1\right) = \frac{1}{2}(\mathbf{S}_1 + \mathbf{S}_1^*) \quad \text{and} \quad j\,\mathrm{Im}\left(\mathbf{S}_1\right) = \frac{1}{2}(\mathbf{S}_1 - \mathbf{S}_1^*).$$

Time Average Power

Reactive Power

## Combing the Poynting vector with Maxwell's Equations -> Leads to Poynting Theorem

1) Instantaneous Poynting Theorem
2) Complex Poynting Theorem

# CONSIDERATION OF POYNTING VECTOR IN AXION ELECTRODYNAMICS: THE ABRAHAM-MINKOWSKI CONTROVERSY

* Poynting vector in Electrodynamics -> Over a century of Controversy, chose $\mathbf{S}_{\mathrm{M}} = \frac{1}{\epsilon_0 \mu_0}(\mathbf{D} \times \mathbf{B})$ or $\mathbf{S}_{\mathrm{A}} = (\mathbf{E} \times \mathbf{H})$ in matter ?

* Pfeifer et. al., Momentum of an electromagnetic wave in dielectric media, Reviews of Modern Physics 79(4), 1197-1216 (2007). -> Addresses the Abraham-Minkowski controversy, conclude: both valid depends on system.

* Kinsler et al., Four Poynting theorems, Eur. J. Phys. 30 (2009) 983–993. Enables interpretation of four Poynting vectors and interaction with the medium -> choosing the best Poynting vector depend on the medium and experimental set up.

* DJ Griffiths, Resource Letter EM-1: Electromagnetic Momentum, Am. J. Phys. 80, 7 (2012) -> Abraham–Minkowski controversy regarding the field momentum in polarizable and magnetizable media: Correct one depends on the detailed nature of the material.

VII. MOMENTUM OF PHOTONS

$$\mathbf{p}_{\text{total}} = \mathbf{p}_{\text{kinetic}} + \int \mathbf{g}_A \, d^3\mathbf{r} = \mathbf{p}_{\text{canonical}} + \int \mathbf{g}_M \, d^3\mathbf{r}$$

$$\begin{cases} p_{\mathrm{A}} = \frac{1}{n}\left(\frac{\hbar\nu}{c}\right) & \text{(Abraham)} \\ p_{\mathrm{M}} = n\left(\frac{\hbar\nu}{c}\right) & \text{(Minkowski)} \end{cases}$$

Size of the central maximum in single-slit diffraction

$$\Delta\theta' = \begin{cases} n\,\Delta\theta & \text{(Abraham)} \\ \frac{1}{n}\,\Delta\theta & \text{(Minkowski)} \end{cases}$$

Measured by Jones et al, when media does not move

# Four Poynting theorems

Paul Kinsler,* Alberto Favaro, and Martin W. McCall
*Blackett Laboratory, Imperial College, Prince Consort Road, London SW7 2AZ, United Kingdom.*
(Dated: November 9, 2016)

The Poynting vector is an invaluable tool for analysing electromagnetic problems. However, even a rigorous stress-energy tensor approach can still leave us with the question: is it best defined as $\vec{E}\times\vec{H}$, or as $\vec{D}\times\vec{B}$? Typical electromagnetic treatments provide yet another perspective: they regard $\vec{E}\times\vec{B}$ as the appropriate definition, because $\vec{E}$ and $\vec{B}$ are taken to be the fundamental electromagnetic fields. The astute reader will even notice the fourth possible combination of fields: i.e. $\vec{D}\times\vec{H}$. Faced with this diverse selection, we have decided to treat each possible flux vector on its merits, deriving its associated energy continuity equation but applying minimal restrictions to the allowed host media. We then discuss each form, and how it represents the response of the medium. Finally, we derive a propagation equation for each flux vector using a directional fields approach; a useful result which enables further interpretation of each flux and its interaction with the medium.

*Published in Eur. J. Phys. 30, 983 (2009).*[1]
This arXiv version has updates not present in the published version.

arXiv:0908.1721v4

## II. MAXWELL'S EQUATIONS

Maxwell's equations for the electric field $\vec{E}$ and magnetic field $\vec{B}$ in a medium are

$$\nabla\cdot\vec{E} = \frac{1}{\epsilon_0}\rho_b + \frac{1}{\epsilon_0}\rho_f \quad = \frac{1}{\epsilon_0}\rho \tag{1}$$

$$\nabla\cdot\vec{B} = 0 \tag{2}$$

$$\nabla\times\vec{E} = -\partial_t\vec{B} \tag{3}$$

$$\nabla\times\vec{B} = \mu_0\vec{J}_b + \mu_0\vec{J}_f + \mu_0\epsilon_0\partial_t\vec{E}, \tag{4}$$

where $(\rho_b,\vec{J}_b)$ and $(\rho_f,\vec{J}_f)$ are respectively the bound and free (charge, current) densities. As an alternative, we can define an electric polarization $\vec{P}$ and magnetization $\vec{M}$, and

$$\vec{J}_b = \vec{J}_P + \vec{J}_M \quad = \partial_t\vec{P} + \nabla\times\vec{M} \tag{5}$$

$$\rho_b = -\nabla\cdot\vec{P} \tag{6}$$

$$\vec{D} = \epsilon_0\vec{E} + \vec{P} \tag{7}$$

$$\vec{H} = \frac{1}{\mu_0}\vec{B} - \vec{M}. \tag{8}$$

These allow us to rewrite Maxwell's equations as

$$\nabla\cdot\vec{D} = \rho_f \tag{9}$$

$$\nabla\cdot\vec{B} = 0 \tag{10}$$

$$\nabla\times\vec{E} = -\mu_0\partial_t\left(\vec{H}+\vec{M}\right) \tag{11}$$

$$\nabla\times\vec{H} = \vec{J}_f + \partial_t\vec{D} \quad = \vec{J}_f + \partial_t\left(\epsilon_0\vec{E}+\vec{P}\right), \tag{12}$$

We can even rewrite eqn. (11) in the unconventional form

$$\nabla\times\vec{D} = -\epsilon_0\mu_0\partial_t\left(\vec{H}+\vec{M}\right) + \nabla\times\vec{P} \tag{13}$$

$$= -\epsilon_0\mu_0\partial_t\vec{H} - \epsilon_0\mu_0\vec{K}_b, \tag{14}$$

where we have defined

$$\vec{K}_b = \vec{K}_P + \vec{K}_M \quad = -\frac{1}{\epsilon_0\mu_0}\nabla\times\vec{P} + \partial_t\vec{M}, \tag{15}$$

$$\sigma_b = -\nabla\cdot\vec{M}. \tag{16}$$

This $\vec{K}_b$ appears in the same place as a monopole current would if such were allowed; $\sigma_b$ is the *bound* magnetic pole density. Note that $\vec{K}_b$ and $\sigma_b$ are merely a way of representing the (local) material response; we are not claiming that some process actually generates true magnetic monopoles inside the material [14][2]. Strictly speaking, this is also true of the bound electric charge and its currents – they are a mechanism used solely to represent the behaviour of the medium.

Further, and just as for the ficticious bound electric charge density, the ficticious bound monopole density necessarily integrates to zero over all space. Thus the material response could, in principle, be re-represented as magnetic dipoles instead of monopoles.

# GENERAL FORM OF MAXWELL'S EQUATIONS IN MATTER

## Bound Electric and/or Magnetic Current Models?

### 1) Modified Ampere's Law (mmf generator)

$$\nabla \times B = \mu_0(\vec{J}_f + \vec{J}_b)\,; \quad \vec{J}_b = \vec{J}_P + \vec{J}_M = \partial_t \vec{P} + \nabla \times \vec{M}$$

$$\varrho_P = -\nabla \cdot \vec{P} \quad \leftrightarrow \quad \nabla \cdot \vec{J}_P = -\partial_t \rho_b$$

Dielectric term

Polarization Current

Permanent Magnet term

### 2) Modified Faraday's Law (emf generator)

$$\nabla \times \vec{D} = -\epsilon_0\mu_0\partial_t(\vec{H} + \vec{M}) + \nabla \times \vec{P} = -\epsilon_0\mu_0\partial_t\vec{H} - \epsilon_0\vec{J}_{mb}$$

$$\vec{J}_{mb} = \vec{J}_{mM} + \vec{J}_{mP} = \mu_0\partial_t\vec{M} - \frac{1}{\epsilon_0}\nabla \times \vec{P}$$

$$\varrho_M = -\mu_0\nabla \cdot \vec{M} \quad \leftrightarrow \quad \nabla \cdot \vec{J}_{mM} = -\partial_t\varrho_M$$

Magnetisation Magnetic Current

Permanent Electret term (Non-conservative, Metastable)

Permanent Magnet

$$\rightarrow \nabla \times \vec{M} \neq 0$$

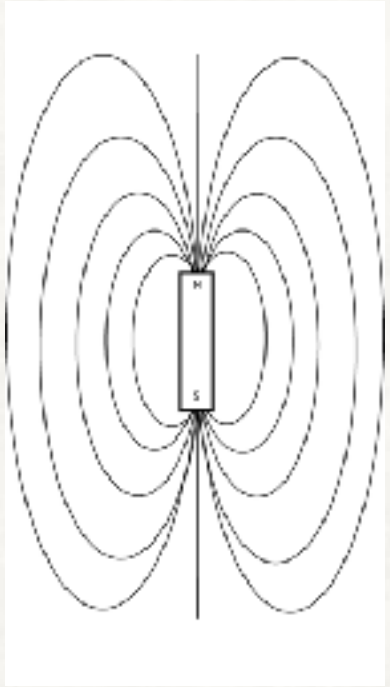

Model as fictitious bound monopole currents or fictitious bound "Ampèrian"currents

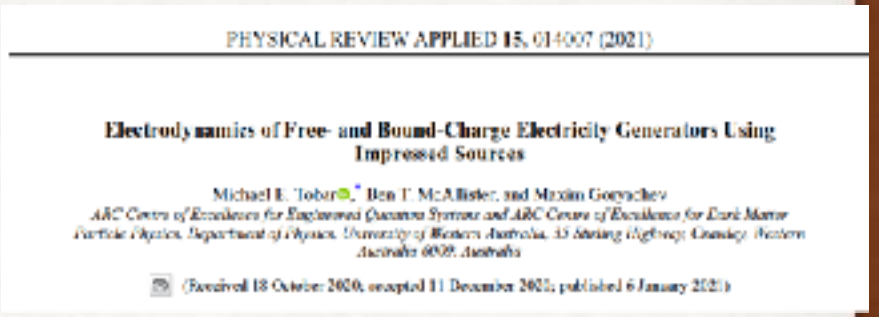

PHYSICAL REVIEW APPLIED 15, 014007 (2021)

**Electrodynamics of Free- and Bound-Charge Electricity Generators Using Impressed Sources**

Michael E. Tobar,* Ben T. McAllister, and Maxim Goryachev

ARC Centre of Excellence for Engineered Quantum Systems and ARC Centre of Excellence for Dark Matter Particle Physics, Department of Physics, University of Western Australia, 35 Stirling Highway Crawley, Western Australia 6009, Australia

(Received 18 October 2020; accepted 11 December 2020; published 6 January 2021)

Bound Charge Voltage Source Electret

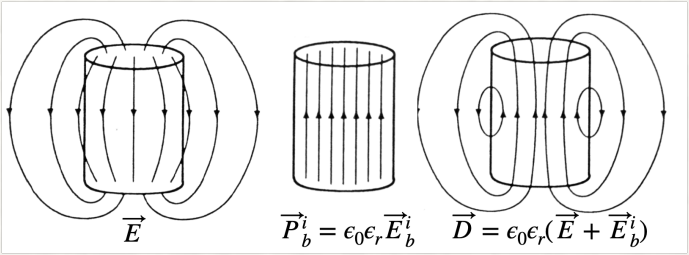


Polarization can also be defined in free charge voltage source

$$\nabla \times \vec{P} \neq 0$$

$$\epsilon_0\nabla \times \vec{E}_i$$

Engineers call impressed field

Could label as Fictitious Electric field

# Electromotive force

From Wikipedia, the free encyclopedia

*Not to be confused with Electromagnetic field.*

In electromagnetism and electronics, **electromotive force (emf,** denoted $\mathcal{E}$ and measured in volts)[1] is the electrical action produced by a non-electrical source.[2] Devices (known as *transducers*) provide an emf[3] by converting other forms of energy into electrical energy,[3] such as batteries (which convert chemical energy) or generators (which convert mechanical energy).[2] Sometimes an analogy to water pressure is used to describe electromotive force.[4] (The word "force" in this case is not used to mean forces of interaction between bodies).

**Fictitious Force**

- EMF per unit length [V/m], is like a Fictitious Electric field
- Does not conform to Maxwell's equations
- Outside Maxwell's equations
- Identify a similar non-conservative term in Axion Modified Electrodynamics

$$\nabla \times \vec{P} \neq 0$$

# NON CONSERVATIVE MAXWELL'S EQUATIONS

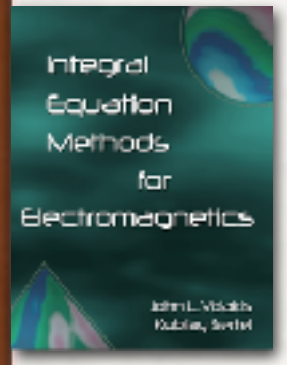


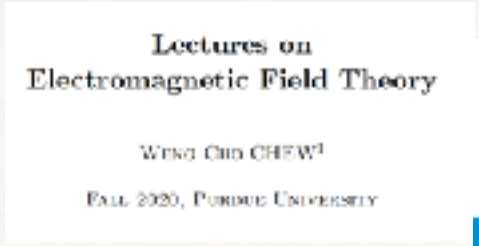





**Model of Current and Voltage Source (Impressed)**

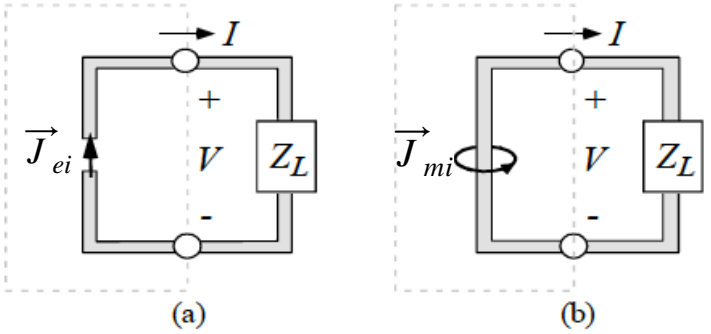


**Figure 1.5** Electromagnetic representation of independent circuit sources. (a) Current generator (impressed electric current filament); (b) Voltage generator (impressed magnetic current loop).

- Engineering Systems are in general "non-conservative"
- Engineers keep Maxwell's equations general, with both fictitious magnetic and electric sources
- Magnetic monopoles do not exist, but magnetic dipoles do!
- Magnetic charge occurs in pairs, does not contradict no monopoles

**Phasor Form for AC Sources**

$$\mathbf{J}_e = \mathbf{J}_{ei} + \mathbf{J}_{ec} = \mathbf{J}_{ei} + \sigma_e \mathbf{E}$$
$$\mathbf{J}_m = \mathbf{J}_{mi} + \mathbf{J}_{mc} = \mathbf{J}_{ei} + \sigma_m \mathbf{H}$$

- Subscript *i* -> Impressed (or excitation Currents}
- Subscript c -> Loss term (conductivity)

$$\nabla \times \mathbf{H} = \mathbf{J}_{ei} + j\omega\epsilon_o\tilde{\epsilon}_r\mathbf{E}$$
$$\nabla \times \mathbf{E} = -\mathbf{J}_{mi} - j\omega\mu_o\tilde{\mu}_r\mathbf{H}$$

**$\rho_m$: magnetic pole distribution integrates to 0**

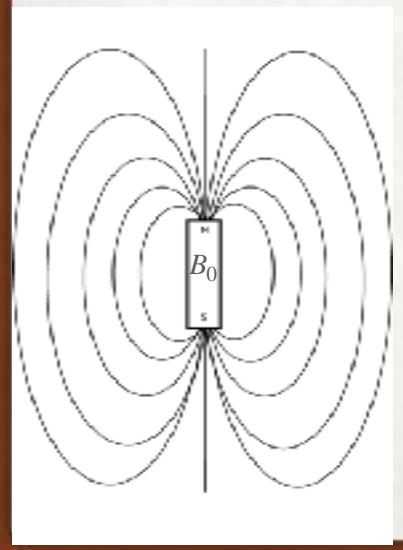


**Surface Magnetic Charge**

$+\sigma_m = B_0$

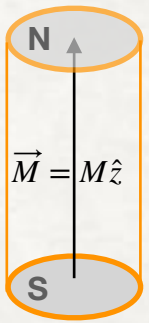


$-\sigma_m = -B_0$

**Spinning magnet of radius R**
**Unipolar Generator**

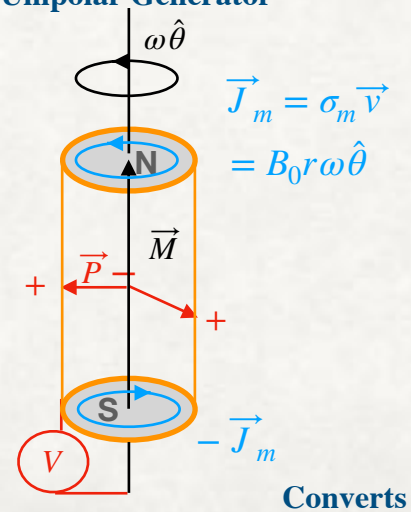


$V = B_0 R\omega$

**Converts mechanical motion to EM energy**
**Fictitious electric field: External Lorentz force/unit charge**

# COMPLEX POYNTING THEOREM: CIRCUITS/ANTENNAS

SECOND EDITION

## ADVANCED ENGINEERING ELECTROMAGNETICS

Constantine A. Balanis

Even though magnetic sources do not exist, they can be engineered

**Model of Current and Voltage Source (Impressed)**

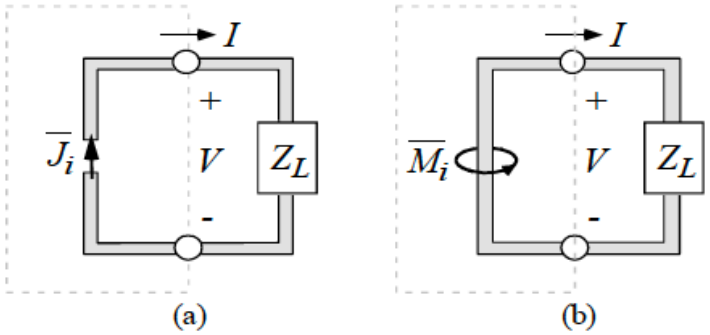


**Figure 1.5** Electromagnetic representation of independent circuit sources. (a) Current generator (impressed electric current filament); (b) Voltage generator (impressed magnetic current loop).

Here Balanis uses $\overrightarrow{M}$ as magnetic current

$$-\iiint_V \nabla\cdot(\tfrac{1}{2}\mathbf{E}\times\mathbf{H}^*)\,dv = -\oint_S (\tfrac{1}{2}\mathbf{E}\times\mathbf{H}^*)\cdot d\mathbf{s}$$

$$= \frac{1}{2}\iiint_V (\mathbf{H}^*\cdot\mathbf{M}_i \mid \mathbf{E}\cdot\mathbf{J}_i^*)\,dv$$

$$+\frac{1}{2}\iiint_V \sigma|\mathbf{E}|^2\,dv + j2\omega\iiint_V (\tfrac{1}{4}\mu|\mathbf{H}|^2 - \tfrac{1}{4}\varepsilon|\mathbf{E}|^2)\,dv$$

or

$$\frac{1}{2}\iiint_V (\mathbf{H}^*\cdot\mathbf{M}_i \mid \mathbf{E}\cdot\mathbf{J}_i^*)\,dv = \oint_S (\tfrac{1}{2}\mathbf{E}\times\mathbf{H}^*)\cdot d\mathbf{s} \mid \frac{1}{2}\iiint_V \sigma|\mathbf{E}|^2\,dv$$

$$+j2\omega\iiint_V (\tfrac{1}{4}\mu|\mathbf{H}|^2 - \tfrac{1}{4}\varepsilon|\mathbf{E}|^2)\,dv \qquad (1\text{-}76)$$

which can be written as

$$P_s = P_e \mid P_d \mid j2\omega(W_m \quad W_e) \qquad (1\text{-}76a)$$

where

$$P_s = -\frac{1}{2}\iiint_V (\mathbf{H}^*\cdot\mathbf{M}_i + \mathbf{E}\cdot\mathbf{J}_i^*)\,dv = \text{supplied complex power (W)} \qquad (1\text{-}76b)$$

$$P_e \quad \oint_S \left(\frac{1}{2}\mathbf{E}\times\mathbf{H}^*\right)\cdot d\mathbf{s} \quad \text{exiting complex power (W)} \qquad (1\text{-}76c)$$

$$P_d \quad \frac{1}{2}\iiint_V \sigma|\mathbf{E}|^2\,dv \quad \text{dissipated real power (W)} \qquad (1\text{-}76d)$$

$$\overline{W}_m \quad \iiint_V \tfrac{1}{4}\mu|\mathbf{H}|^2\,dv \quad \text{time-average magnetic energy (J)} \qquad (1\text{-}76e)$$

$$W_e = \iiint_V \tfrac{1}{4}\varepsilon|\mathbf{E}|^2\,dv = \text{time-average electric energy (J)} \qquad (1\text{-}76f)$$

# COMPLEX POYNTING THEOREM: CIRCUITS/ANTENNAS

$$P_{av} = \frac{1}{2}\,\mathrm{Re}\oint_{S_c} (\mathbf{E}\times\mathbf{H}^*)\cdot d\mathbf{s}$$

Average radiated power outside V

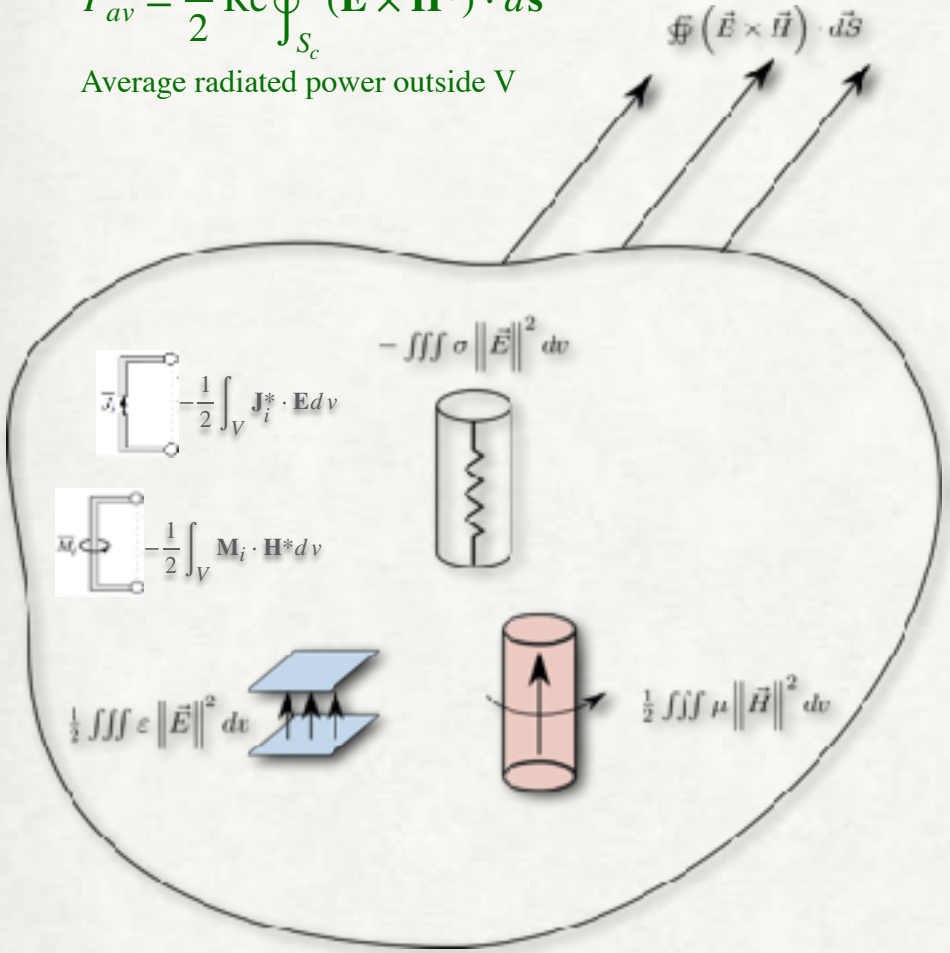


Here Balanis uses $\vec{M}$ as magnetic current

**Maxwell's Equations Phasor Form**

$$\mathbf{E}\cdot\nabla\times\mathbf{H}^* = \mathbf{J}_i^*\cdot\mathbf{E} - j\omega\epsilon^*\mathbf{E}^*\cdot\mathbf{E} = \mathbf{J}_i^*\cdot\mathbf{E} - j\omega\epsilon^*|\mathbf{E}|^2$$

$$\mathbf{H}^*\cdot\nabla\times\mathbf{E} = -\mathbf{M}_i\cdot\mathbf{H}^* - j\omega\mu\mathbf{H}\cdot\mathbf{H}^* = -\mathbf{M}^i\cdot\mathbf{H}^* - j\omega\mu|\mathbf{H}|^2$$

**Vector Identity**

$$\nabla\cdot(\mathbf{E}\times\mathbf{H}^*) = \mathbf{H}^*\cdot\nabla\times\mathbf{E} - \mathbf{E}\cdot\nabla\times\mathbf{H}^*$$

$$\nabla\cdot(\mathbf{E}\times\mathbf{H}^*) = j\omega\epsilon^*|\mathbf{E}|^2 - j\omega\mu|\mathbf{H}|^2 - \mathbf{J}_i^*\cdot\mathbf{E} - \mathbf{M}_i\cdot\mathbf{H}^*$$

**Integrate over volume, apply Divergence theorem**

$$\frac{1}{2}\oint_{S_c}(\mathbf{E}\times\mathbf{H}^*)\cdot d\mathbf{s} = \frac{1}{2}\int_V \left[j\omega\epsilon^*|\mathbf{E}|^2 + j\omega\mu|\mathbf{H}|^2 - \mathbf{J}_i^*\cdot\mathbf{E} - \mathbf{M}_i\cdot\mathbf{H}^*\right] dv$$

**Real part is average power: Imaginary part is complex power**

$$\frac{1}{2}\,\mathrm{Re}\oint_{S_c}(\mathbf{E}\times\mathbf{H}^*)\cdot d\mathbf{s} = P_{ei} + P_{mi} - P_d$$

$$P_d = \frac{1}{2}\int_V \sigma|\mathbf{E}|^2 dv = \text{ average power dissipated in } V$$

$$P_{ei} = -\frac{1}{2}\int_V \mathrm{Re}\left(\mathbf{J}_i^*\cdot\mathbf{E}\right) dv = \text{ average outgoing power due to the source } \mathbf{J}_i^*$$

$$P_{mi} = -\frac{1}{2}\int_V \mathrm{Re}\left(\mathbf{M}_i\cdot\mathbf{H}^*\right) dv = \text{ average outgoing power due to the source } \mathbf{M}_i$$

**complex power**

$$\frac{1}{2}Im\oint_{S_c}(\mathbf{E}\times\mathbf{H}^*)\cdot d\mathbf{s} = 2\omega\left[W_e - W_m\right] - \frac{1}{2}Im\int\left[\mathbf{J}_i^*\cdot\mathbf{E} + \mathbf{M}_i\cdot\mathbf{H}^*\right] dv$$

$$W_e = \frac{1}{4}\int_V \epsilon_o\epsilon_r|\mathbf{E}|^2 dv = \text{ average electric energy in } V$$

$$W_m = \frac{1}{4}\int_V \mu_o\mu_r|\mathbf{H}|^2 dv = \text{ average magnetic energy in } V$$

# IMAGINARY POYNTING VECTOR INSIDE CAVITY

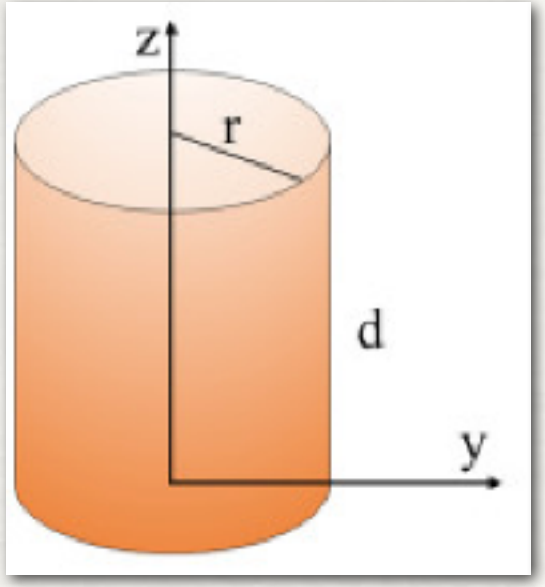


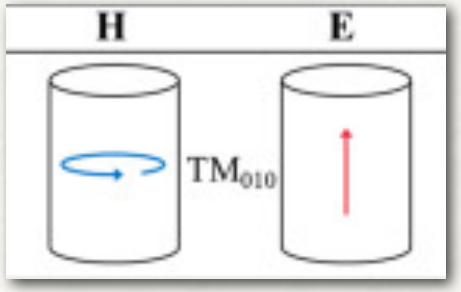


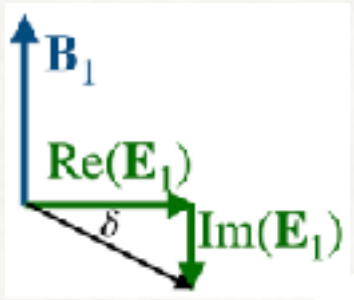


$TM_{0n0}$

$$\tilde{H}_\phi = -j\tilde{E}_0(\omega\epsilon)\frac{r_c}{\chi_{0n}}J_0'\left(\frac{\chi_{0n}}{r_c}r\right)$$

$$\tilde{E}_z = \tilde{E}_0 J_0\left(\frac{\chi_{0n}}{r_c}r\right)$$

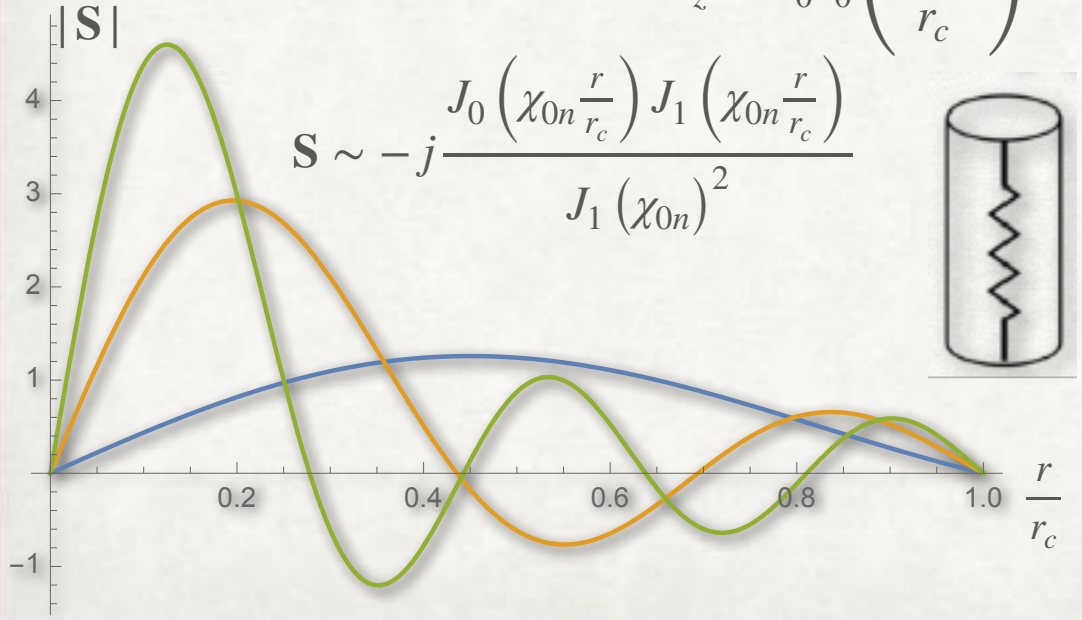


$$\mathbf{S} \sim -j\frac{J_0\left(\chi_{0n}\frac{r}{r_c}\right)J_1\left(\chi_{0n}\frac{r}{r_c}\right)}{J_1\left(\chi_{0n}\right)^2}$$



However Dissipation Gives real part of Poynting vector

$$\vec{S} = \vec{E} \times \vec{H}$$

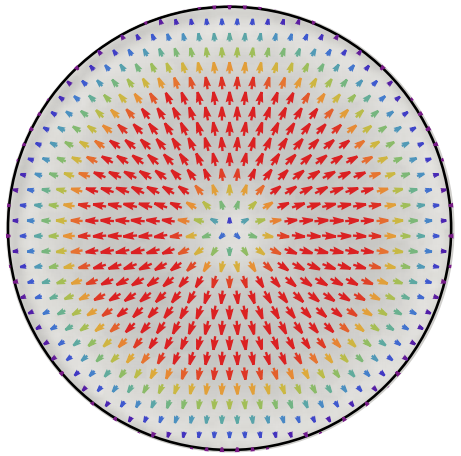

$TM_{010}$

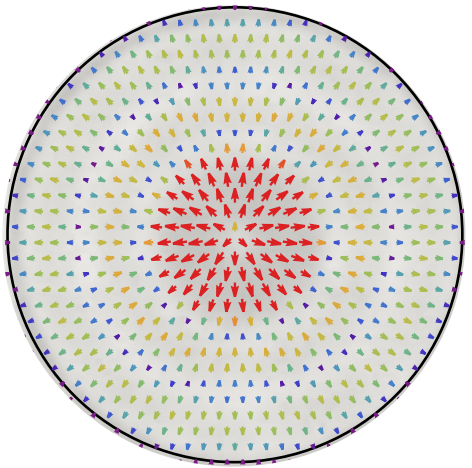

$TM_{020}$

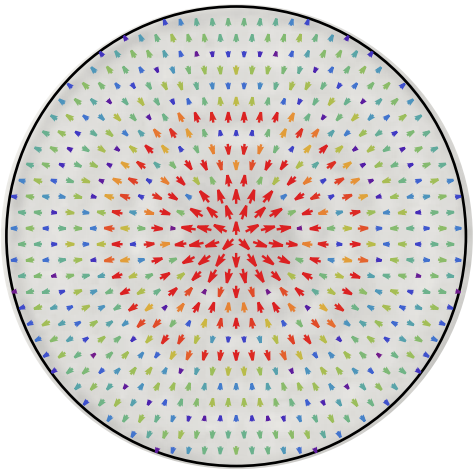

$TM_{030}$

At resonance Poynting vector is REAL
Small dissipation: Power builds up
Enhanced power per cycle with large Q

# EQUIVALENT CIRCUIT AND POYNTING VECTOR

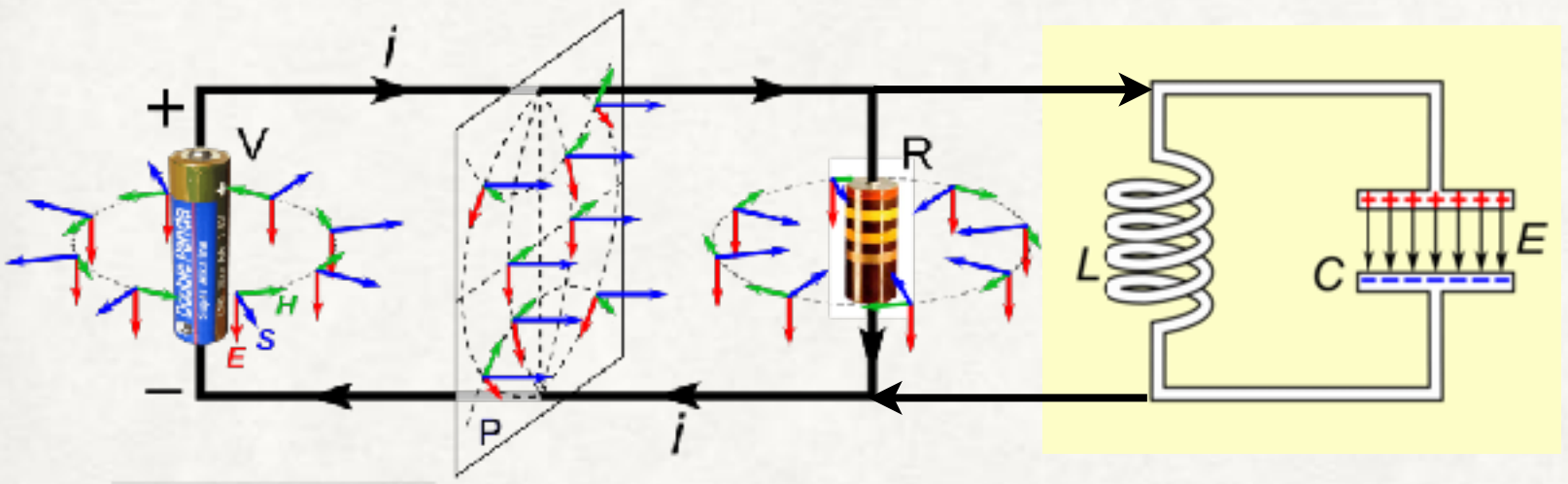


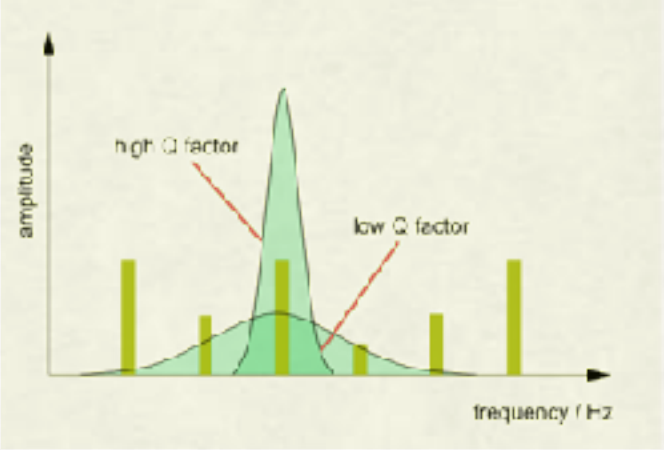


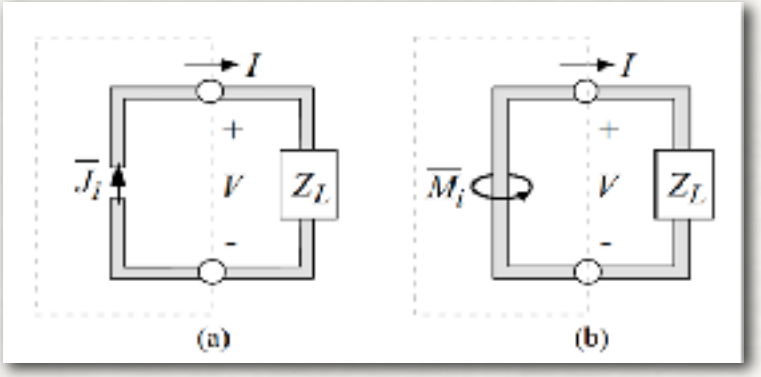


$$P_{in} = \frac{1}{2}VI^* = \frac{1}{2}II^*\left(R + j\omega L + \frac{1}{j\omega C}\right)$$

$$P_{in} = P_{loss} + 2j\omega\left(U_m - U_e\right)$$

$$U_m = \tfrac{1}{4}LII^* \text{ and } U_e = \tfrac{1}{4}CVV^* \qquad P_{loss} = \tfrac{1}{2}RII^*$$

$$U_m = \frac{1}{4}\mathrm{Re}\iiint \overline{H}^* \cdot \overline{B}\, dV \qquad U_e = \frac{1}{4}\mathrm{Re}\iiint \overline{E} \cdot \overline{D}^* dV$$

- Reactive Power Oscillates between Electric and Magnetic field in the cavity as Stored Energy
- Source does not need to provide reactive power on resonance
- Steady state: Source power balanced by dissipative power in resonator
- High-Q, low-loss per cycle, power in resonator builds up (circulating power put into narrow frequency bandwidth)

**Here Balanis uses $\overrightarrow{M}$ as magnetic current**

# PROPAGATING POYNTING VECTOR IS REAL

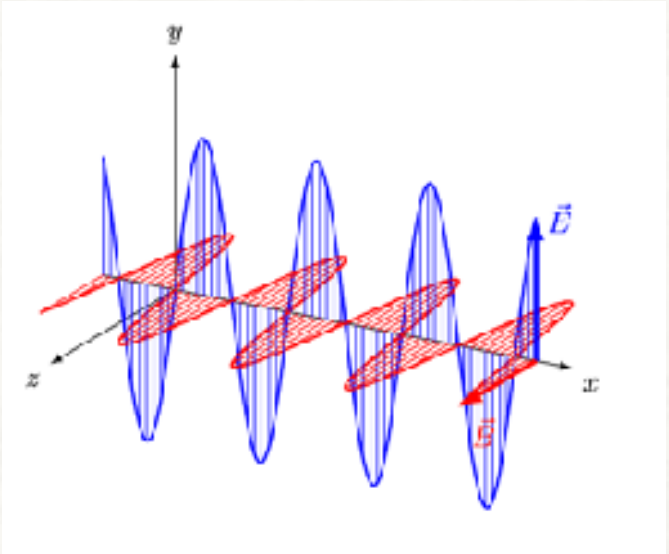


# INDUCTOR OR CAPACITOR HAS AN IMAGINARY POYNTING VECTOR

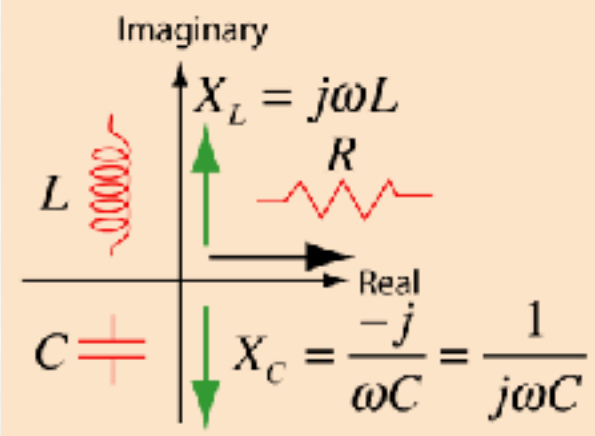


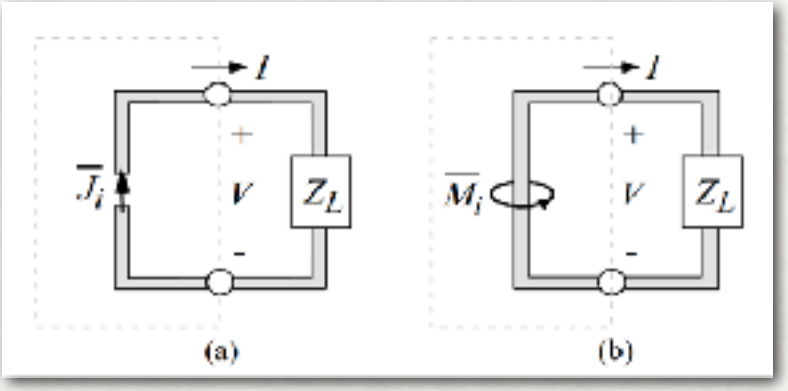

# Axion-Photon Coupling

- Axion is predicted to couple to photons, coupling parameter, $g_{a\gamma\gamma}$
- Two-photon transition, interaction Hamiltonian density
  $\mathscr{H} = \mathscr{H}_{\mathrm{EM}} + \mathscr{H}_a + \mathscr{H}_{int}: \quad \mathscr{H}_{int} = \varepsilon_0 c g_{a\gamma\gamma} a \mathbf{E}\cdot\mathbf{B}$

**Equation of Motion: Maxwell's Equations**

$$\nabla \times \vec{B}_1 = \mu_0\epsilon_0\partial_t \vec{E}_1 + \mu_0 \vec{J}_{e1}$$
$$\nabla \times \vec{E}_1 = -\partial_t \vec{B}_1$$
$$\nabla \cdot \vec{B}_1 = 0$$
$$\nabla \cdot \vec{E}_1 = \epsilon_0^{-1}\rho_{e_1}$$

**Axion Equation of Motion: Klein–Gordon equation for massive spin 0 particle**

$$\left(\Box + \frac{m_a^2 c^2}{\hbar^2}\right) a = -\, g_{a\gamma\gamma}\varepsilon_0 c \mathbf{E}\cdot\mathbf{B}$$

$$\Box = c^{-2}\partial_t\partial_t - \nabla^2$$

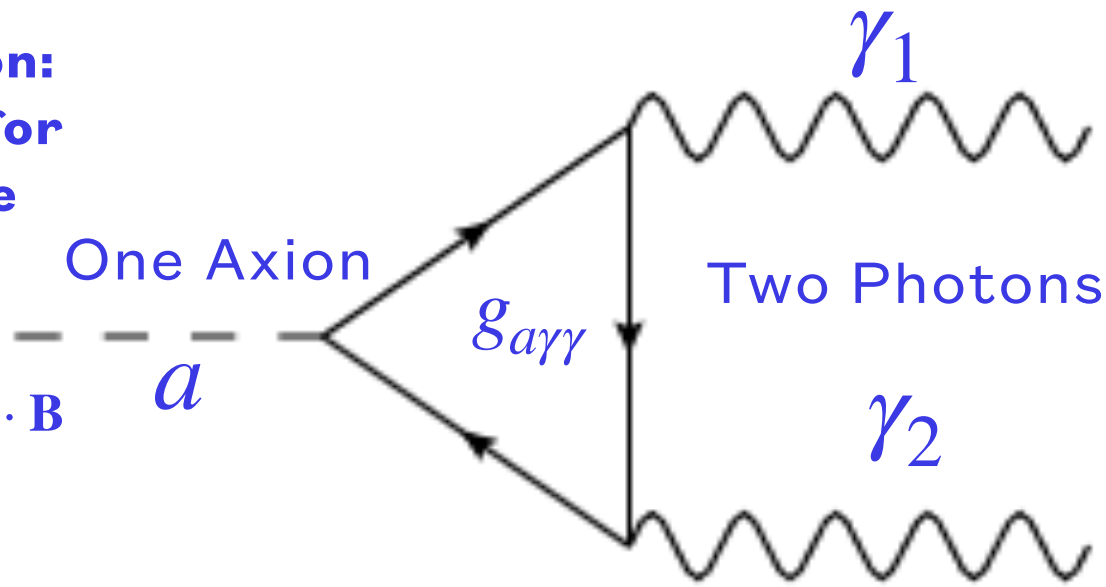


$$\nabla \times \vec{B}_2 = \mu_0\epsilon_0\partial_t \vec{E}_2 + \mu_0 \vec{J}_{e2}$$
$$\nabla \times \vec{E}_2 = -\partial_t \vec{B}_2$$
$$\nabla \cdot \vec{B}_2 = 0$$
$$\nabla \cdot \vec{E}_2 = \epsilon_0^{-1}\rho_{e_2}$$

**Axion Coupling to two Photonic Degree of Freedoms Modifies Electrodynamics**

# Haloscopes

- Axions convert into photons in presence of strong background electromagnetic field

Axion Equation of Motion:

Klein-Gordon equation for massive spin 0 particle

$$a(t) = \frac{1}{2}\left(\tilde{a}e^{-j\omega_a t} + \tilde{a}^* e^{j\omega_a t}\right)$$
$$= \mathrm{Re}\left(\tilde{a}e^{-j\omega_a t}\right)$$

Modified Axion Electrodynamics

(Represents two photons)

$$\nabla \cdot \vec{E} = \frac{\rho_e}{\varepsilon_0} + c g_{a\gamma\gamma} \vec{B} \,.\, \nabla a$$
$$\nabla \times \vec{B} - \frac{1}{c^2}\partial_t \vec{E} =$$
$$\mu_0 \vec{J}_e - g_{a\gamma\gamma}\epsilon_0 c\left(\vec{B}\partial_t a + \nabla a \times \vec{E}\right)$$
$$\nabla \cdot \vec{B} = 0$$
$$\nabla \times \vec{E} + \partial_t \vec{B} = 0$$

1) Background field (subscript zero)

2) Created Photon Field (subscript 1)

$$\epsilon_0 \nabla \cdot \vec{E}_1 = \rho_{e1} + \rho_{ab}$$
$$\frac{1}{\mu_0}\nabla \times \vec{B}_1 - \epsilon_0 \partial_t \vec{E}_1 = \vec{J}_{e1} + \vec{J}_{ab} + \vec{J}_{ae}$$

$$\rho_{ab} = g_{a\gamma\gamma}\epsilon_0 c \nabla \cdot \left(a(t)\vec{B}_0(\vec{r},t)\right)$$
$$\vec{J}_{ab} = -g_{a\gamma\gamma}\epsilon_0 c \partial_t \left(a(t)\vec{B}_0(\vec{r},t)\right)$$
$$\vec{J}_{ae} = -g_{a\gamma\gamma}\epsilon_0 c \nabla \times \left(a(t)\vec{E}_0(\vec{r},t)\right)$$
$$\nabla \cdot \vec{J}_{ab} = -\partial_t \rho_{ab}$$

**Source Terms generate Photons-> From background fields mixing with axion**

# Photonic Haloscope Equations in terms of Auxiliary Fields

## Modified Axion Electrodynamics

**(Represents two photons)**

$$\nabla \cdot \vec{E} = \frac{\rho_e}{\varepsilon_0} + c g_{a\gamma\gamma} \vec{B} \cdot \nabla a$$

$$\nabla \times \vec{B} - \frac{1}{c^2}\partial_t \vec{E} = \mu_0 \vec{J}_e - g_{a\gamma\gamma}\epsilon_0 c \left( \vec{B}\partial_t a + \nabla a \times \vec{E} \right)$$

$$\nabla \cdot \vec{B} = 0$$

$$\nabla \times \vec{E} + \partial_t \vec{B} = 0$$

## Applied Background Field

$$\nabla \times \vec{B}_0 = \mu_0 \epsilon_0 \partial_t \vec{E}_0 + \mu_0 \vec{J}_{e_0}$$

$$\nabla \times \vec{E}_0 = -\partial_t \vec{B}_0$$

$$\nabla \cdot \vec{B}_0 = 0$$

$$\nabla \cdot \vec{E}_0 = \epsilon_0^{-1} \rho_{e_0}$$

## Measure Created Photon

$$\nabla \cdot \left( \vec{E}_1(\vec{r},t) - g_{a\gamma\gamma} a(t) c \vec{B}_0(\vec{r},t) \right) = \frac{\rho_{e_1}}{\epsilon_0}$$

$$\nabla \times \left( \vec{B}_1(\vec{r},t) + \frac{g_{a\gamma\gamma} a(t)}{c} \vec{E}_0(\vec{r},t) \right)$$

$$-\frac{1}{c^2}\partial_t \left( \vec{E}_1(\vec{r},t) - g_{a\gamma\gamma} a(\vec{r},t) c \vec{B}_0(\vec{r},t) \right) = \mu_0 \vec{J}_{e_1}$$

$$\nabla \cdot \vec{B}_1(\vec{r},t) = 0$$

$$\nabla \times \vec{E}_1(\vec{r},t) + \partial_t \vec{B}_1(\vec{r},t) = 0.$$

$$\nabla \cdot \vec{D}_1 = \rho_{e_1}$$

$$\nabla \times \vec{H}_1 - \partial_t \vec{D}_1 = \vec{J}_{e_1}$$

$$\nabla \cdot \vec{B}_1(\vec{r},t) = 0$$

$$\nabla \times \vec{E}_1(\vec{r},t) + \partial_t \vec{B}_1(\vec{r},t) = 0,$$

## Constitutive Relations(Include Matter)

$$\vec{H}_1(\vec{r},t) = \frac{\vec{B}_1}{\mu_0} - \vec{M}_1 - \vec{M}_{a1};$$

$$\vec{D}_1(\vec{r},t) = \epsilon_0 \vec{E}_1 + \vec{P}_1 + \vec{P}_{a1}$$

$$\vec{M}_{a1} = -g_{a\gamma\gamma} a(t) c \epsilon_0 \vec{E}_0(\vec{r},t) \text{ and } \frac{1}{\epsilon_0}\vec{P}_{a1} = -g_{a\gamma\gamma} a(t) c \vec{B}_0(\vec{r},t)$$

$$\nabla \times \vec{D}_1(\vec{r},t) = -\partial_t \vec{B}_1(\vec{r},t) + \nabla \times (\vec{P}_1 + \vec{P}_{a1})$$

$$\nabla \times \vec{P}_{a1} \neq 0 = -g_{a\gamma\gamma} a(t) c \nabla \times \vec{B}_0(\vec{r},t) \quad (\nabla a = 0)$$

$$\vec{J}_{ab}(\vec{r},t) = \frac{\partial \vec{P}_{a1}(\vec{r},t)}{\partial t}$$

$$\lambda_a = \frac{h}{m_a c}$$

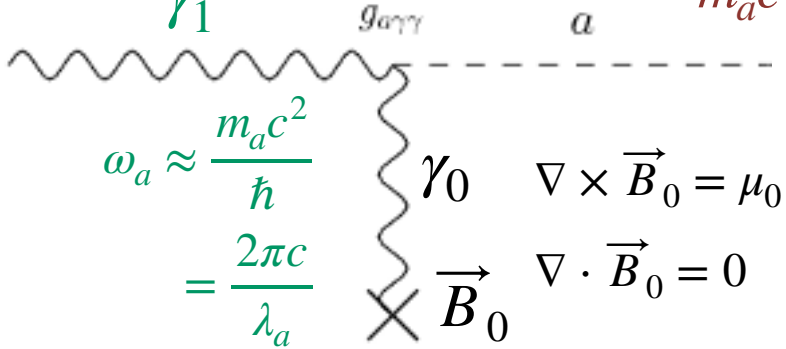


$$\omega_a \approx \frac{m_a c^2}{\hbar} = \frac{2\pi c}{\lambda_a}$$

$$\nabla \times \vec{B}_0 = \mu_0 \vec{J}_{e_0}$$

$$\nabla \cdot \vec{B}_0 = 0$$

# Poynting vector analysis of photonic conversion of the dark matter axion mixing with a background DC magnetic Field

- Apply Poynting theorem to axion modified electrodynamics
- Two possible Poynting vectors, analogous to the Abraham Poynting vector and Minkowski Poynting vector
- Minkowski picks up the extra non-conservative terms
- The non-conservative terms -> categorised as "curl forces" -> non-conservative and non-dissipative forces
- Fictitious Electric Field: Outside of the conservative Maxwell's Equations.
- Both give the same sensitivity for a resonant cavity axion haloscope, but predict markedly different sensitivity for low-mass broad band reactive haloscopes.

# Curl Force

PRL 103, 106101 (2009) PHYSICAL REVIEW LETTERS week ending 4 SEPTEMBER 2009

## Direct Measurement of the Nonconservative Force Field Generated by Optical Tweezers

Pinyu Wu,[1] Rongxin Huang,[1] Christian Tischer,[2] Alexandr Jonas,[3] and Ernst-Ludwig Florin[1,*]
[1]Center for Nonlinear Dynamics and Department of Physics, University of Texas at Austin, Austin, Texas 78712, USA
[2]European Molecular Biology Laboratory, 69117 Heidelberg, Germany
[3]Institute of Scientific Instruments, Academy of Sciences of the Czech Republic, 61264 Brno, Czech Republic
(Received 15 March 2009; published 1 September 2009)

$$\mathbf{F} = -\underbrace{\nabla V}_{\text{conservative}} + \underbrace{\nabla \times \mathbf{A}}_{\text{non-conservative}} \equiv \underbrace{\mathbf{F}_{\text{grad}}}_{\text{conservative}} + \underbrace{\mathbf{F}_{\text{curl}}}_{\text{non-conservative}}. \quad (1)$$

where the nonconservative force $\mathbf{F}_{\text{curl}}$ satisfies

$$\nabla \times \mathbf{F} - \nabla \times \mathbf{F}_{\text{curl}} - \nabla(\nabla \cdot \mathbf{\Lambda}) - \nabla^2 \mathbf{\Lambda} \neq 0.$$

## Classical and quantum complex Hamiltonian curl forces

M V Berry
H H Wills Physics Laboratory, Tyndall Avenue, Bristol BS8 1TL, United Kingdom

Received 23 June 2020, revised 29 July 2020
Accepted for publication 7 August 2020
Published 10 September 2020

Abstract

## Quantized Hamiltonian Curl Forces and Squeezed Light

P Strange

[Dated: July 3, 2018]

In this paper we discuss quantum curl forces. We present both the classical and quantum theory of linear curl forces. The quantum theory is shown to reproduce the classical theory precisely if appropriate combinations of eigenfunctions are chosen. A series of examples are used to illustrate the theory and to demonstrate its limitations. Furthermore we are able to point out an analogy between the quantum theory of curl forces and some of the squeezed light states of quantum optics.

IOP Publishing Journal of Physics A: Mathematical and Theoretical
J. Phys. A: Math. Theor. 46 (2013) 422001 (5pp) doi:10.1088/1751-8113/46/42/422001
IOP FTC

FAST TRACK COMMUNICATION

## Physical curl forces: dipole dynamics near optical vortices

KEY ISSUES REVIEW

## Non-conservative optical forces

Journal of Physics A: Mathematical and Theoretical
FAST TRACK COMMUNICATION

## Physical curl forces: dipole dynamics near optical vortices

THE EUROPEAN PHYSICAL JOURNAL D
Regular Article

## Curl forces and their role in optics and ion trapping

Electret-> Curl Force
Electric Vector Potential

$$\nabla \times \vec{D} = -\epsilon_0 \mu_0 \partial_t(\vec{B}) + \nabla \times \vec{P}$$

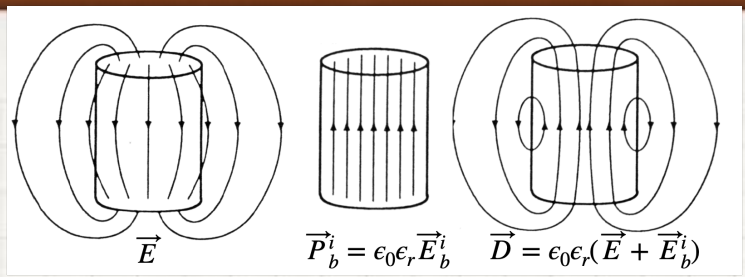


Curl Force in Axions Electrodynamics

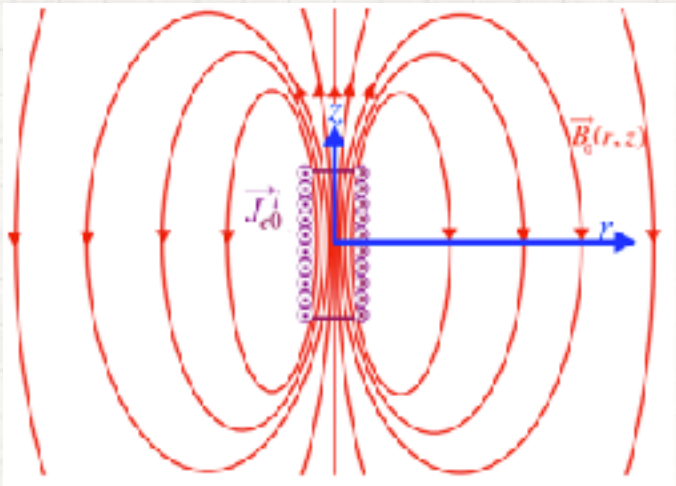


$$\vec{B}_0(\vec{r}) = \frac{\mu_0}{4\pi}\int_\Omega \frac{\vec{\nabla} \times \vec{J}^i_{DC}(\vec{r}')}{|\vec{r} - \vec{r}'|} d^3\vec{r}'$$

$$\vec{E}_{a1}(\vec{r},t) = -g_{a\gamma\gamma} a(t) c \vec{B}_0(\vec{r})$$

$$= -\frac{1}{4\pi}\int_\Omega \frac{\vec{\nabla} \times \vec{J}^i_{ma}(\vec{r}',t)}{|\vec{r} - \vec{r}'|} d^3\vec{r}'$$

Fictitious Electric field

$$\vec{J}_{m1a} = g_{a\gamma\gamma} a(t) \mu_0 c \vec{J}_{e0}$$

Axion Modified Faraday's Law

$$\frac{1}{\epsilon_0}\nabla \times \vec{D}_1 = \nabla \times \vec{E}_1 - g_{a\gamma\gamma} c \nabla \times (a\vec{B}_0) = -(\partial_t \vec{B}_1 + g_{a\gamma\gamma} a(t) c \mu_0 \vec{J}_{e0})$$







Magnetic Vector Potential generates a Conservative Force -> Not a non-conservative Curl force

# AXION ELECTRODYNAMICS IN HARMONIC PHASOR FORM
# DC BACKGROUND FIELD

Cavity Electric Field

$$\vec{E}_1(\vec{r},t) = \frac{1}{2}\left(\mathbf{E}_1(\vec{r})e^{-j\omega_1 t} + \mathbf{E}_1^*(\vec{r})e^{j\omega_1 t}\right) = \mathrm{Re}\left[\mathbf{E}_1(\mathbf{r})e^{-j\omega_1 t}\right]$$

Cavity Electric Field Phasor

$$\tilde{\mathbf{E}}_1(\vec{r},t) = \mathbf{E}_1(\vec{r})e^{-j\omega_1 t} \qquad \tilde{\mathbf{E}}_1^*(\vec{r},t) = \mathbf{E}_1^*(\vec{r})e^{j\omega_1 t}$$

Axion Scalar Field

$$a(t) = \frac{1}{2}\left(\tilde{a}e^{-j\omega_a t} + \tilde{a}^* e^{j\omega_a t}\right) = \mathrm{Re}\left(\tilde{a}e^{-j\omega_a t}\right)$$

Axion Phasor

$$\tilde{A} = \tilde{a}e^{-j\omega_a t} \qquad \tilde{A}^* = \tilde{a}^* e^{j\omega_a t}$$

Ampere's law in phasor form

$$\frac{1}{\mu_0}\nabla\times\tilde{\mathbf{B}}_1 = \tilde{\mathbf{J}}_{e1} - j\omega_1\epsilon_0\tilde{\mathbf{E}}_1 + j\omega_a g_{a\gamma\gamma}\epsilon_0 c\tilde{A}\vec{B}_0$$

$$\frac{1}{\mu_0}\nabla\times\tilde{\mathbf{B}}_1^* = \tilde{\mathbf{J}}_{e1}^* + j\omega_1\epsilon_0\tilde{\mathbf{E}}_1^* - j\omega_a g_{a\gamma\gamma}\epsilon_0 c\tilde{A}^*\vec{B}_0,$$

Ampere's law in time dependent form

$$\frac{1}{\mu_0}\nabla\times\vec{B}_1(\vec{r},t)) = \vec{J}_{e_1} + \partial_t\left(\epsilon_0\vec{E}_1(\vec{r},t) - g_{a\gamma\gamma}a(\vec{r},t)\epsilon_0 c\vec{B}_0(\vec{r},t)\right)$$

Alternative Faraday's law in phasor form (Minkowski)

$$\frac{1}{\epsilon_0}\nabla\times\tilde{\mathbf{D}}_1 = j\omega_1\tilde{\mathbf{B}}_1 - g_{a\gamma\gamma}c\mu_0\tilde{A}\vec{J}_{e0}$$

$$\frac{1}{\epsilon_0}\nabla\times\tilde{\mathbf{D}}_1^* = -j\omega_1\tilde{\mathbf{B}}_1^* - g_{a\gamma\gamma}c\mu_0\tilde{A}^*\vec{J}_{e0}$$

Faraday's law in phasor form (Abraham)

$$\nabla\times\tilde{\mathbf{E}}_1 = j\omega_1\times\tilde{\mathbf{B}}_1$$

$$\nabla\times\tilde{\mathbf{E}}_1^* = -j\omega_1\times\tilde{\mathbf{B}}_1^*,$$

# COMPLEX ABRAHAM POYNTING VECTOR FOR A DC AXION HALOSCOPE

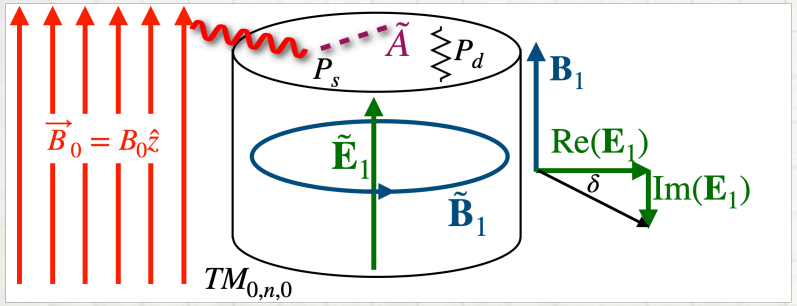


$$\mathbf{S}_{EH} = \frac{1}{2\mu_0}\mathbf{E}_1 \times \mathbf{B}_1^* \text{ and } \mathbf{S}_{EH}^* = \frac{1}{2\mu_0}\mathbf{E}_1^* \times \mathbf{B}_1$$

$$\nabla \cdot \mathbf{S} = \frac{1}{2\mu_0}\nabla \cdot (\mathbf{E}_1 \times \mathbf{B}_1^*) = \frac{1}{2\mu_0}\mathbf{B}_1^* \cdot (\nabla \times \mathbf{E}_1) - \frac{1}{2\mu_0}\mathbf{E}_1 \cdot (\nabla \times \mathbf{B}_1^*)$$

$$\nabla \cdot \mathbf{S}^* = \frac{1}{2\mu_0}\nabla \cdot (\mathbf{E}_1^* \times \mathbf{B}_1) = \frac{1}{2\mu_0}\mathbf{B}_1 \cdot (\nabla \times \mathbf{E}_1^*) - \frac{1}{2\mu_0}\mathbf{E}_1^* \cdot (\nabla \times \mathbf{B}_1)$$

Can show

Real part of Poynting Theorem

$$\oint \mathrm{Re}\left(\mathbf{S}\right) \cdot \hat{n} ds = \int \left( \frac{j\omega_a}{4}\epsilon_0 g_{a\gamma\gamma} c\vec{B}_0 \cdot (\tilde{a}^*\mathbf{E}_1 - \tilde{a}\mathbf{E}_1^*) \right.$$
$$\left. -\frac{1}{4}(\mathbf{E}_1 \cdot \mathbf{J}_{e1}^* + \mathbf{E}_1^* \cdot \mathbf{J}_{e1}) \right) d\tau$$

Can show

Reactive part of Poynting Theorem

$$\oint j\,\mathrm{Im}\left(\mathbf{S}\right) \cdot \hat{n} ds = \int \left( \frac{j\omega_1}{2}\left(\frac{1}{\mu_0}\mathbf{B}_1^* \cdot \mathbf{B}_1 - \epsilon_0 \mathbf{E}_1 \cdot \mathbf{E}_1^*\right) \right.$$
$$+\frac{j\omega_a}{4}\epsilon_0 g_{a\gamma\gamma} c\vec{B}_0 \cdot (\tilde{a}^*\mathbf{E}_1 + \tilde{a}\mathbf{E}_1^*)$$
$$\left. -\frac{1}{4}(\mathbf{E}_1 \cdot \mathbf{J}_{e1}^* - \mathbf{E}_1^* \cdot \mathbf{J}_{e1})) \right) d\tau$$

= 0 on resonance

$$\oint \langle \mathbf{S} \rangle \cdot dS = -\frac{1}{4}\int (\mathbf{E}_1 \cdot \mathbf{J}_{e1}^* + \mathbf{E}_1^* \cdot \mathbf{J}_{e1})\, d\tau + \frac{j\omega_a \epsilon_0 g_{a\gamma\gamma}}{4}\int c\vec{B}_0 \cdot (A^*\mathbf{E}_1 - A\mathbf{E}_1^*)\, d\tau$$

Cavity Power dissipation

Axion power input

= 0 for closed system

$$P_d = \frac{\omega_a \epsilon_0}{2Q}\int \mathbf{E}_1 \cdot \mathbf{E}_1^*\, d\tau = \frac{\omega_a U}{Q}$$

$$C_1 = \frac{\left(\int \vec{B}_0 \cdot \mathrm{Re}(\mathbf{E}_1)\, dV\right)^2}{B_0^2 V_1 \int \mathbf{E}_1 \cdot \mathbf{E}_1^*\, dV}$$

$$P_1 = \omega_a Q U_1 = g_{a\gamma\gamma}^2 \langle a_0 \rangle^2 \omega_a Q_1 \epsilon_0 c^2 B_0^2 V_1 C_1$$
$$= g_{a\gamma\gamma}^2 \rho_a Q_1 \epsilon_0 c^5 B_0^2 V_1 C_1 \frac{1}{\omega_a},$$

known power output
for a Sikivie Haloscope

# COMPLEX MINKOWSKI POYNTING VECTOR FOR A DC AXION HALOSCOPE

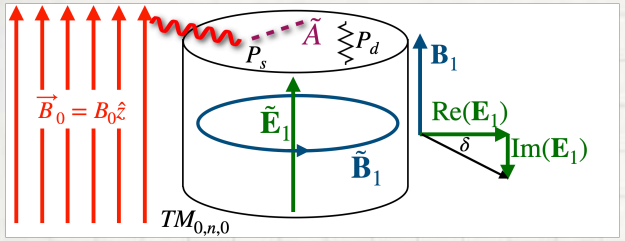


Real part of Poynting Theorem

$$\oint \mathrm{Re}\left(\mathbf{S}_{DB}\right)\cdot\hat{n}ds = \int\Big(\frac{j(\omega_1-\omega_a)}{4}\epsilon_0 g_{a\gamma\gamma}c\vec{B}_0\cdot(\tilde{a}\mathbf{E}_1^* - \tilde{a}^*\mathbf{E}_1) + \frac{1}{4}g_{a\gamma\gamma}c\vec{B}_0\cdot(\tilde{a}\mathbf{J}_{e_1}^* + \tilde{a}^*\mathbf{J}_{e_1}) - \frac{1}{4}g_{a\gamma\gamma}\vec{J}_{e_0}\cdot(\tilde{a}^*c\mathbf{B}_1 + \tilde{a}c\mathbf{B}_1^*) - \frac{1}{4}(\mathbf{E}_1\cdot\mathbf{J}_{e_1}^* + \mathbf{E}_1^*\cdot\mathbf{J}_{e_1})\Big)\,dV,$$

Reactive part of Poynting Theorem

$$\oint j\,\mathrm{Im}\left(\mathbf{S}_{DB}\right)\cdot\hat{n}ds = \int\Big(\frac{j\omega_1}{2}\Big(\frac{1}{\mu_0}\mathbf{B}_1^*\cdot\mathbf{B}_1 - \epsilon_0\mathbf{E}_1\cdot\mathbf{E}_1^*\Big) + \frac{j(\omega_1+\omega_a)\epsilon_0 g_{a\gamma\gamma}}{4}c\vec{B}_0\cdot(\tilde{a}\mathbf{E}_1^* + \tilde{a}^*\mathbf{E}_1) + \frac{1}{4}g_{a\gamma\gamma}c\vec{B}_0\cdot(\tilde{a}\mathbf{J}_{e_1}^* - \tilde{a}^*\mathbf{J}_{e_1}) + \frac{1}{4}g_{a\gamma\gamma}\vec{J}_{e_0}\cdot(\tilde{a}^*c\mathbf{B}_1 - \tilde{a}c\mathbf{B}_1^*) - \frac{1}{4}(\mathbf{E}_1\cdot\mathbf{J}_{e_1}^* - \mathbf{E}_1^*\cdot\mathbf{J}_{e_1})\Big)\,dV$$

= 0 on resonance

Axion frequency tuned to resonance $\omega_a = \omega_1$: If Halocope is inside the magnet $\frac{1}{4}g_{a\gamma\gamma}\vec{J}_{e0}\cdot(Ac\mathbf{B}_1^* + A^*c\mathbf{B}_1) = 0$

$$\oint\langle\mathbf{S}\rangle\cdot\hat{n}ds = -\frac{1}{4}\int(\mathbf{E}_1\cdot\mathbf{J}_{e1}^* + \mathbf{E}_1^*\cdot\mathbf{J}_{e1})\,d\tau + \frac{1}{4}\int c\vec{B}_0\cdot(g_{a\gamma\gamma}A\mathbf{J}_{e1}^* + g_{a\gamma\gamma}A^*\mathbf{J}_{e1})\,d\tau$$

Cavity Power dissipation — Axion power input

$$P_d = \frac{1}{4}\int(\mathbf{E}_1\cdot\mathbf{J}_{e1}^* + \mathbf{E}_1^*\cdot\mathbf{J}_{e1}) \qquad P_s = \frac{1}{4}\int c\vec{B}_0\cdot(g_{a\gamma\gamma}A\mathbf{J}_{e1}^* + g_{a\gamma\gamma}A^*\mathbf{J}_{e1})\,d\tau$$

= 0 for closed system

$$P_d = \frac{\omega_a\epsilon_0}{2Q}\int\mathbf{E}_1\cdot\mathbf{E}_1^*\,d\tau = \frac{\omega_a U}{Q}$$

$$C_1 = \frac{\left(\int\vec{B}_0\cdot\mathrm{Re}(\mathbf{E}_1)\,dV\right)^2}{B_0^2V_1\int\mathbf{E}_1\cdot\mathbf{E}_1^*\,dV}$$

$$P_1 = \omega_a Q U_1 = g_{a\gamma\gamma}^2\langle a_0\rangle^2\omega_a Q_1\epsilon_0 c^2 B_0^2 V_1 C_1 = g_{a\gamma\gamma}^2\rho_a Q_1\epsilon_0 c^5 B_0^2 V_1 C_1\frac{1}{\omega_a},$$

known power output for a Sikivie Haloscope

# Capacitor under DC Magnetic Field: Quasi-static limit

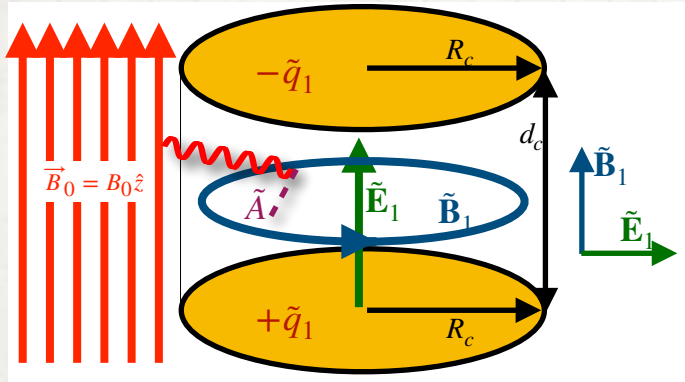


**To First order: Real part of Poynting Theorem $= 0$: Reactive part of Poynting Theorem $\neq 0$**

$$\oint j\,\mathrm{Im}\left(\mathbf{S}_{EH}\right)\cdot\hat{n}\,ds = j\omega_a\int\left(\frac{1}{2\mu_0}\mathbf{B}_1^*\cdot\mathbf{B}_1 - \frac{\epsilon_0}{2}\mathbf{E}_1^*\cdot\mathbf{E}_1 + \frac{\epsilon_0}{2}g_{a\gamma\gamma}a_0 c\vec{B}_0\cdot Re(\mathbf{E}_1)\right)dV$$

$$\oint j\,\mathrm{Im}\left(\mathbf{S}_{DB}\right)\cdot\hat{n}\,ds = j\omega_a\int\left(\frac{1}{2\mu_0}\mathbf{B}_1^*\cdot\mathbf{B}_1 - \frac{\epsilon_0}{2}\mathbf{E}_1^*\cdot\mathbf{E}_1 + \epsilon_0 g_{a\gamma\gamma}a_0 c\vec{B}_0\cdot Re(\mathbf{E}_1)\right)dV$$

**First order: Ignore fringing**

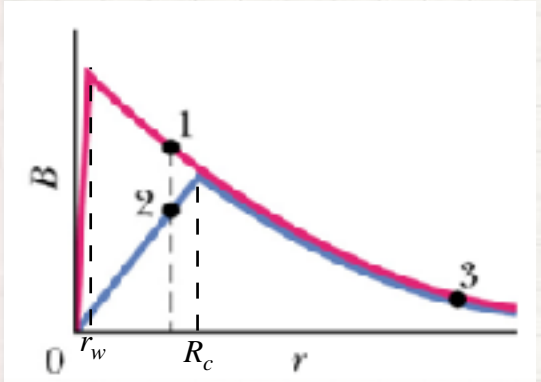


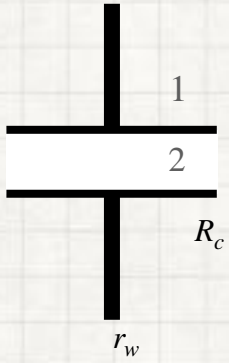


$$\mathbf{E}_1 = \frac{\tilde{q}_1}{\pi R_c^2\epsilon_0}\hat{z} \qquad \mathbf{B}_1 = -j\omega_a\mu_0\tilde{q}_1\frac{r}{\pi R_c^2}\hat{\theta} \qquad \frac{U_m}{U_e} = \frac{\int_{V_c}\mathbf{B}_1\cdot\mathbf{B}_1^* dV}{\epsilon_0\mu_0\int_{V_c}\mathbf{E}_1\cdot\mathbf{E}_1^* dV} = \frac{R_c^2\omega_a^2}{8c^2} = \frac{\pi^2 R_c^2}{2\lambda_a^2}$$

**Sensitivity assuming the Modified Abraham Poynting Vector**

$$\nabla\times\vec{E}_1 = -\partial_t\vec{B}_1$$

$$jP_a = \oint j\,\mathrm{Im}\left(\mathbf{S}_{EH}\right)\cdot\hat{n}\,ds = \frac{j\omega_a g_{a\gamma\gamma}a_0\epsilon_0 c}{2}\int\left(\vec{B}_0\cdot\mathrm{Re}(\mathbf{E}_1)\right)\frac{\pi^2 r^2}{\lambda_a^2}\,dV$$

$$P_a = \omega_a U_c, \text{ where } U_c = g_{a\gamma\gamma}^2\langle a_0\rangle^2\epsilon_0 c^2 B_0^2 V_1\left(\frac{\pi^2 R c^2}{2\lambda_a^2}\right)^2 \qquad U_c = \frac{1}{2}\tilde{\mathscr{V}}\tilde{\mathscr{V}}^* C_a \qquad \left(C_a = \frac{\pi R_c^2\epsilon_0}{d_c}\right)$$

$$\mathscr{V}_{rms} = g_{a\gamma\gamma}\langle a_0\rangle c B_0 d_c\left(\frac{\pi R_c}{\sqrt{2}\lambda_a}\right)^2 = g_{a\gamma\gamma}d_c\frac{c}{\omega_a}B_0\sqrt{\rho_a c^3}\left(\frac{\pi R_c}{\sqrt{2}\lambda_a}\right)^2$$

**Sensitivity assuming the Modified Minkowski Poynting Vector**

$$\nabla\times\vec{D}_1 = \epsilon_0\nabla\times\vec{E}_1 - g_{a\gamma\gamma}\epsilon_0 c\nabla\times(a\vec{B}_0) = -\epsilon_0(\partial_t\vec{B}_1 + g_{a\gamma\gamma}a(t)\mu_0 c\vec{J}_{e0})$$

$$jP_a = \oint j\,\mathrm{Im}\left(\mathbf{S}_{DB}\right)\cdot\hat{n}\,ds = \frac{j\omega_a g_{a\gamma\gamma}a_0\epsilon_0 c}{2}\int\left(\vec{B}_0\cdot\mathrm{Re}(\mathbf{E}_1)\right)dV$$

$$U_c = g_{a\gamma\gamma}^2\langle a_0\rangle^2\epsilon_0 c^2 B_0^2 V_1$$

$$\mathscr{V}_{rms} = g_{a\gamma\gamma}\langle a_0\rangle c B_0 d_c = g_{a\gamma\gamma}d_c\frac{c}{\omega_a}B_0\sqrt{\rho_a c^3}$$

# Electric Action of the Axion, $a(t)$, mixing with $\vec{B}_0$
# -> Creates Electromagnetic Energy at $\omega_a$

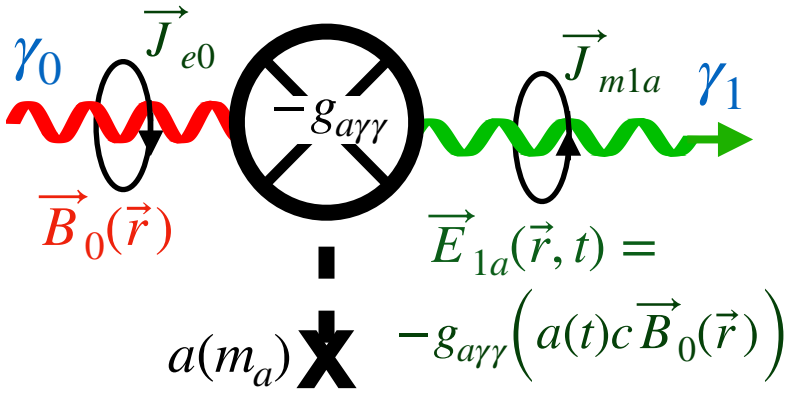


$$\vec{E}_{1a}(\vec{r},t) = -g_{a\gamma\gamma}\left(a(t)c\vec{B}_0(\vec{r})\right)$$

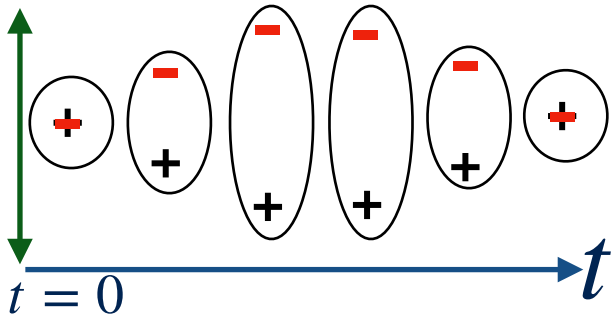


$$\vec{J}_{ab}(\vec{r},t) = \epsilon_0 \frac{\partial \vec{E}_{1a}(\vec{r},t)}{\partial t}$$

$$a(t) = a_0 \sin(\omega_a t)$$

AXION energy

$\vec{E}_{1a}$

A fictitious Electric Field

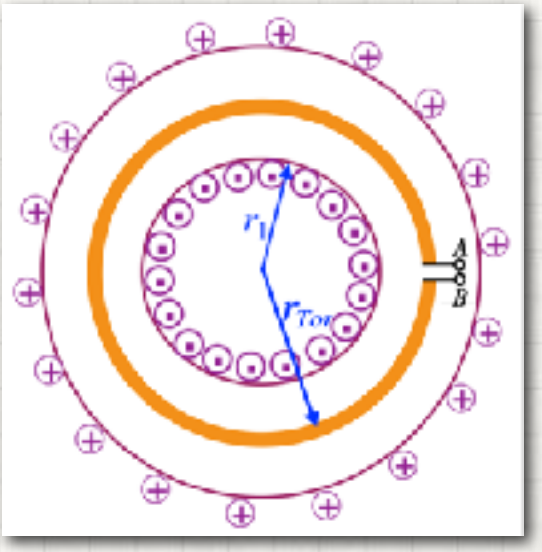



Physics of the Dark Universe

Broadband electrical action sensing techniques with conducting wires for low-mass dark matter axion detection

Michael E. Tobar, Ben T. McAllister, Maxim Goryachev

$$\oint \langle \vec{S} \rangle \cdot dS = -\frac{1}{4}\int (\mathbf{E}_1 \cdot \mathbf{J}_{e1}^* + \mathbf{E}_1^* \cdot \mathbf{J}_{e1})\, d\tau + \frac{1}{4}\int c\vec{B}_0 \cdot (g_{a\gamma\gamma} A \mathbf{J}_{e1}^* + g_{a\gamma\gamma} A^* \mathbf{J}_{e1})\, d\tau - \int \frac{1}{4} g_{a\gamma\gamma} \vec{J}_{e0} \cdot (Ac\mathbf{B}_1^* + A^* c\mathbf{B}_1)\, d\tau$$



Professor Mike Tobar
Director



Dr Maxim Goryachev
Research Associate



Dr Ben McAllister
Research Associate



Professor Eugene Ivanov
Winthrop Research Professor—Dept of Physics



Dr Jeremy Bourhill
Postdoctoral Research Associate

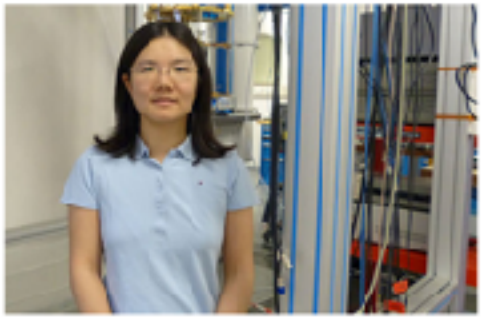

Dr Cindy Zhao
Deborah Jin Fellow—EQUS



Professor Alexey Veryaskin
Adjunct Professor



Graeme Flower
PhD




Aaron Quiskamp
PhD



Will Campbell
PhD



Catriona Thomson
PhD



Elrina Hartman
PhD



Jay Mummery
Masters



Robert Crew
BPhil (Hons) Placement

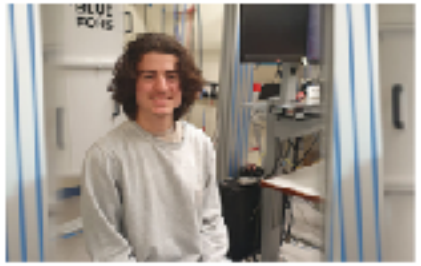

Daniel Tobar
BPhil (Hons) Placement



Michael Hatzon
BPhil (Hons)Placement



Steve Osborne
Technician

**THE END**
**THE**
**TEAM**